https://ntrs.nasa.gov/search.jsp?R=19800020796 2020-03-21T17:44:35+00:00Z

NASA CR-159,472

3 1176 01326 6169

NASA-CR-159472
19800020796

A Reproduced Copy

NASA CR-159,472

Reproduced for NASA

by the

NASA Scientific and Technical Information Facility

LIBRARY COPY

AUG 2 9 1988

LANGLEY RESEARCH CENTER
LIBRARY NASA
HAMPTON, VIRGINIA

NF01190

FFNo 672 Aug 65

NASA CR-159472
R78AEG574

QUIET CLEAN SHORT-HAUL EXPERIMENTAL ENGINE (QCSEE) UNDER-THE-WING (UTW) COMPOSITE NACELLE TEST REPORT

Volume II - Acoustic Performance

November 1979

by
D. L. Stimpert
Advanced Engineering and Technology Programs Department
Aircraft Engine Engineering Division
GENERAL ELECTRIC COMPANY

Prepared For
National Aeronautics and Space Administration

NASA-Lewis Research Center
NAS3-18021

(NASA-CR-159472) QUIET CLEAN SHORT-HAUL EXPERIMENTAL ENGINE (QCSEE) UNDER-THE-WING (UTW) COMPOSITE NACELLE TEST REPORT. VOLUME 2: ACOUSTIC PERFORMANCE (General Electric Co.) 124 p HC A06/MF A01 CSCL 21E
N80-29297
Unclas
G3/07 25904

N80-29297 #

1. Report No.	2. Government Accession No.	3. Recipient's Catalog No.
NASA CR-159472		

4. Title and Subtitle	5. Report Date
Quiet Clean Short-Haul Experimental Engine (QCSEE) Under-The-Wing (UTW) Composite Nacelle Test Report, Volume II - Acoustic Performance	November 1979
	6. Performing Organization Code
7. Author(s)	8. Performing Organization Report No.
D.L. Stimpert	R78AEG574
	10. Work Unit No.
9. Performing Organization Name and Address	11. Contract or Grant No.
General Electric Company One Neumann Way Cincinnati, Ohio 45215	NAS3-18021
	13. Type of Report and Period Covered
12. Sponsoring Agency Name and Address	Contractor Report
National Aeronautics and Space Administration Washington, D.C. 20546	14. Sponsoring Agency Code

15. Supplementary Notes

Experimental Report, Project Manager, C.C. Ciepluch, QCSEE Project Office, Technical Adviser, I.J. Loeffler, NASA-Lewis Research Center, Cleveland, Ohio 44135

16. Abstract

The Quiet Clean Short-Haul Experimental Engine (QCSEE) Program includes the design and testing of high bypass geared turbofan engines with nacelles forming the propulsion system for short-haul passenger aircraft. These flight systems contain the technology required for externally blown flap-type aircraft for introduction into passenger service in the 1980's.

This report covers testing of the Under-The-Wing (UTW) engine and composite nacelle components. The report consists of two volumes and two appendices as follows:

Volume I	Summary, Mechanical and Aerodynamic Performance (CR-159471)
Volume II	Acoustic Performance (CR-159472)
Appendix A	Detailed Engine Performance
Appendix B	Acoustic Data

System noise levels for a four-engine, UTW-powered aircraft operating in the powered-lift mode were calculated to be 97.2 and 95.7 EPNdB at takeoff and approach, respectively, on a 152.4 m (500 ft) sideline compared to a goal of 95.0 EPNdB.

17. Key Words (Suggested by Author(s))

Variable Pitch Fan
Aircraft Propulsion and Power
Integrated Engine Nacelle Structure
Propulsion System Testing
Acoustics
Jet Engine Acoustics

19. Security Classif. (of this report)	20. Security Classif. (of this page)	21. No. of Pages	22. Price
Unclassified	Unclassified	118	

TABLE OF CONTENTS

PRECEDING PAGE BLANK NOT FILMED

LIST OF ILLUSTRATIONS

LIST OF ILLUSTRATIONS (Continued)

LIST OF ILLUSTRATIONS (Continued)

LIST OF ILLUSTRATIONS (Concluded)

LIST OF TABLES

1.0 SUMMARY

As part of the Quiet Clean Short-Haul Experimental Engine (QCSEE) Program sponsored by the NASA-Lewis Research Center, the General Electric Company conducted a series of acoustic tests on an Under-the-Wing (UTW) engine suitable for use on an aircraft with powered lift capability. These tests evaluated the fully suppressed noise levels in both forward and reverse thrust modes of operation and provided a means to evaluate selected component suppression effectiveness.

System noise levels, using a contract specified calculation procedure, indicate that the in-flight noise level on a 152 m (500 ft) sideline at takeoff and approach are 97.2 and 95.7 EPNdB, respectively, compared to a goal of 95.0 EPNdB. In reverse thrust, the maximum level of thrust achieved was 27% (relative to takeoff thrust) and, at this level, the aircraft system noise level was 106.4 EPNdB.

Baseline noise levels were higher than predicted by 4 to 5 PNdB in the high frequency, broad band noise region. The high throat Mach number inlet with wall treatment (hybrid inlet) demonstrated 14 to 15 PNdB suppression of inlet radiated noise at 0.79 throat Mach number. Suppression of aft radiated noise on the engine was within 2 PNdB of predicted; and suppression of up to 2 dB was demonstrated in the high frequencies by the treated OGV's.

2.0 INTRODUCTION

The General Electric Company is currently engaged in the Quiet Clean Short-Haul Experimental Engine (QCSEE) program under Contact NAS3-18021 to the NASA-Lewis Research Center. An Under-the-Wing (UTW) experimental engine was designed and built under the program to develop and demonstrate technology applicable to engines for future commercial short-haul turbofan aircraft. The initial buildup of the UTW engine and boilerplate nacelle was tested at the General Electric Company's Peebles Test Operation from September 2, 1976 to December 17, 1976. Initial tests included mechanical and systems checkout along with fan performance characteristics over a range of blade settings including reverse thrust operation. Failure of an exhaust nozzle support ring and subsequent ingestion of a fan nozzle flap resulted in a premature conclusion of testing before any acoustic data could be acquired. A second buildup of the UTW engine - this time with a composite nacelle - was tested during the period from September 2, 1977 to July 21, 1978. Acoustic data were acquired on this second buildup and are reported in this volume.

This volume of the UTW propulsion system test report includes the results of the analysis of internal and far-field acoustic measurements and the comparison of the fully suppressed noise levels to the noise goals for a four-engine, 66,681-kg (147,000-lb), UTW-powered aircraft. Detailed acoustic data used in the analyses of this volume may be found in a separate volume, Appendix B, which is limited in distribution to the General Electric Company and Government agencies only.

3.0 TEST CONFIGURATIONS

The QCSEE UTW composite nacelle engine was tested on pad IV-D (the prime acoustic test site) at the General Electric Company's Peebles Test Operation near Peebles, Ohio. Acoustic tests were conducted over a period of time from October 5, 1977 to July 21, 1978.

Many low noise design features were incorporated into this engine including source noise reduction techniques and sound absorbing material (References 1 through 4). Table I lists the acoustic design parameters and Figure 1 is a schematic of the engine which points out the acoustic features. The engine had a low pressure ratio, low tip speed fan with wide rotor-OGV spacing, and a vane/blade ratio optimized to reduce second harmonic tone generation. Treatment was installed on the inlet, fan frame, and fan exhaust duct walls. The OGV's were treated on the pressure side for high frequency broadband suppression, and an acoustic splitter was used in the fan exhaust. Core suppression was achieved with a "stacked" suppressor which consisted of thin single-degree-of-freedom (SDOF) treatment for high frequency turbine noise suppression and deep low frequency panels for low frequency combustor noise suppression. At takeoff, inlet suppression was achieved primarily with an accelerating high Mach number inlet.

More details of the acoustic design procedure, philosophy, and component test programs are available in References 1, 2, 3, and 4.

Five engine configurations were tested. An overview of the five is presented in Table II which indicates the general setup of each.

A photograph of the baseline engine is shown in Figure 2 with a cross section in Figure 3. The inlet was a hardwall bellmouth and the fan exhaust walls were taped as shown in Figure 4 to give an acoustically hardwall surface. Fan frame wall treatment, compressor inlet treatment, and vane pressure surface treatment were present on the baseline configuration. This baseline configuration was tested twice during the program. Initially, it was tested with a gravel sound field and then later (including a removal and re-installation on the stand) with a concrete sound field. The engine configuration was identical in both cases. Table III presents the specific acoustic data points and corresponding engine operating parameters for the baseline engine tests.

An evaluation of the effect of the vane treatment was conducted on the configuration shown in Figure 5. This configuration differs from the baseline only in that the acoustically treated surfaces of the vanes were covered with metallic tape to render them acoustically hardwall. Approximately 0.67 m^2 (7.2 ft^2) of vane treatment were taped. Data points for the taped vane configuration are tabulated in Table IV.

A schematic of the fully suppressed configuration is shown in Figure 6. Treatment included the inlet wall, fan frame, fan exhaust wall, splitter, and core walls. In addition, a hybrid inlet employed on an inlet flow acceleration effect at takeoff to achieve suppression was used. A photograph of the

Table I. Acoustic Design Parameters.

- 41.2 m/sec (80 knots) Aircraft Speed
- 61 m (200 ft) Altitude
- Takeoff Conditions

Number of Fan Blades	18
Fan Diameter	180.4 cm (71 in.)
Fan Pressure Ratio	1.27
Fan rpm	3089 (3244 at 100%)
Fan Tip Speed	289.6 m/sec (950 ft/sec)
Number of OGV's	33 (32 + pylon)
Fan Weight Flow (Corrected)	405.5 kg/sec (894 lbm/sec)
Inlet Mach Number (Throat)	0.79
Rotor OGV Spacing	1.5 Rotor Tip Aerodynamic Chords
Fan Exhaust Area	1.615 m^2 (2504 $in.^2$)
Core Exhaust Area	0.348 m^2 (540 $in.^2$)
Gross Thrust (SLS Uninstalled)	81.39 kN (18,300 lbf)
Blade Passing Frequency	927 Hz
Core Exhaust Flow	31.3 kg/sec (69.1 lbm/sec)
Fan Exhaust Velocity	197.8 m/sec (649 ft/sec)
Core Exhaust Velocity	238.9 m/sec (784 ft/sec)
Bypass Ratio	12.1
Inlet Treatment Length/Fan Diameter	0.74
Vane/Blade Ratio	1.83

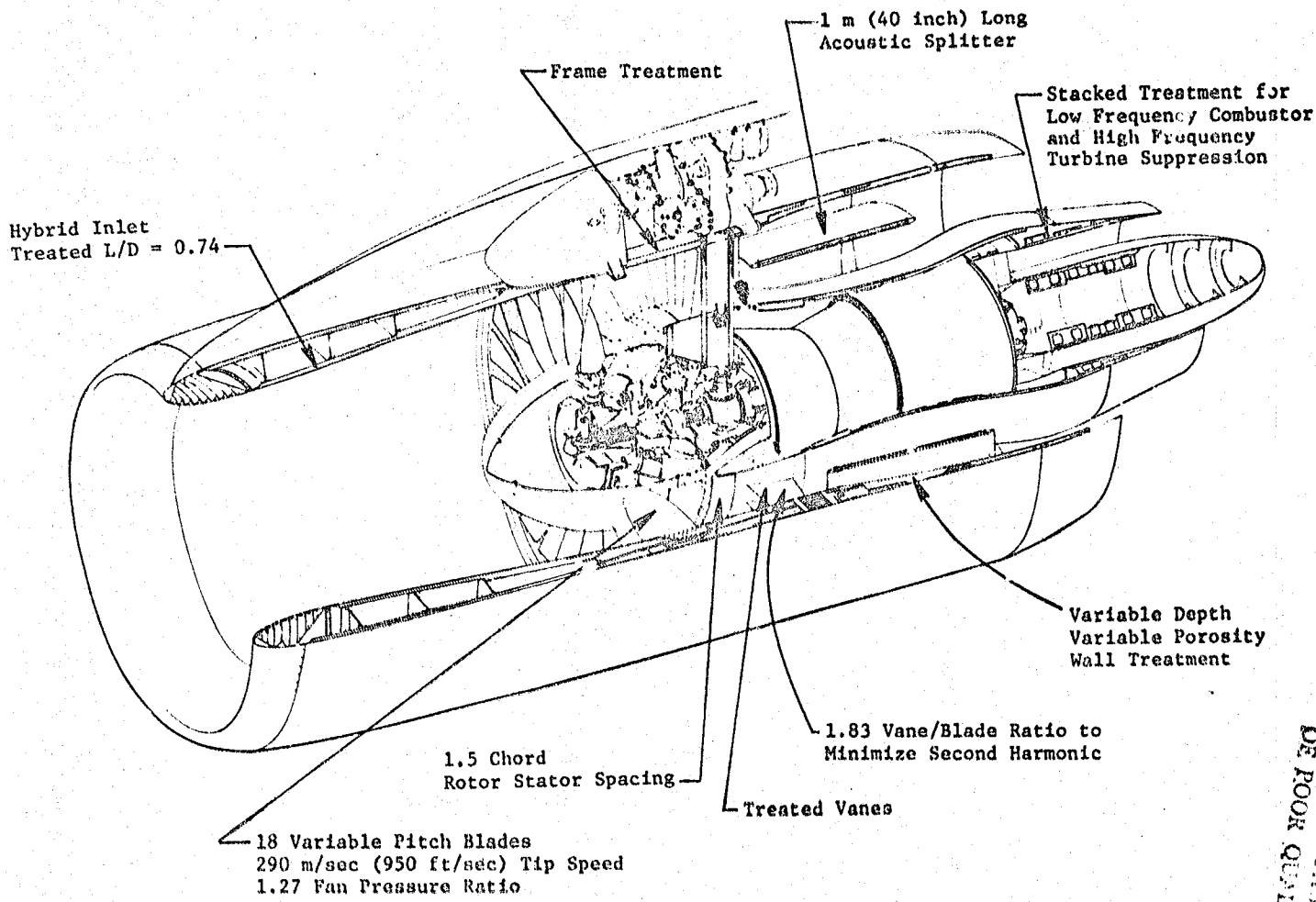

Figure 1. Acoustic Design Features.

ORIGINAL PAGE IS
OF POOR QUALITY

Table II. QCSEE UTW Acoustic Test Configurations.

- All configurations have fan frame wall treatment and compressor wall treatment

Configuration	Inlet Type	Vane Treatment	Fan Wall Treatment	Acoustic Splitter	Core Treatment
Baseline	Hardwall/ Bellmouth	Yes	Taped	No	Hardwall
Vane Treatment Effect	Hardwall/ Bellmouth	Taped	Taped	No	Hardwall
Fully Suppressed	Hybrid	Yes	Yes	Yes	Yes
Splitter Treatment Effect	Hybrid	Yes	Yes	No	Yes
Core Treatment Effect	Hybrid	Yes	Yes	Yes	Hardwall

ORIGINAL PAGE IS
OF POOR QUALITY

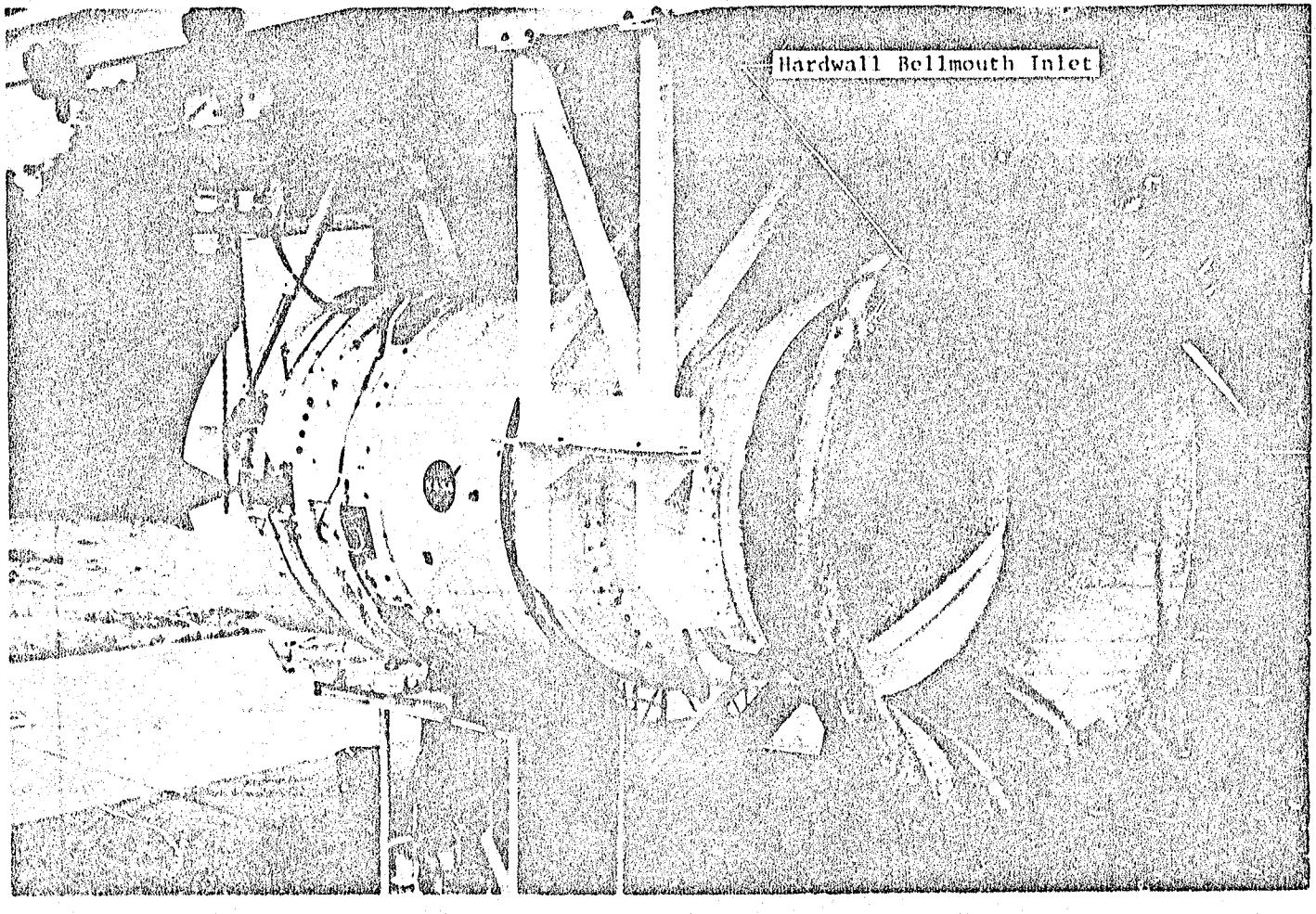

Figure 2. QCSEE UTW Baseline Engine.

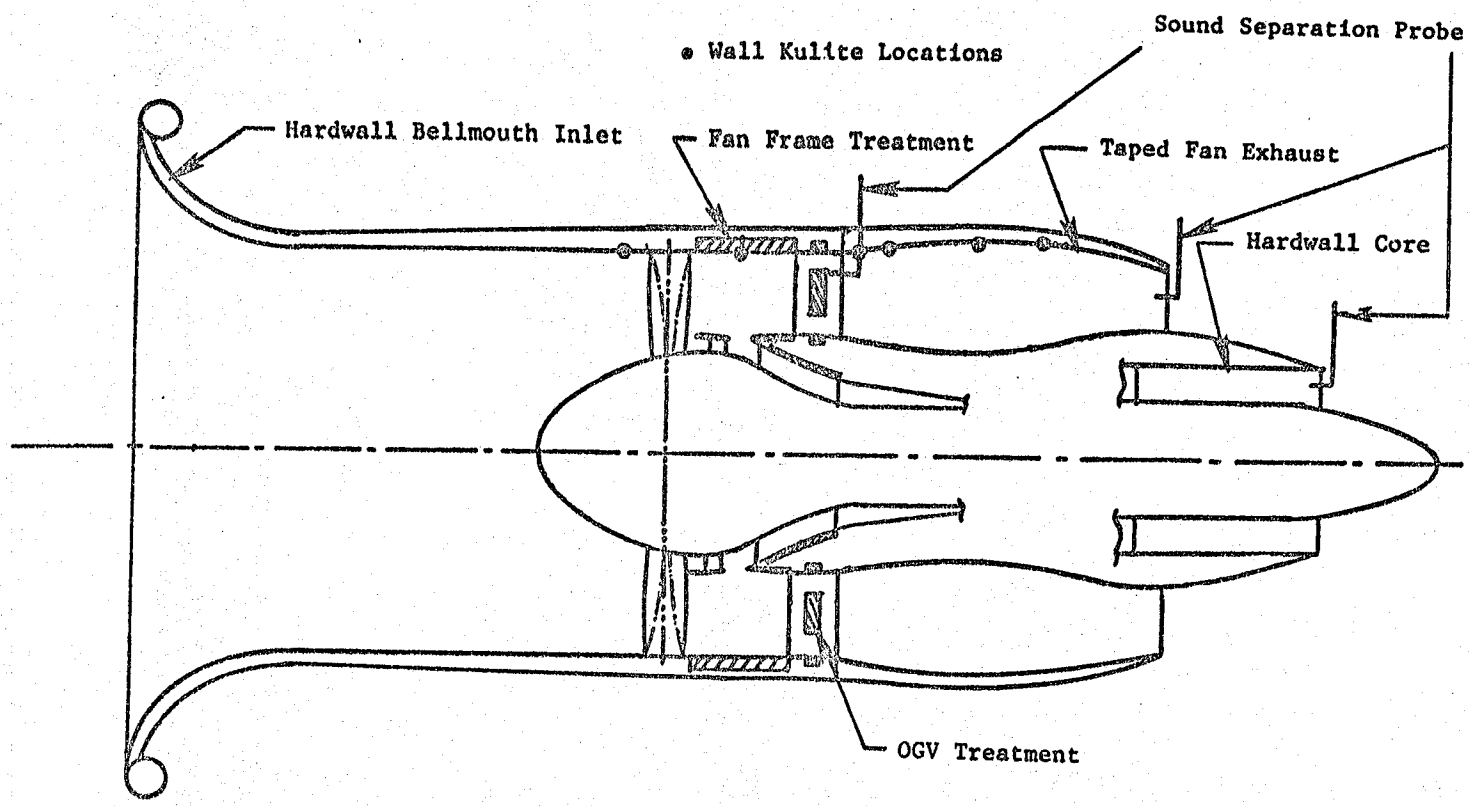

Figure 3. UTW Baseline Configuration.

ORIGINAL PAGE IS
OF POOR QUALITY

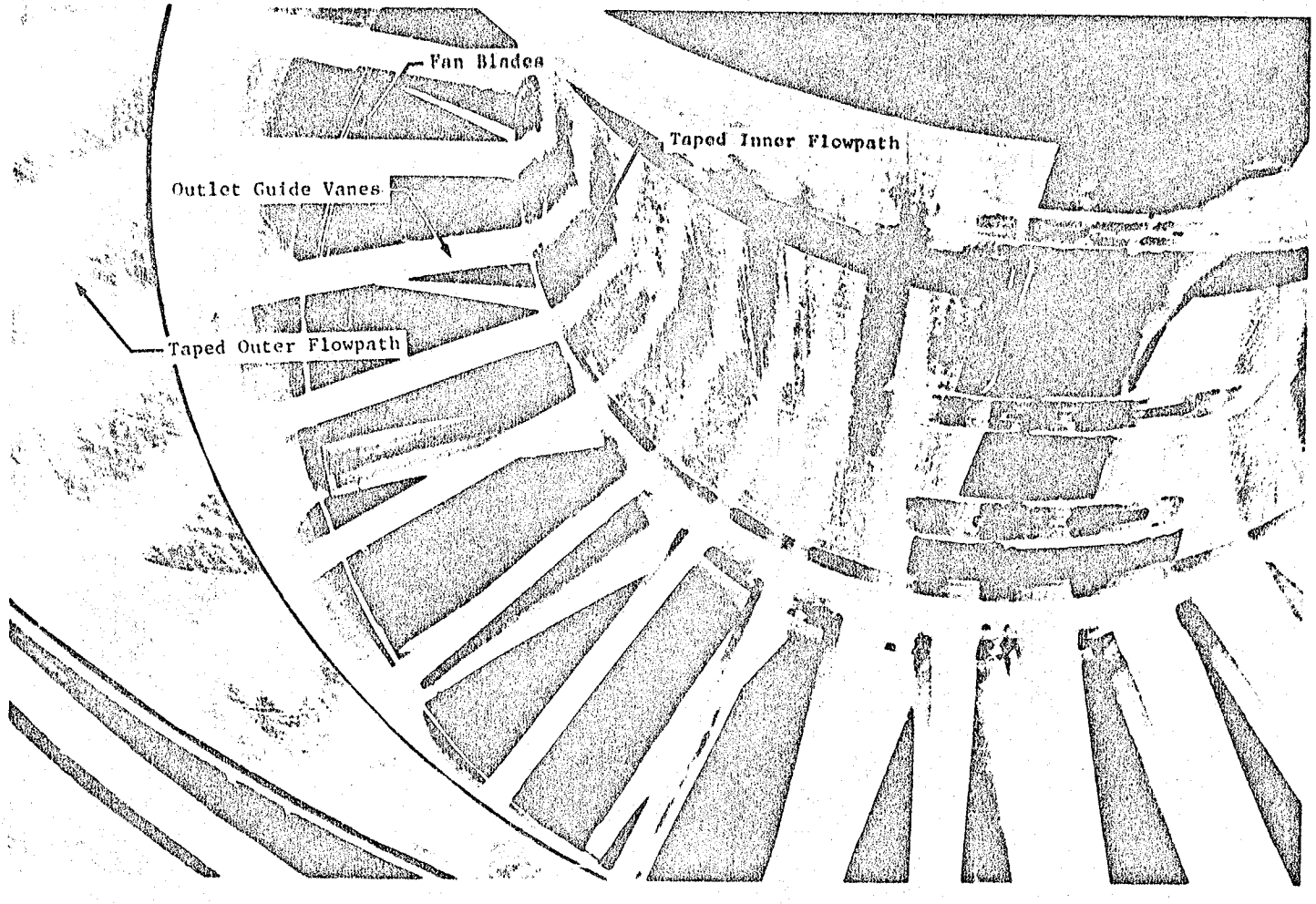

Figure 4. Taped Fan Bypass Duct.

Table III. Baseline (Frame-Treated) Acoustic Data Points.

Acoustic Readings	Comments*	Date	PCNLR	XNL	XNH	ROPDEG	A18 m^2	A18 $in.^2$	FNRIN N	FNRIN lb	XM11	Probe Immersions
1	Background Noise	10-5-77	0	0	0	-	-	-	0	0		
2	250 Counts Core Cowl Cooling	10-5-77	0	0	0	-	-	-	0	0		
3	500 Counts Core Cowl Cooling	10-5-77	0	0	0	-	-	-	0	0		
4	1000 Counts Core Cowl Cooling	10-5-77	0	0	0	-	-	-	0	0		
5	Idle	10-5-77	55.5	1805	11020	4.9	1.518	2353	-	-		
6		10-5-77	91.5	2969	12424	-5.5	1.608	2493	73805	16592		
7		10-5-77	91.2	2970	13000	-5.4	1.580	2449	73818	16595		
8		10-5-77	90.9	2963	12992	-5.4	1.548	2399	73511	16526		
9		10-5-77	90.9	2962	12930	-5.4	1.517	2352	73551	16535		
10	1000 Counts Core Cowl Cooling	10-6-77	0	0	0	-	-	-	0	0		
11		10-6-77	97.0	3143	12[illegible]5	-5.1	1.625	2519	77688	17465		
12		10-6-77	97.1	3144	12917	-4.8	1.556	2412	77608	17447		
13		10-6-77	94.5	3058	12872	-5.0	1.613	2501	74895	16837		
14		10-6-77	94.3	3056	12933	-4.8	1.582	2453	79886	17359		
15		10-6-77	94.4	3058	12945	-5.2	1.540	2418	77568	17438		
16		10-6-77	94.5	3059	12964	-5.1	1.519	2355	78520	17652		
17		10-6-77	94.4	3058	12925	-4.5	1.457	2259	77679	17463		
18	Repeat (12)	10-6-77	96.9	3137	12963	-4.6	1.559	2417	76096	17107		
19		10-6-77	96.2	3112	12981	-5.3	1.561	2419	78080	17553		
20		10-6-77	80.6	2608	12290	-4.1	1.684	2610	56635	12732		
21		10-6-77	80.6	2608	12298	-3.9	1.886	2923	55705	12523		
22	Repeat (21)	10-6-77	80.6	2608	12295	-4.0	1.891	2931	55100	12387		
23		10-6-77	84.3	2728	12294	-2.5	1.877	2910	56613	12727		
24	1000 Counts Core Cowl Cooling	10-7-77	0	0	0	-	-	-	0	0		
25		10-7-77	87.2	2769	12440	-3.7	2.003	3105	-	-		
26		10-7-77	83.6	2819	12577	-1.0	1.893	2934	56279	12652		
27		10-7-77	95.4	3099	13157	-6.9	1.615	2504	79561	17886		
28	Abort											
29		10-7-77	95.0	3067	12375	+0.4	1.875	2906	56541	12711		
30		10-7-77	94.9	3067	12357	1.0	1.681	2605	57040	12823		
31		10-7-77	94.9	3066	12906	-4.6	1.561	2420	76140	17117		
32		10-7-77	96.8	3126	12986	-5.0	1.558	2415	78204	17581		
33		10-7-77	89.8	2901	12091	-5.1	1.550	2403	69917	15718		
34		10-7-77	79.9	2579	12399	-4.6	1.548	2400	57827	13000		
35	Idle	10-7-77	55.5	1793	11398	-5.9	1.558	2415	28340	6371		
36	Idle	10-7-77	55.6	1794	11358	-5.2	1.887	2925	28842	6484		
37		10-7-77	79.9	2578	12324	-5.5	1.890	2929	56319	12661		
38		10-7-77	89.8	2899	12739	-5.0	1.880	2914	68596	15421		
39		10-7-77	95.3	3075	13028	-5.3	1.904	2951	-	-		
40		10-7-77	97.0	3133	13070	-5.0	1.890	2930	73591	16544		
41		10-7-77	97.0	3133	13049	-5.3	1.733	2686	75758	17031		
163		7-16-78	92.5	3045	12880	-3.1	1.536	2381	68285	15351		
164		7-16-78	94.3	3099	12954	-3.2	1.535	2380	69873	15708		
165		7-16-78	85.0	2791	12564	-3.1	1.535	2380	57440	12913		
166		7-16-78	80.2	2632	12487	-3.1	1.535	2380	-	-		
167		7-16-78	94.2	3095	13001	-3.2	1.536	2381	71679	16114		

*Readings 1 to 41 - gravel surface
Readings 163 to 167 - concrete surface

Table III. Baseline (Frame-Treated) Acoustic Data Points. (Continued)

Acoustic Readings	Comments*	Date	PCNLR	XNL	XNH	ROPDEG	A18 m^2	A18 $in.^2$	FNRIN N	FNRIN lb	XM11	Probe Immersions
168	Decel/Accel	7-16-78	-	-	-	-3.2	1.536	2381	-	-		
169		7-16-78	94.5	3100	13156	-4.6	1.535	2380	-	-		
170		7-16-78	89.6	2939	12826	-4.6	1.537	2383	66038	14846		
171		7-16-78	79.6	2612	12457	-4.6	1.536	2382	53161	11951		
172		7-16-78	79.6	2613	12501	-4.9	1.535	2379	54299	12207		
173		7-16-78	84.9	2785	12740	-5.0	1.535	2380	61999	13938		
174		7-16-78	90.0	2953	12927	-5.0	1.535	2380	70322	15809		
175		7-16-78	92.5	3034	13116	-5.0	1.536	2381	74272	16697		
176		7-16-78	94.3	3095	13225	-5.1	1.536	2381	77359	17391		
177	Accel	7-16-78	-	-	-	-5.1	1.536	2381	-	-		
178	Abort	7-16-78	-	-	-	-	-	-	-	-		
179		7-16-78	94.3	3094	13220	-4.9	1.536	2381	77661	17459		
180		7-17-78	92.3	3027	13054	-5.0	1.484	2300	-	-		
181		7-17-78	92.5	3033	13222	-5.0	1.484	2300	-	-		
182		7-17-78	90.0	2953	13126	-5.0	1.484	2300	-	-		
183		7-17-78	92.3	3027	13054	-5.2	1.595	2473	73431	16508		
184		7-17-78	94.5	3099	13265	-4.8	1.595	2473	78084	17554		
185		7-17-78	90.1	2955	12962	-5.0	1.595	2472	71283	16025		
186	Directional Array	7-17-78	94.2	3082	12466	4.4	1.661	2574	54308	12209		
187	Directional Array	7-17-78	94.6	3091	13180	-5.0	1.536	2382	76865	17280		
188		7-17-78	94.4	3082	12356	5.0	1.535	2380	53294	11981		
189		7-17-78	94.4	3082	12638	0.0	1.535	2380	62729	14102		
190		7-17-78	94.4	3082	12822	-2.0	1.535	2379	68280	15350		
191		7-17-78	94.5	3082	13007	-4.1	1.535	2380	73943	16623		
192		7-17-78	94.4	3082	13162	-6.0	1.536	2381	77524	17428		
193		7-17-78	94.4	3081	13287	-7.1	1.536	2381	79481	17868		
194		7-17-78	94.4	3082	13315	-7.8	1.536	2381	80166	18022		
195		7-17-78	92.2	3008	13269	-7.8	1.536	2381	78226	17586		
196		7-17-78	90.0	2937	13143	-7.9	1.536	2381	73589	16993		
197		7-17-78	85.1	2776	12943	-7.9	1.536	2381	69566	15639		
198		7-17-78	80.3	2620	12667	-8.1	1.535	2380	61421	13808		
199		7-17-78	89.4	2916	12249	3.3	1.877	2909	48059	10804		
200		7-17-78	94.6	3085	12454	1.5	1.695	2627	56510	12704		
201		7-17-78	95.0	3097	12479	0.3	1.877	2910	56021	12594		

*Concrete Surface

Table III. Baseline (Frame-Treated) Acoustic Data Points. (Concluded)

Acoustic Readings	Comments*	Date	PCNLR	XNL	XNH	ROPDEG	A18 m^2	A18 $in.^2$	FNRIN N	FNRIN lb	XM11	Probe Immersions
202		7-17-78	94.8	3089	12926	-3.3	1.594	2470	71923	16169		
203		7-17-78	92.4	3014	12841	-3.3	1.594	2471	69343	15589		
204		7-17-78	89.9	2932	12716	-3.3	1.594	2470	-	-		
205		7-17-78	90.4	2948	12878	-3.6	1.486	2303	-	-		
206		7-17-78	92.5	3018	12991	-3.6	1.486	2303	-	-		
207		7-17-78	94.7	3084	13111	-3.6	1.485	2302	-	-		
208	OGV Probe	7-17-78	94.6	3083	13040	-5.0	1.523	2361	-	-		15
209		7-17-78	90.3	2949	13172	-7.8	1.579	2447	-	-		
210		7-17-78	92.0	3004	13300	-7.8	1.579	2447	-	-		
211		7-17-78	92.1	3007	13358	-8.0	1.484	2300	-	-		
212	90%	7-17-78	90.0	2940	13153	-8.0	1.484	2300	-	-		
213		7-17-78	93.7	3059	13445	-8.1	1.484	2300	-	-		
214	Fan Nozzle Probe	7-17-78	90.5	3007	12650	0.0	1.645	2550	57747	12982		15
215	Core Probe	7-17-78	90.7	3006	12694	0.0	1.659	2572	58309	13086		2
216	Core Probe	7-17-78	90.7	3006	12629	0.0	1.880	2914	55265	12424		2
217	Core Probe	7-17-78	85.0	2818	12366	0.0	1.880	2915	48294	10857		2
218	Core Probe	7-17-78	80.1	2656	12234	0.0	1.879	2913	43682	9820		4
219	Core Probe	7-17-78	54.3	1801	11307	-0.1	1.879	2912	22081	4964		2
220	Core Probe Accel/Decel	7-17-78	-	-	-	-	-	-	-	-		1
221	Core Probe	7-17-78	80.4	2665	12322	-0.2	1.759	2726	47565	10693		2
222	OGV Probe	7-17-78	87.8	2908	12607	-0.3	1.661	2574	56995	12813		15
223	Core Probe	7-17-78	80.1	2648	12319	-0.1	1.629	2525	46982	10562		4
224	Fan Nozzle Probe	7-17-78	93.7	3098	13154	-3.0	1.537	2382	74250	16692		15
225	Core Probe	7-17-78	93.8	3102	13188	-5.0	1.535	2380	-	-		4

*Concrete Surface

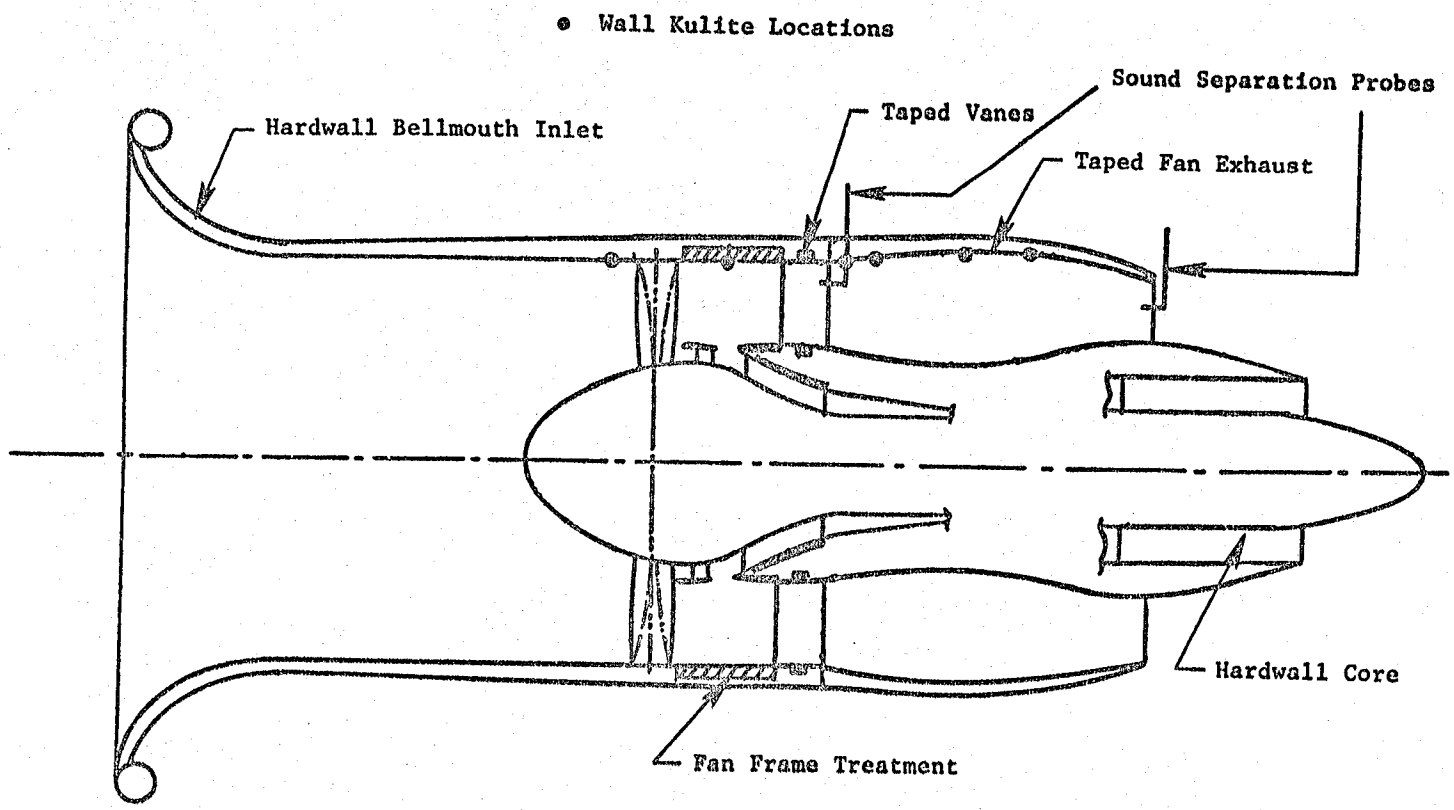

Figure 5. Treated Vane Evaluation Configuration.

Table IV. Taped Vane Acoustic Data Points.

Acoustic Readings	Comments*	Date	PCNLR	XNL	XNH	ROPDEG	A18		FNRIN		Probe Immersions
							m^2	$in.^2$	N	lb	
145	Fan Nozzle Probe	7-16-78	94.1	3094	13165	-5.0	1.535	2380	74227	16687	6
146	OGV Probe	7-16-78	94.2	3096	13250	-5.0	1.535	2380	-	-	6
147	OGV Probe	7-16-78	94.2	3098	12453	+4.3	1.648	2554	-	-	6
148	Fan Nozzle Probe	7-16-78	94.2	3097	12425	+4.3	1.648	2554	-	-	6
149	Idle	7-16-78	54.5	1793	11099	4.8	1.625	2519	-	-	
150		7-16-78	80.1	2606	-	-5.0	1.535	2380	-	-	
151		7-16-78	85.0	2777	12085	-4.7	1.535	2380	-	-	
152		7-16-78	90.0	2950	13154	-4.9	1.535	2380	-	-	
153		7-16-78	92.5	3040	13279	-4.9	1.535	2380	-	-	
154		7-16-78	94.6	3106	13263	-5.0	1.537	2382	76394	17174	
155	Decel/Accel	7-16-78	-	-	-	-5.0	1.537	2382	-	-	
156		7-16-78	94.4	3094	12928	-3.3	1.535	2380	69757	15682	
157		7-16-78	94.4	3095	13117	-4.8	1.542	2390	73778	16586	
158		7-16-78	94.5	3095	13114	-4.9	1.535	2380	74098	16658	
159		7-16-78	94.4	3094	13375	-8.1	1.535	2380	78920	17742	
160		7-16-78	94.5	3094	12580	0.2	1.877	2909	56048	12600	
161		7-16-78	94.5	3094	12496	1.7	1.694	2626	55532	12484	
162		7-16-78	94.4	3094	12369	4.3	1.659	2572	49215	11064	

*Concrete Surface

- Wall Kulite Locations

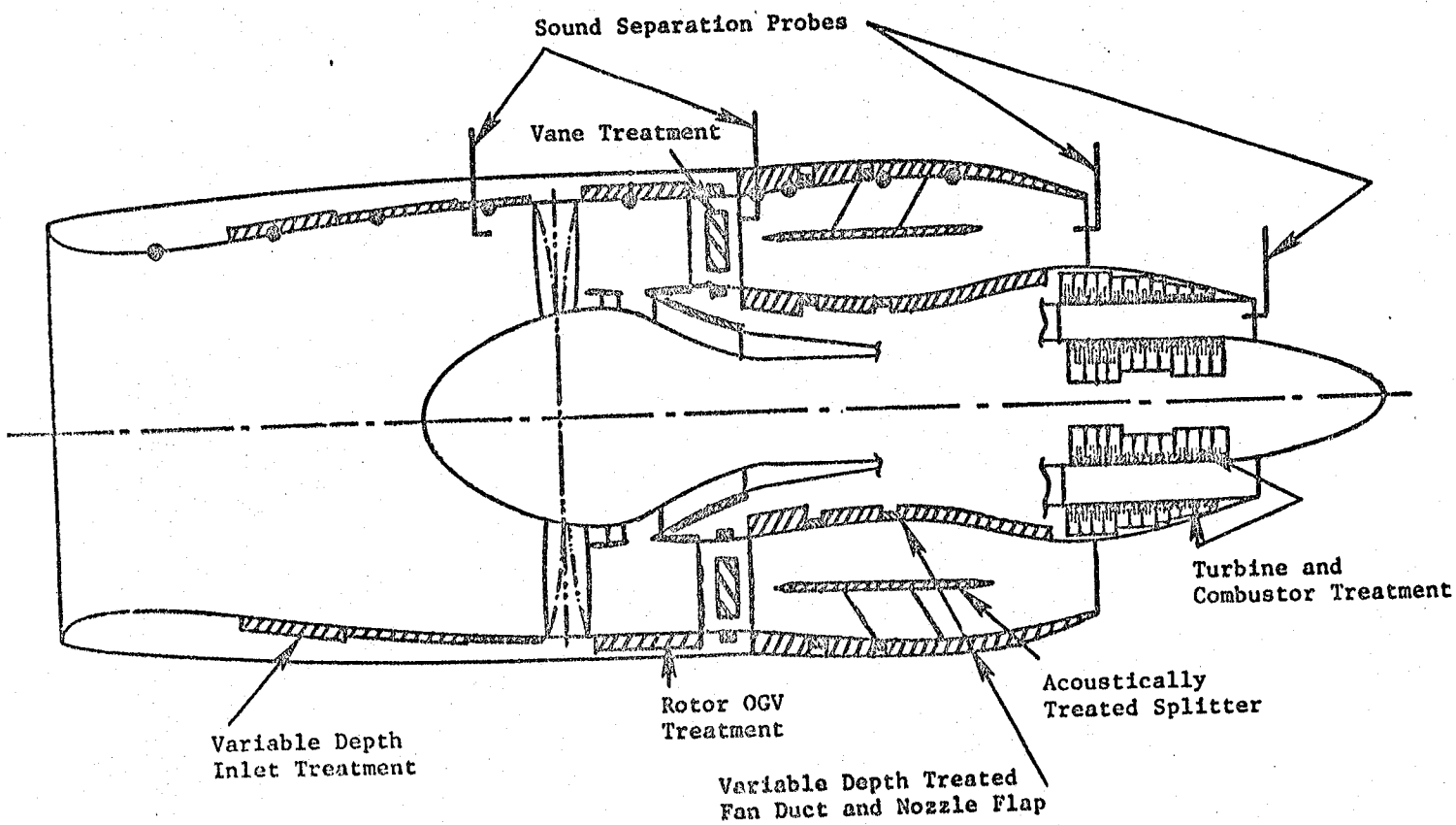

Figure 6. Fully Suppressed Configuration.

UTW fully suppressed engine on the test stand is shown in Figure 7. The specific data points acquired are tabulated in Table V. This fully suppressed configuration was tested in both forward and reverse thrust modes of operation.

Evaluation of the core suppressor stacked treatment was conducted on the configuration shown schematically in Figure 8. Only the stacked treatment in the core was removed and replaced with hardwall panels. Acoustic data points are tabulated in Table VI.

The final configuration tested was fully suppressed with wall treatment only - no splitter - in the fan bypass duct, shown schematically in Figure 9. This configuration was tested at the acoustic data points listed in Table VII.

Figure 7. UTW Composite Nacelle Engine.

ORIGINAL PAGE IS
OF POOR QUALITY

Table V. Fully Suppressed Acoustic Data Points.

Acoustic Readings	Comments*	Date	PCNLR	XNL	XNH	ROPDEG	A18 m^2	A18 $in.^2$	FNRIN N	FNRIN lb	XM11	Probe Immersions
42	Background Noise	1-3-78	0	0	0	-	-	-	-	-	-	
43	500 Counts Core Cowl Cooling	1-3-78	0	0	0	-	-	-	-	-	-	
44	Idle	1-3-78	60.1	1883	10887	5.2	1.613	2500	24843	5585	-	
45		1-3-78	79.6	2489	12111	-4.8	1.526	2366	58005	13040	-	
46		1-3-78	79.7	2497	12126	-4.7	1.527	2367	59055	13276	0.607	
47		1-3-78	89.6	2805	12588	-4.7	1.530	2371	74379	16721	0.739	
48		1-3-78	94.6	2962	12814	-4.6	1.530	2372	79832	17947	0.821	
49		1-3-78	96.5	3023	12868	-4.6	1.530	2372	80864	18179	0.839	
50		1-3-78	96.6	3022	12886	-4.7	1.489	2308	82110	18459	0.822	
51		1-3-78	96.7	3023	12001	3.7	1.859	2882	53468	12020	0.619	
52		1-4-78	96.4	3023	12001	4.3	1.738	2694	53979	12135	0.613	
53		1-4-78	94.7	2971	11983	3.4	1.740	2697	-	-	-	
	Idle	1-4-78	60.3	1894	-	6.0	1.348	2089	-	-	-	
54		1-4-78	94.4	2963	11966	4.3	1.645	2550	53681	12068	0.590	
55		1-4-78	91.9	2872	11974	3.3	1.862	2886	53601	12050	0.623	
56		1-4-78	90.7	2837	11983	3.3	1.738	2694	53285	11979	0.609	
57		1-4-78	91.8	2870	11995	3.2	1.861	2885	53525	12033	0.626	
58		1-4-78	89.4	2801	11997	1.3	1.861	2885	53383	12001	0.629	
59		1-4-78	88.0	2756	11963	1.2	1.740	2698	53561	12041	0.614	
60	Aborted - High Winds	1-4-78	-	-	-	-	-	-	-	-	-	
61	Fan OGV/Nozzle Probe	3-10-78	94.6	3016	12157	5.2	1.648	2555	54566	12267	0.593	6
62	Fan OGV/Nozzle Probe	3-10-78	96.5	3077	12256	3.2	1.862	2886	54793	12318	-	3
63	Core Cowl Cooling	3-10-78	0	0	0	0	-	-	0	0	0	
64	Background Noise	3-10-78	0	0	0	-	-	-	0	0	0	
65	Idle	4-3-78	54.3	1784	11567	-5.0	1.616	2505	26476	5952	0.354	
66		4-3-78	92.2	3028	13243	-5.0	1.587	2460	74899	16838	0.773	
67		4-3-78	97.2	3188	13467	-5.0	1.586	2459	76976	17305	0.831	
68		4-3-78	95.1	3123	13393	-5.0	1.587	2460	75976	17080	0.809	
69	Accel/Decel	4-3-78	-	-	-	-5.0	1.587	2460	-	-	-	
70		4-3-78	92.4	3027	13267	-5.0	1.553	2408	74735	16801	0.765	
71		4-3-78	96.5	3165	13470	-5.0	1.551	2405	77702	17468	0.818	
72		4-3-78	95.3	3128	13438	-5.0	1.552	2406	77110	17335	0.805	
73		4-4-78	75.8	2486	12472	-5.0	1.529	2370	50461	11344	0.549	
74		4-4-78	96.0	3150	13448	-5.0	1.530	2371	77919	17517	0.808	
75		4-4-78	94.8	3110	13415	-5.0	1.530	2371	77408	17402	0.797	
76		4-4-78	91.7	3009	13225	-5.0	1.530	2371	74441	16735	0.747	
77		4-4-78	89.8	2947	13076	-5.0	1.530	2371	71768	16134	0.717	
78	500 Counts Core Cowl Cooling	4-4-78	0	0	0	-	-	-	0	0	0	
79	Background Noise	4-4-78	0	0	0	-	-	-	0	0	0	
80		4-4-78	96.3	3122	13438	-5.0	1.489	2308	79178	17800	0.789	
81		4-4-78	96.5	3129	13499	-5.0	1.419	2199	-	-	0.731	
82		4-4-78	91.8	3011	13229	-5.0	1.421	2203	74232	16688	0.698	

*Gravel Surface

Table V. Fully Suppressed Acoustic Data Points. (Continued)

Acoustic Readings	Comments*	Date	PCNLR	XNL	XNH	ROPDEG	A18 m^2	A18 $in.^2$	FNRIN N	FNRIN lb	XM11	Probe Immersions
83		4-4-78	92.0	3011	13242	-5.0	1.49	2310	74681	16789	0.731	
84	Background Noise	4-7-78	0	0	0	-5.0	-	-	-	-	-	
85		4-7-78	54.6	1782	11594	-95.0	Flare**		-11419	-2567	-	
86		4-7-78	57.8	1889	11783	-95.0	Flare		-12646	-2843	-	
87		4-7-78	61.3	2002	11989	-95.0	Flare		-14283	-3211	-	
88		4-7-78	66.9	2185	12309	-95.0	Flare		-16970	-3815	-	
89	Reverse Thrust	4-7-78	63.9	2084	12114	-95.0	Flare		-15476	-3468	-	
90		4-7-78	67.1	2189	12327	-95.0	Flare		-16997	-3821	-	
91		4-7-78	61.1	1993	11973	-95.0	Flare		-14074	-3164	-	
92	Accel/Decel	4-7-78	-	-	-	-95.0	Flare		-	-	-	
93	Background Noise	4-7-78	0	0	0	-95.0	-	-	-	-	-	
94	500 Counts Core Cowl Cooling	4-8-78	0	0	0	-8.0	1.619	2510	-	-	-	
95	Idle	4-8-78	55.5	1792	11531	-8.0	1.619	2510	29959	6735	-	
96	Background Noise	4-8-78	0	0	0	-8.0	-	-	-	-	-	
97		4-8-78	94.0	3013	13271	-8.0	1.526	2365	81376	18294	0.853	
98		4-8-78	89.1	2856	12991	-8.0	1.526	2365	75944	17073	0.753	
99		4-8-78	86.8	2782	1284'	-8.0	1.526	2365	72039	16195	0.715	
100		4-8-78	90.9	2914	13118	-8.0	1.526	2365	78240	17589	-	
101		4-8-78	80.0	2564	12503	-8.0	1.526	2365	60198	13533	0.615	
102		4-8-78	96.4	3090	13353	-8.0	1.581	2451	79712	17920	0.906	
103		4-8-78	90.8	2910	13063	-8.0	1.581	2451	76634	17228	0.793	
104		4-8-78	86.9	2784	12809	-8.0	1.581	2451	71647	16107	0.725	
105		4-8-78	96.6	3095	13399	-8.0	1.548	2400	-	-	-	
106		4-8-78	90.8	2909	13180	-8.0	1.548	2400	79530	17879	0.838	
107		4-8-78	86.8	2781	12900	-8.0	1.548	2400	73582	16542	0.735	
108		4-8-78	86.8	2781	12863	-8.0	1.484	2300	72951	16400	0.708	
109		4-8-78	90.8	2909	13220	-8.0	1.484	2300	80197	18029	0.790	
110		4-8-78	92.3	2959	13334	-8.0	1.484	2300	-	-	-	
111	Core Cowl Cooling	4-8-78	0	0	0	-8.0	1.484	2300	-	-	-	
112	Background Noise	4-8-78	0	0	0	-8.0	1.484	2300	-	-	-	
113	Background Noise	4-16-78	0	0	0	-3.3	1.484	2300	-	-	-	
114	500 Counts Core Cowl Cooling	4-16-78	0	0	0	-3.3	1.484	2300	-	-	-	
115		4-16-78	57.2	1840	11309	-3.3	1.612	2499	-	-	-	
116		4-16-78	96.0	3088	12948	-3.3	1.612	2499	-	-	-	
117		4-16-78	96.0	3088	12983	-3.3	1.522	2360	77168	17348	0.764	
118		4-16-78	95.0	3056	12938	-3.3	1.522	2360	75918	17067	0.748	
119		4-16-78	91.1	2930	12686	-3.3	1.522	2360	71083	15980	0.695	
120		4-16-78	87.0	2799	12531	-3.3	1.522	2360	64771	14561	0.653	
121		4-16-78	79.8	2567	12287	-3.3	1.522	2360	55127	12393	0.570	
122		4-16-78	76.1	3089	12923	-3.3	1.645	2550	74881	16834	0.784	
123		4-16-78	95.0	3053	12884	-3.3	1.645	2550	74227	16687	0.770	
124		4-16-78	91.9	2952	12604	-3.3	1.645	2550	70202	15782	0.718	
125		4-16-78	90.9	2918	12687	-3.3	1.58	2450	71132	15991	0.701	
126		4-17-78	96.1	3087	12957	-3.3	1.58	2450	76398	17175	0.761	
127		4-17-78	94.6	3035	12913	-3.3	1.58	2450	74503	16749	0.743	

*Gravel Surface
**See Figure 67

Table V. Fully Suppressed Acoustic Data Points. (Concluded)

Acoustic Readings	Comments*	Date	PCNLR	XNL	XNH	ROPDEG	A18 m^2	A18 $in.^2$	FNRIN N	FNRIN lb	XM11	Probe Immersions
128		4-17-78	94.7	3036	12900	-3.3	1.548	2400	74552	16760	0.737	
129		4-17-78	96.2	3086	13002	-3.3	1.548	2400	76687	17240	0.749	
130		4-17-78	90.7	2909	12730	-3.3	1.548	2400	69027	15518	0.685	
131		4-17-78	90.9	2913	12758	-3.3	1.484	2300	-	-	-	
132	Reverse Thrust	4-17-78	96.2	3083	13027	-3.3	1.484	2300	77897	17512	0.742	
133		4-17-78	94.8	3040	13007	-3.3	1.484	2300	-	-		
134		4-17-78	56.2	1813	11400	-3.3	1.871	2900	-	-		
135	Background Noise	4-21-78	0	0	0	-100	Flared		0	0		
136	Facility On	4-21-78	0	0	0	-100	Flared		0	0		
137	Idle	4-21-78	56.8	1806	11227	-100	Flared		-11361	-2554		1
138		4-21-78	82.4	2625	12435	-100	Flared		-21120	-4748		1
139	Facility Off	4-27-78	0	0	0				0	0		1
140	Facility On	4-27-78	0	0	0				0	0		
141	Idle	4-27-78	57.8	1874	10870	-5.7	1.875	2906	-	-		
142 **	Approximately 80%	4-27-78	80.3	2597	11941	+3.3	1.875	2906	-	-		
143	Approximately 92%	4-27-78	92.8	2998	12050	+3.3	1.875	2906	-	-		
144	Idle	4-27-78	53.7	1736	10960	+3.3	1.875	2906	-	-		

*Gravel Surface

**Core Probe and One Far-Field Microphone at 110° on a 47.2 m (155 ft) arc.

● Wall Kulite Locations

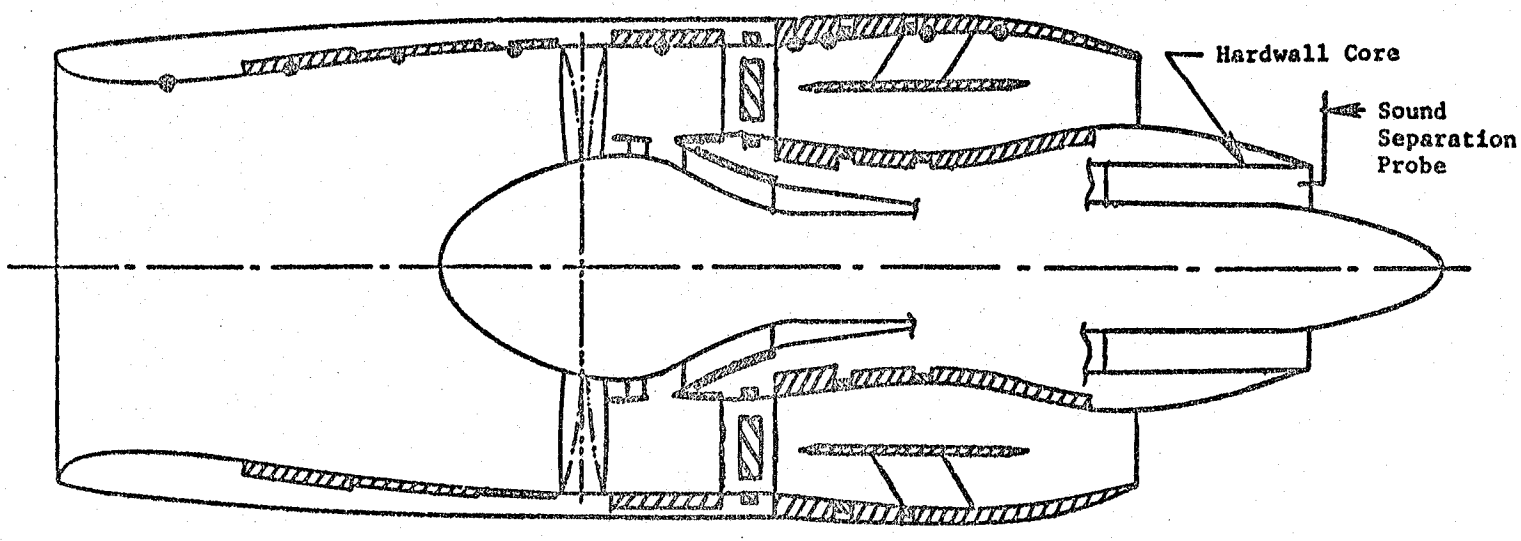

Figure 8. Configuration for Core Suppressor Evaluation.

Table VI. Fully Suppressed/Hard-Core Acoustic Data Points.

Acoustic Readings	Comments*	Date	PCNLR	XNL	XNH	ROPDEG	A18 m^2	A18 $in.^2$	FNRIN N	FNRIN lb	XM11	Probe Immersions
226	Idle	7-19-78	50.4	1657	11002	-0.4	1.877	2910	18852	4238	0.313	
227		7-19-78	79.9	2625	12257	-0.1	1.879	2913	46422	10436	0.552	
228		7-19-78	85.1	2796	12416	-0.1	1.879	2912	50510	11355	0.587	
229		7-19-78	89.9	2954	12580	-0.1	1.879	2912	55211	12412	0.628	
230	Accel/Decel	7-19-78	-	-	-	-0.1	1.879	2912	-	-	-	
231		7-19-78	79.7	2621	12228	0.1	1.750	2712	44656	10039	0.527	
232		7-19-78	79.7	2623	12264	-0.3	1.628	2523	45599	10251	0.515	
233		7-19-78	88.8	2918	12593	-0.1	1.660	2573	55856	12557	0.603	
234	Inlet Probe	7-19-78	89.8	2918	12593	0	1.660	2573	55856	12557	0.603	6
235		7-19-78	91.8	3018	12367	3.2	1.878	2911	47663	10715	0.563	
236		7-19-78	94.0	3093	12546	1.8	1.693	2625	53726	12078	0.592	
237		7-19-78	94.1	3093	12608	0.2	1.879	2913	54807	12321	0.625	
238		7-19-7b	88.9	2922	12488	0.0	1.660	2574	53263	11974	0.581	
239		7-19-78	94.3	3089	12948	-3.3	1.537	2383	69116	15538	0.682	
240		7-19-78	94.1	3088	13145	-5.1	1.538	2384	73133	16441	0.735	
241	Inlet Probe	7-19-78	94.1	3088	13145	-5.1	1.538	2384	73133	16441	0.735	6
242		7-19-78	92.6	3035	13035	-5.2	1.537	2383	70656	15884	0.700	
243		7-19-78	90.0	2950	12897	-5.1	1.537	2383	67008	15064	0.666	
244		7-19-78	85.2	2796	12703	-5.0	1.537	2383	61332	13788	0.619	
245		7-19-78	79.9	2625	12521	-5.1	1.538	2384	54184	12181	0.559	
246	Accel/Decel	7-19-78	-	-	-	-5.1	1.538	2384	-	-	-	
247		7-19-78	94.1	3089	13399	-8.0	1.539	2385	77110	17335	0.775	
248	Array 50°	7-19-78	92.1	3056	13288	-5.3	1.537	2383	73996	16635	0.737	
249	Array 60°	7-19-78	92.1	3055	13275	-5.3	1.537	2382	72613	16324	0.721	
250	Array 80°	7-19-78	92.1	3055	13275	-5.3	1.537	2382	72613	16324	0.721	
251	Array 100°	7-19-78	92.1	3055	13275	-5.3	1.537	2382	72613	16324	0.721	
252	Array 110°	7-19-78	92.1	3055	13275	-5.3	1.537	2382	72613	16324	0.721	
253	Array 120°	7-19-78	92.1	3055	13275	-5.3	1.537	2382	72613	16324	0.721	
254	Array 120°	7-19-78	89.4	2965	12661	0.0	1.537	2550	72613	16324	0.721	
255	Array 110°	7-19-78	89.4	2965	12661	0.0	1.537	2550	72613	16324	0.721	
256	Array 100°	7-19-78	89.4	2965	12661	0.0	1.537	2550	72613	16324	0.721	
257	Array 80°	7-19-78	89.4	2965	12661	0.0	1.537	2550	72613	16324	0.721	
258	Array 60°	7-19-78	89.4	2965	12661	0.0	1.537	2550	72613	16324	0.721	
259	Array 50°	7-19-78	89.4	2965	12661	0.0	1.537	2550	72613	16324	0.721	
260	Core Probe	7-19-78	89.4	2965	12661	0.0	1.537	2550	72613	16324	0.721	2
261	OGV Probe	7-19-78	89.4	2965	12616	0.0	1.537	2550	72613	16324	0.721	6
262	Fan Nozzle Probe	7-19-78	89.4	2964	12620	0.0	1.537	2550	72613	16324	0.721	6
263	Core Probe	7-19-78	89.9	2987	12634	0.1	1.879	2912	52894	11891	0.616	2
264	Core Probe	7-19-78	85.0	2827	12418	0.1	1.880	2914	47467	10671	0.566	2

*Concrete Surface

Table VI. Fully Suppressed/Hard-Core Acoustic Data Points. (Concluded)

Acoustic Readings	Comments*	Date	PCNLR	XNL	XNH	ROPDEG	A18		FNRIN		XM11	Probe Immersions
							m^2	$in.^2$	N	lb		
265	Core Probe	7-19-78	80.0	2657	12268	0.1	1.879	2913	43032	9674	0.522	4
266	Core Probe	7-19-78	54.1	1799	11347	-0.2	1.877	2910	21654	4868	0.343	2
267	Core Probe Accel/Decel	7-19-78	-	-	-	-0.2	1.877	2910	-	-	-	
268	Core Probe	7-19-78	79.9	2656	12352	-0.3	1.757	2724	46150	10375	0.534	2
269	Core Probe	7-19-78	79.9	2656	12357	0.1	1.628	2524	46168	10379	0.521	4
270	Core Probe	7-19-78	93.1	3094	13189	-4.8	1.537	2382	71541	16083	0.713	4
271	OGV Probe	7-20-78	93.1	3094	13189	-4.8	1.537	2382	71541	16083	0.713	6
272	Fan Nozzle Probe	7-20-78	93.2	3093	13212	-4.8	1.537	2382	71541	16083	0.711	6
273	Undercowl Cooling	7-20-78	0	0	0	-	-	-	0	0	0	
274	Background Noise	7-20-78	0	0	0	-	-	-	0	0	0	

*Concrete Surface

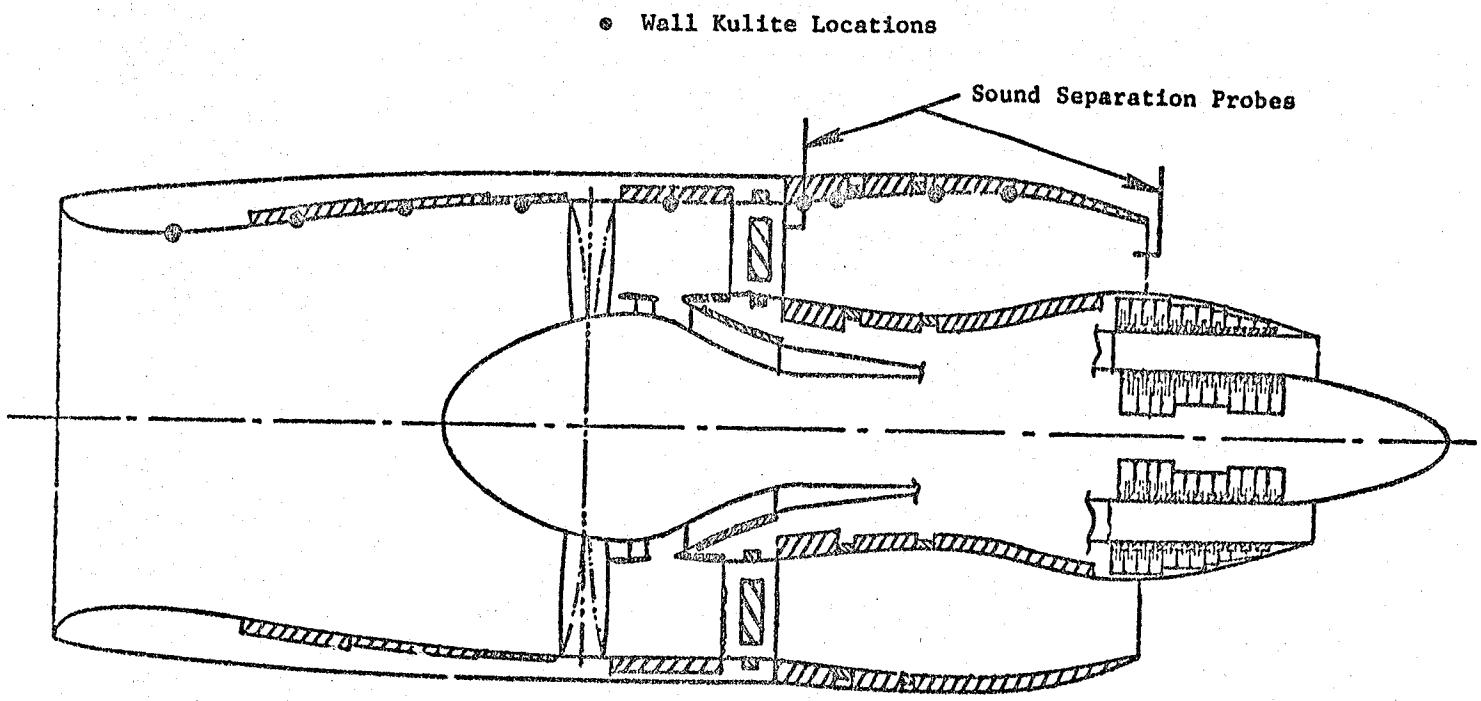

Figure 9. Splitter Effect Configuration.

Table VII. Fully Suppressed/No Splitter Acoustic Data Points.

Acoustic Readings	Comments*	Date	PCNLR	XNL	XNH	ROPDEG	A18 m^2	A18 $in.^2$	W11R	FNRIN N	FNRIN lb	XM11	Probe Immersions
274	Background Noise	7-20-78	0	0	0	-	-	-	-	-	-	-	
275		7-20-78	53.9	1792	11344	0.0	1.875	2907	514	21970	4939	0.346	
276		7-21-78	79.7	2650	12340	0.2	1.877	2910	724	44424	9987	0.536	
277		7-21-78	83.1	2830	12536	0.1	1.877	2910	764	49526	11134	0.583	
278		7-21-78	90.1	2996	12710	0.0	1.877	2909	798	54415	12233	0.627	
279		7-21-78	80.0	2671	12355	0.0	1.742	2700	-	-	-	-	
280		7-21-78	80.0	2671	12386	0.0	1.626	2521	702	45719	10278	0.512	
281		7-21-78	89.2	2954	12725	0.1	1.650	2557	779	55420	12459	0.602	
282		7-21-78	91.9	3060	12456	3.3	1.871	2900					
283		7-21-78	79.8	2652	12675	-5.1	1.535	2379	753	54784	12316	0.510	
284		7-21-78	84.9	2818	12917	-5.1	1.535	2379	798	61764	13885	0.627	
285		7-21-78	90.4	2996	13164	-5.1	1.535	2379	843	69713	15672	0.701	
286		7-21-78	92.7	3074	13298	-5.1	1.535	2380	860	72880	16384	0.729	
287		7-21-78	93.4	3097	13320	-5.0	1.535	2380	858	73071	16427	0.726	
288	OGV Probe	7-21-78	93.2	3094	13332	-5.1	1.535	2380	868	73102	16434	0.746	15
289	Decel/Accel	7-21-78	-	-	-	-5.1	1.535	2380	-	-	-	-	
290		7-21-78	93.0	3100	13358	-5.0	1.535	2380	-	-	-	-	
291		7-21-78	92.3	3063	13470	-7.9	1.535	2380	878	74534	16756	0.768	
292	Core Probe Idle	7-21-78	48.3	1603	10971	0	1.871	2900	-	-	-	-	2
293	Core Probe	7-21-78	80.1	2657	12300	0.3	1.871	2900	-	-	-	-	4
294	Core Probe	7-21-78	85.0	2819	12490	0.1	1.871	2900	-	-	-	-	2
295	Core Probe	7-21-78	90.0	2985	12651	0	1.871	2900	-	-	-	-	2
296	Fan Nozzle Probe	7-21-78	93.3	3093	13184	-5.0	1.535	2380	-	-	-	-	15
297	OGV Probe	7-21-78	89.0	2944	12570	0.0	1.659	2572	764	52649	11836	0.582	15
298	Fan Nozzle Probe	7-21-78	89.0	2944	12570	0.0	1.659	2572	-	-	-	-	6

*Concrete Surface

4.0 ACOUSTIC INSTRUMENTATION

4.1 DATA ACQUISITION

Acoustic data were acquired on this engine using a variety of acoustic instrumentation including far-field microphones, a directional acoustic array, in-duct wall-mounted Kulites, and in-duct sound separation probes.

4.1.1 Far-Field Instrumentation

The far-field data acquisition system is presented schematically in Figure 10. Initial testing (through acoustic Reading 144) was conducted over a gravel surface. This surface consisted of a leveled semicircle of approximately 76 m (250 ft) radius with a crushed rock surface composed of rock sizes of approximately 2.5 to 5 cm (1 to 3 in.) diameter. Far-field microphones were located at acoustic angles of 10° through 160° in 10° increments on a 45.7 m (150 ft) arc centered near the fan rotor plane. Standard microphone height over the gravel surface was 12.2 m (40 ft). This height was selected in the early 1970's to simulate ground reflection patterns for the flight case, experienced with a 1.22 m (4 ft) microphone height. To aid in establishing the free-field corrections over the gravel surface, four microphones were located 1.22 m (4 ft) off the ground at acoustic angles of 60, 100, 110, and 120° during portions of the testing. A photograph of the gravel sound field and 12.2 m (40 ft) towers is shown in Figure 11.

Subsequent testing was conducted after the acoustic arena had been paved with concrete. Microphones were located at engine centerline height 3.96 m (13 ft) above the concrete and 1.27 cm (0.5 in.) above the concrete at acoustic angles of 20 to 160° in 10° increments. Figure 12 shows the concrete sound field used for the QCSEE test program. Microphone stands were located on a 46.5 m (152.4 ft) arc, centered on the fan rotor plane. A photograph of the microphone system and support stands for the concrete field is shown in Figure 13.

Other far-field acoustic instrumentation included a Directional Acoustic Array, as shown in Figure 14. Details of the directional characteristics of the Array can be found in Reference 5. The Array was positioned on a 30 m (100 ft) arc at acoustic angles of 50, 60, 80, 100, 110, and 120°. While at each angle, it was aimed at seven different positions on the engine including the inlet, fan bypass exhaust nozzle, and core nozzle. Postrun analysis then determined the relative contribution from each aiming point on the engine at each of the six far-field acoustic angles.

A schematic of the far-field acoustic data acquisition system used is shown on Figure 15. The system is used for obtaining data from 50 Hz through the 20 kHz 1/3-octave center frequency band. Microphone types utilized for far-field data acquisition are the Bruel and Kjaer (B&K) 4133 and 4134 1.27 cm (0.5 in.) condenser microphones. The 4134 microphones, oriented for 90° incidence, were utilized for ground plane measurements and 4133 microphones, orien-

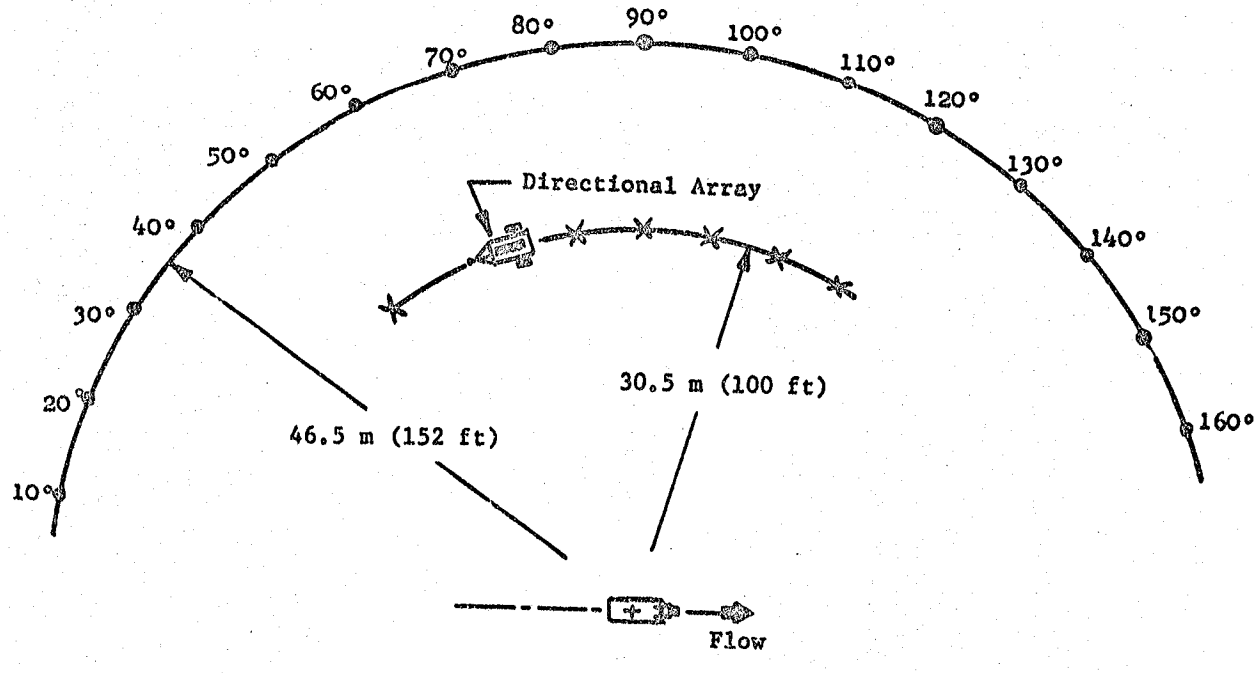

Figure 10. Sound Field Acoustic Instrumentation.

ORIGINAL PAGE IS
OF POOR QUALITY

Figure 11. General Electric Company Acoustic Test Facility (Gravel).

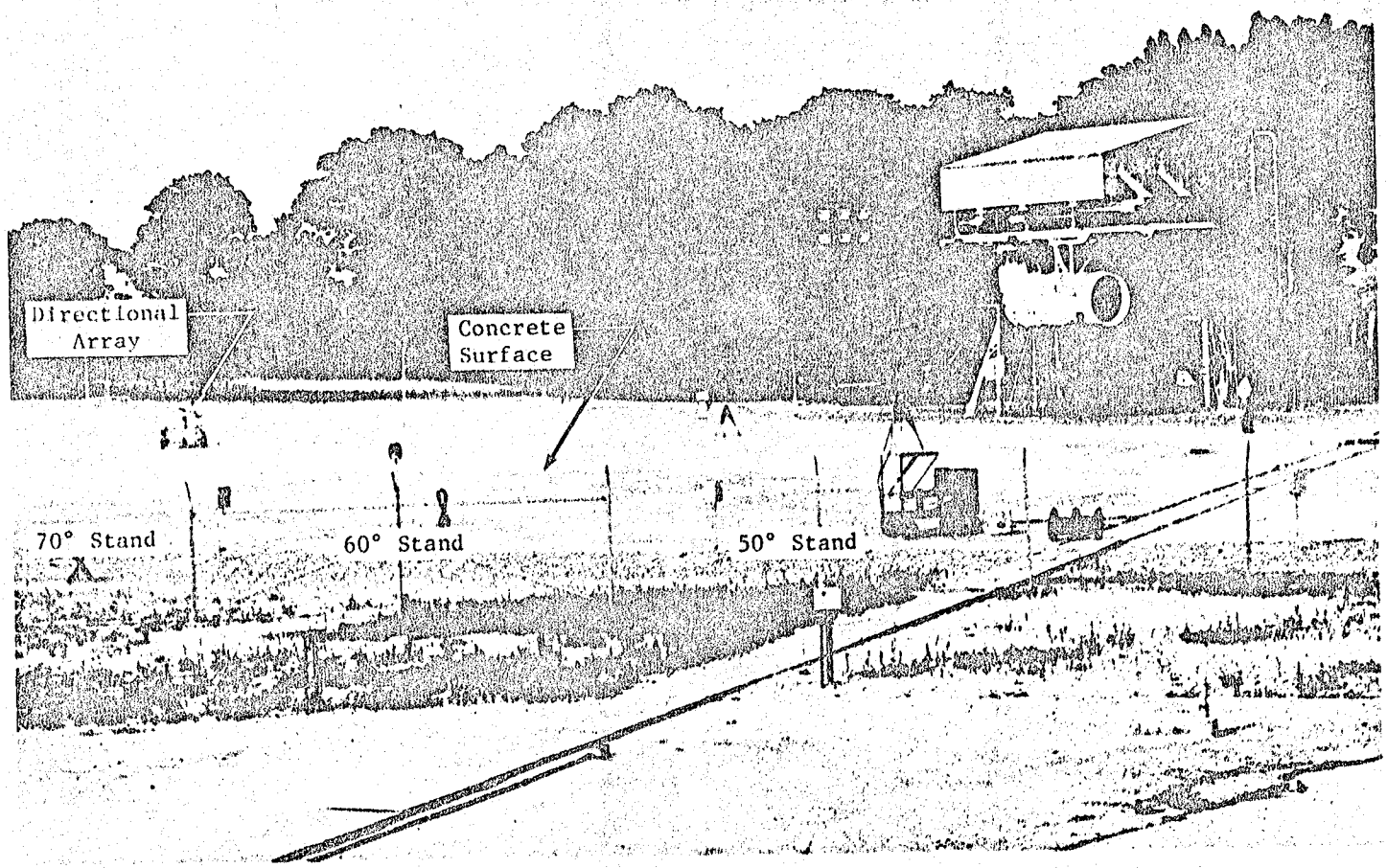

Figure 12. General Electric Company Acoustic Test Facility (Concrete).

ORIGINAL PAGE IS
OF POOR QUALITY

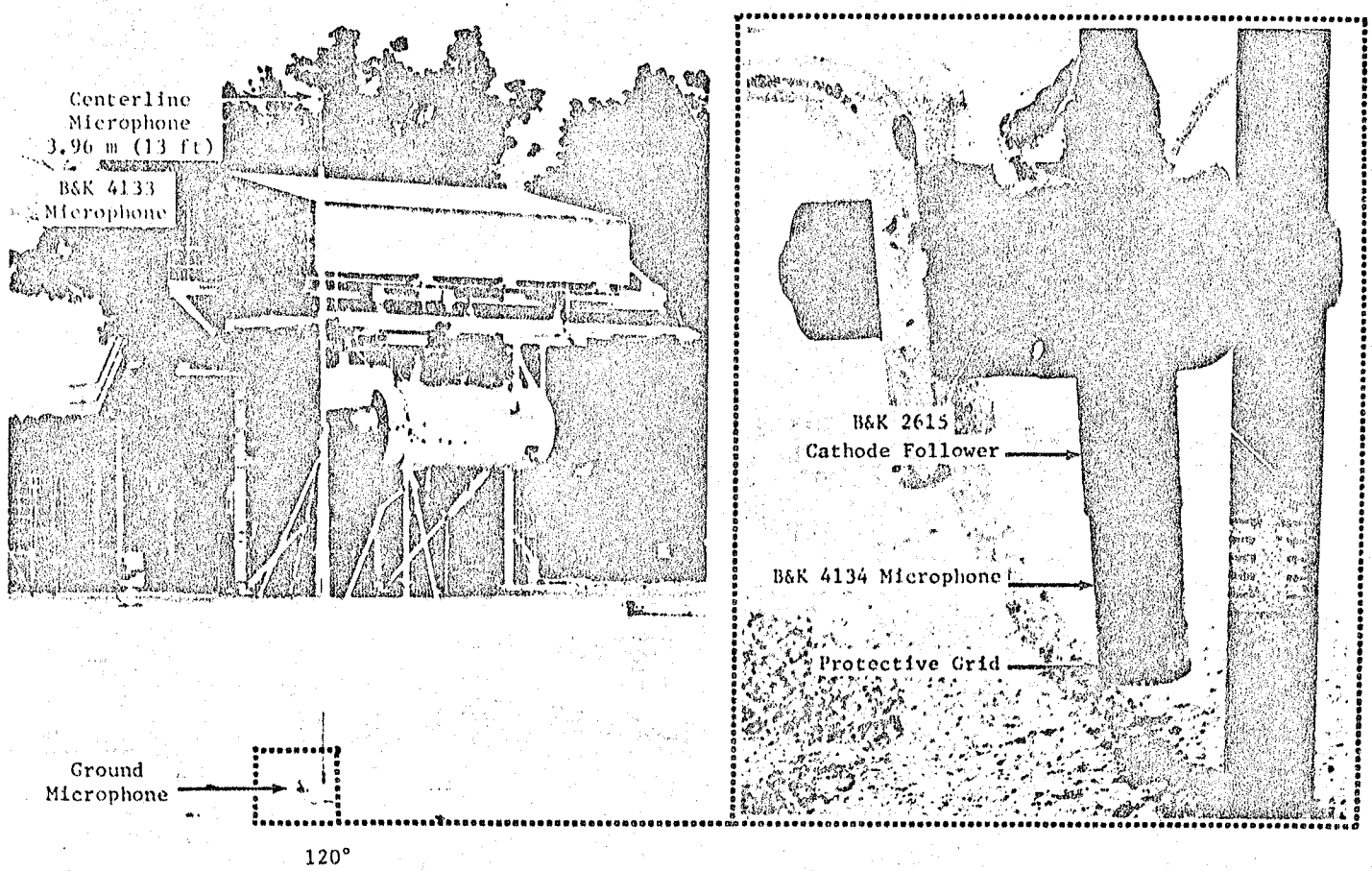

Figure 13. Centerline and Ground Microphone System.

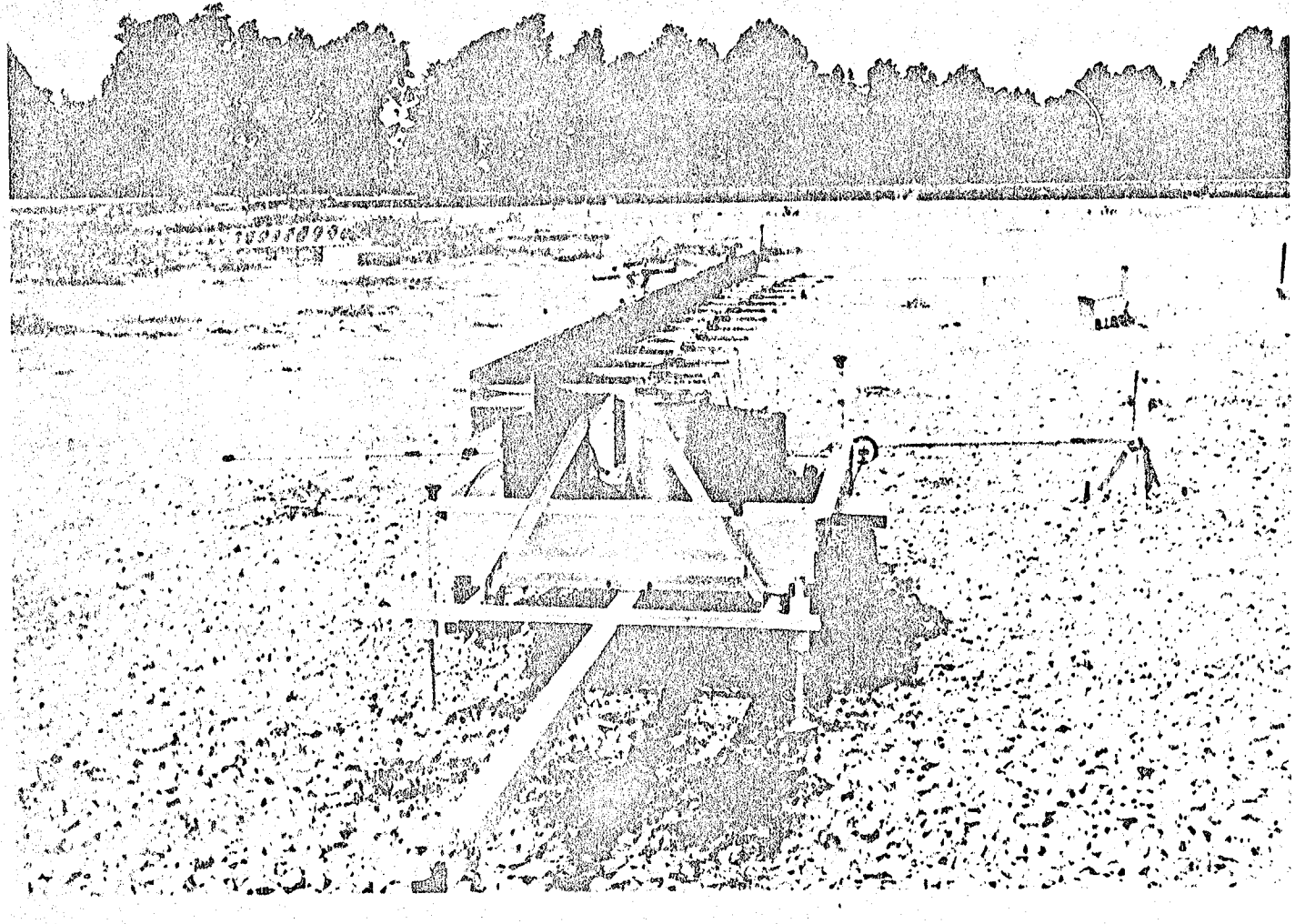

Figure 14. Directional Broadside Acoustic Array.

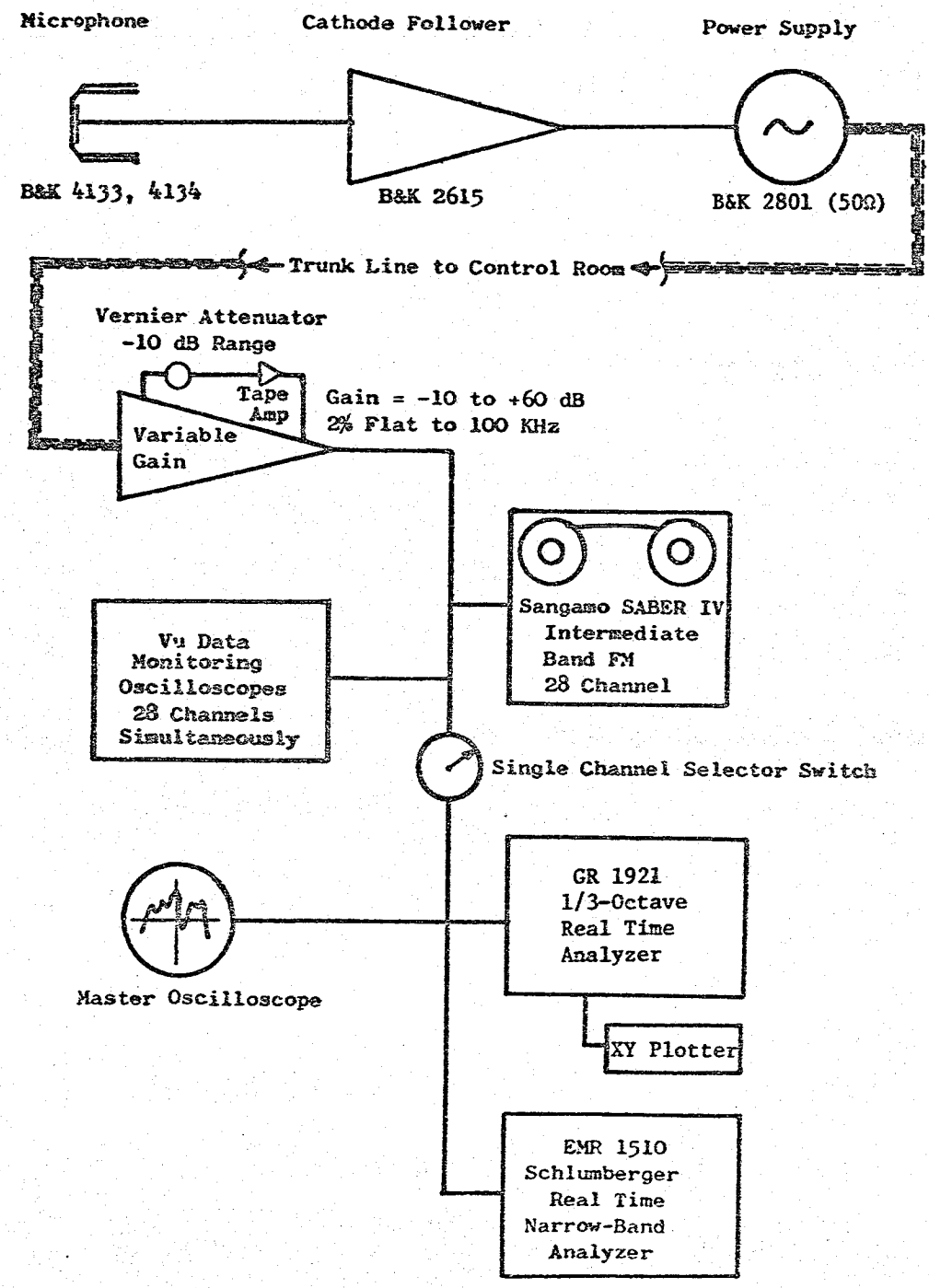

Figure 15. Acoustic Microphone Data Acquisition System.

ted for 0° incidence, were utilized for centerline height measurements. All microphone systems utilized the B&K 2615 cathode follower and B&K 2801 power supply with the 50Ω output option to provide a flat reaponse through the 20 kHz region of interest.

All data were recorded using two Sangamo Sabre IV FM tape systems operated in IRIG intermediate band mode at a tape speed of 76 cm per second (30 ips). The overall frequency response of the acquisition and reduction system was determined for each channel by recording a pink noise signal through the cathode follower with playback and processing through the data reduction system. These corrections were then included in the data processing to account for flatness deviations in system response.

During testing, on-line quick-look 1/3-octave data were obtained using a General Radio 1921 spectrum analyzer and plots obtained with an X-Y plotter. Normalization of the tape amplifiers and a selector switch permitted obtaining absolute level spectra (without system corrections) of any of the far field microphones.

4.1.2 In-Duct Kulites

Internal acoustic instrumentation for these tests consisted of Kulites flush-mounted on the flowpath walls and probe-mounted Kulites which could be immersed into the flow. All in-duct instrumentation is tabulated in Table VIII. A schematic of the Kulite data acquisition system is given in Figure 16.

The probes used in the fan duct had either two or three flush-mounted Kulite sensors on them. A three-element probe is shown in the insert in Figure 16. The probe used in the core nozzle had two elements and was water-cooled to permit immersion in the hot exhaust. These multiple-element probes, as reported previously in Reference 6, are known as sound separation probes and permit discrimination between broad band sound and turbulence in duct probe measurements. All probes were traversible radially to provide data across the duct.

4.2 DATA REDUCTION

Off-line reduction of the recorded data was performed using an automated 1/3-octave reduction system, shown schematically on Figure 17. The recorded data were played back on a CEC 3700B, 28-track system, with electronics capable of reproducing IRIG wide band Groups I and II and intermediate band data. All 1/3-octave analyses were performed using a General Radio 1921 1/3-octave analyzer. A normal integration time of 32 seconds was used to provide adequate sampling of the low frequency portion of the data signal. The data frequency range for the QCSEE UTW test series was 50 Hz through 20 kHz. Each data channel is passed through an interface to a GEPAC 30 computer, where data are corrected for frequency response of the acquisition and reduction system and for microphone head response. A "quick-look" display of results is provided by means of a Terminet 300 console with data transferred and stored

Table VIII. In-Duct Acoustic Instrumentation.

Item	Engine Station	Angle*
Inlet Throat Probe (3-element SSP)	115.0	120
Inlet Wall Kulite	106.6	270
Inlet Wall Kulite	122.8	270
Inlet Wall Kulite	136.4	270
Inlet Wall Kulite	157.0	280
Fan Face Probe (2-element SSP)	154.8	180
Fan Frame Wall Kulite	188.5	110
OGV Exit Probe (3-element SSP)	204.5	282
Fan Exhaust Wall Kulite	204.1	112
Fan Exhaust Wall Kulite	213.0	110
Fan Exhaust Wall Kulite	230.0	110
Fan Exhaust Wall Kulite	242.0	110
Fan Nozzle Probe (3-element SSP)	267.4	90
Core Nozzle Probe (2-element water-cooled SSP)	289.7	270

*aft looking forward

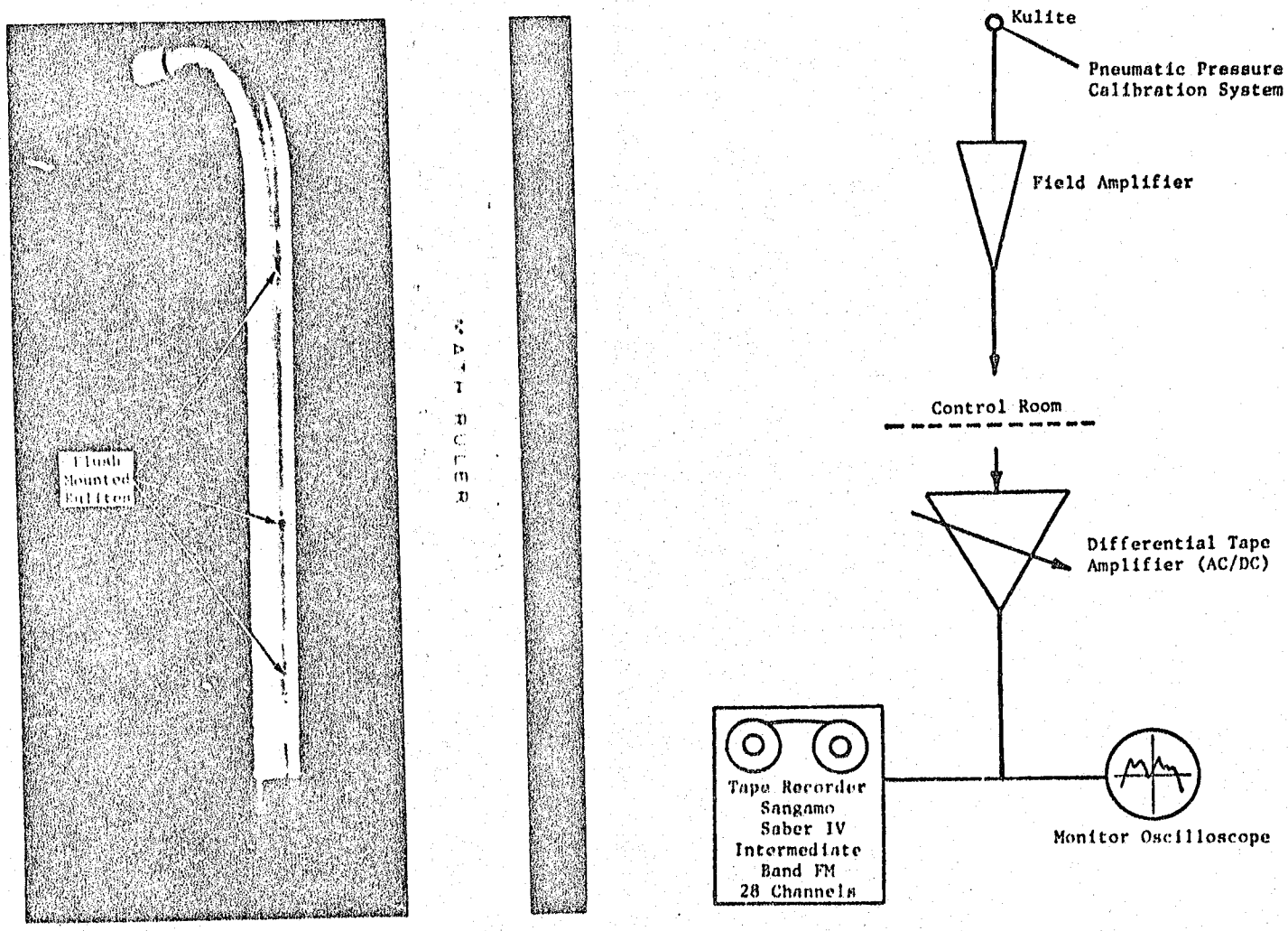

Figure 16. Kulite Data Acquisition System.

- Time Code Comparator Starts Integration on G.R. Analyzer
- Tape Automatically Shuttles to Restart on Each Recording Channel

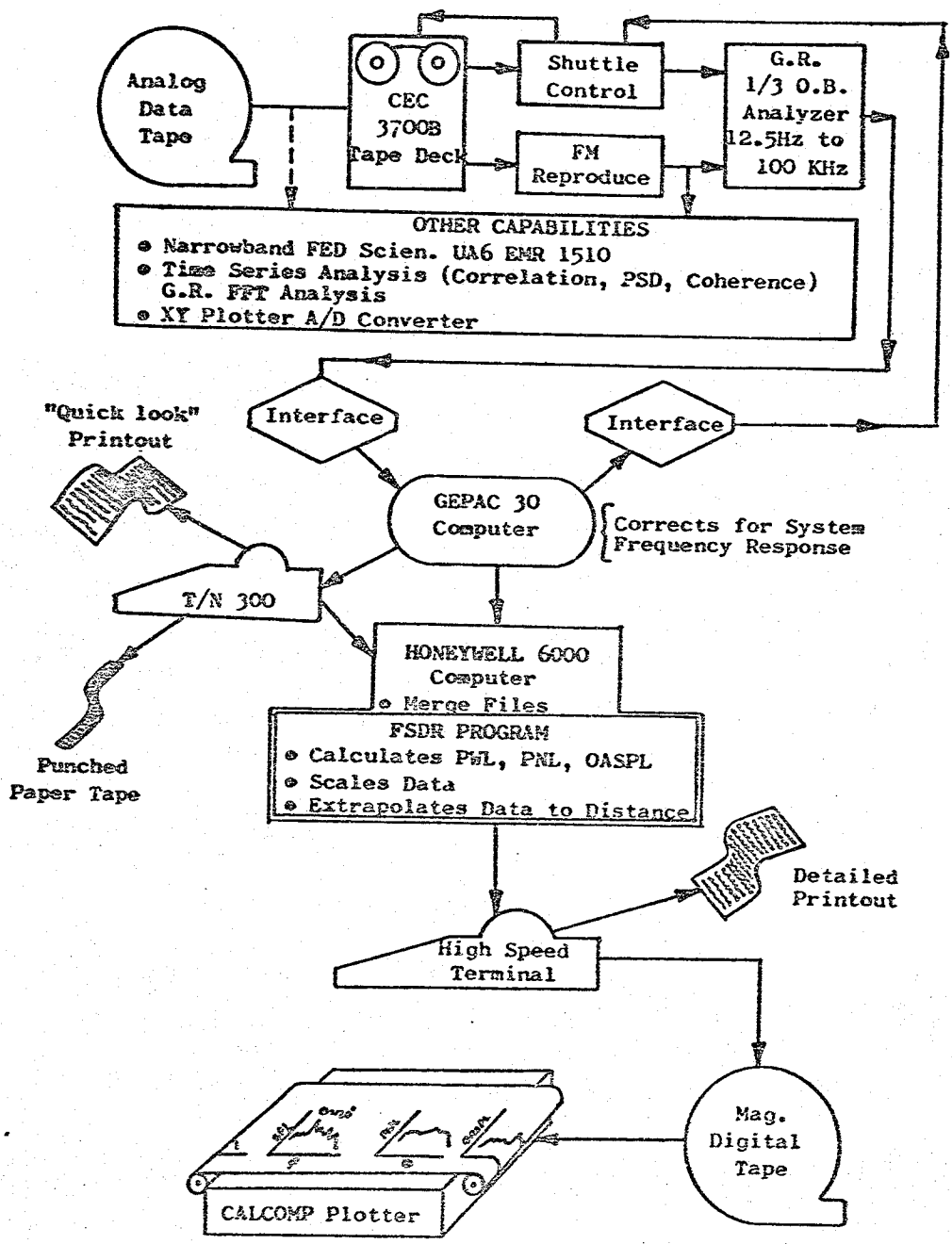

Figure 17. General Electric Company Acoustic Data Reduction System.

in the Honeywell 6000 system by a direct timesharing link. Processing in the 6000 system is performed with the Full-Scale Data Reduction (FSDR) program, where calculations are performed correcting data for atmospheric attenuation in accordance with Reference 7 with all data output corrected to 298 K (77° F), 70% relative humidity, acoustic standard day. Additional calculations, including data scaling, extrapolations, perceived noise level (PNL), overall sound pressure level (OASPL), and sound power level (PWL) also are performed. As an option, the output of FSDR is written to digital magnetic tape for subsequent data plotting with Calcomp plotter routines.

Other data reduction techniques were also used. Constant bandwidth narrow band spectra were reduced on the Federal Scientific UA6. Complex time series analysis such as cross correlation, coherence functions, and probability density were processed through the General Radio/Time Data System, a computer based system incorporating analysis techniques in both the time and frequency domains.

5.0 FORWARD THRUST ACOUSTIC RESULTS

The bulk of the testing on the UTW composite nacelle was devoted to measuring and evaluating forward thrust noise levels. Approximately 275 acoustic data points were taken on four configurations. Reporting on these data will be accomplished by investigating the inlet-radiated and exhaust-radiated noise and then evaluating the engine system noise levels and how these levels compare to the noise goals of the QCSEE program.

5.1 INLET-RADIATED NOISE

Analysis of the inlet-radiated noise is divided into two main categories - basic source noise levels and the suppression achieved with the hybrid inlet.

5.1.1 Baseline Noise Levels

The inlet for the baseline configuration was a hardwall cylindrical bellmouth as shown in Figures 2 and 3, and the fan exhaust duct walls were rendered hardwall with metallic tape over the treatment. There was frame treatment between the rotor and the OGV's plus treatment on the pressure side of the vanes.

As part of the engine design procedure, detailed estimates of the far-field noise were made at select angles. These estimates utilized model data where available and empirical correlations from General Electric experience on other engines. Figure 18 compares predicted constituents, their total, and measured spectra at 60° on a 46.5 m (152.4 ft) arc at takeoff thrust. Several different combinations of speed, blade angle, and fan bypass nozzle area give representative measured results. In the low frequencies below 250 Hz, there is good agreement; however, at higher frequencies, the measured levels are consistently higher than predicted. Measured PNL's are 3.4 to 4.5 PNdB higher than predicted. Higher-than-predicted noise levels are evident in the 1/3-octave bands which contain the fan BPF (1000 Hz), its second harmonic (2000 Hz), and the fan third harmonic (2500 Hz). In an effort to understand whether higher-than-predicted tones or fan broadband noise caused the PNL to be higher than predicted, a study was made by arbitrarily reducing the BPF and its harmonics by 5 dB in various combinations. The study indicated that a 5 dB reduction on the BPF reduced the PNL by 0.5 PNdB. Individual reductions of 5 dB on the band containing the second or third harmonic lowered the PNL by only 0.2 PNdB. Reducing all three bands by 5 dB lowered the PNL by 1.2 PNdB. It appears that while higher-than-predicted fan tones can contribute up to 1.2 PNdB of the 3.4 to 4.5 PNdB increase over predicted, the remaining increase must be due to fan broadband noise above 250 Hz.

At approach, measured levels are also higher than predicted over the entire frequency spectrum as shown in Figure 19, and range from 1.1 to 2.7 PNdB higher. Note the variations in fan speeds, blade angles, and fan bypass nozzle area that could be used to give approach thrust.

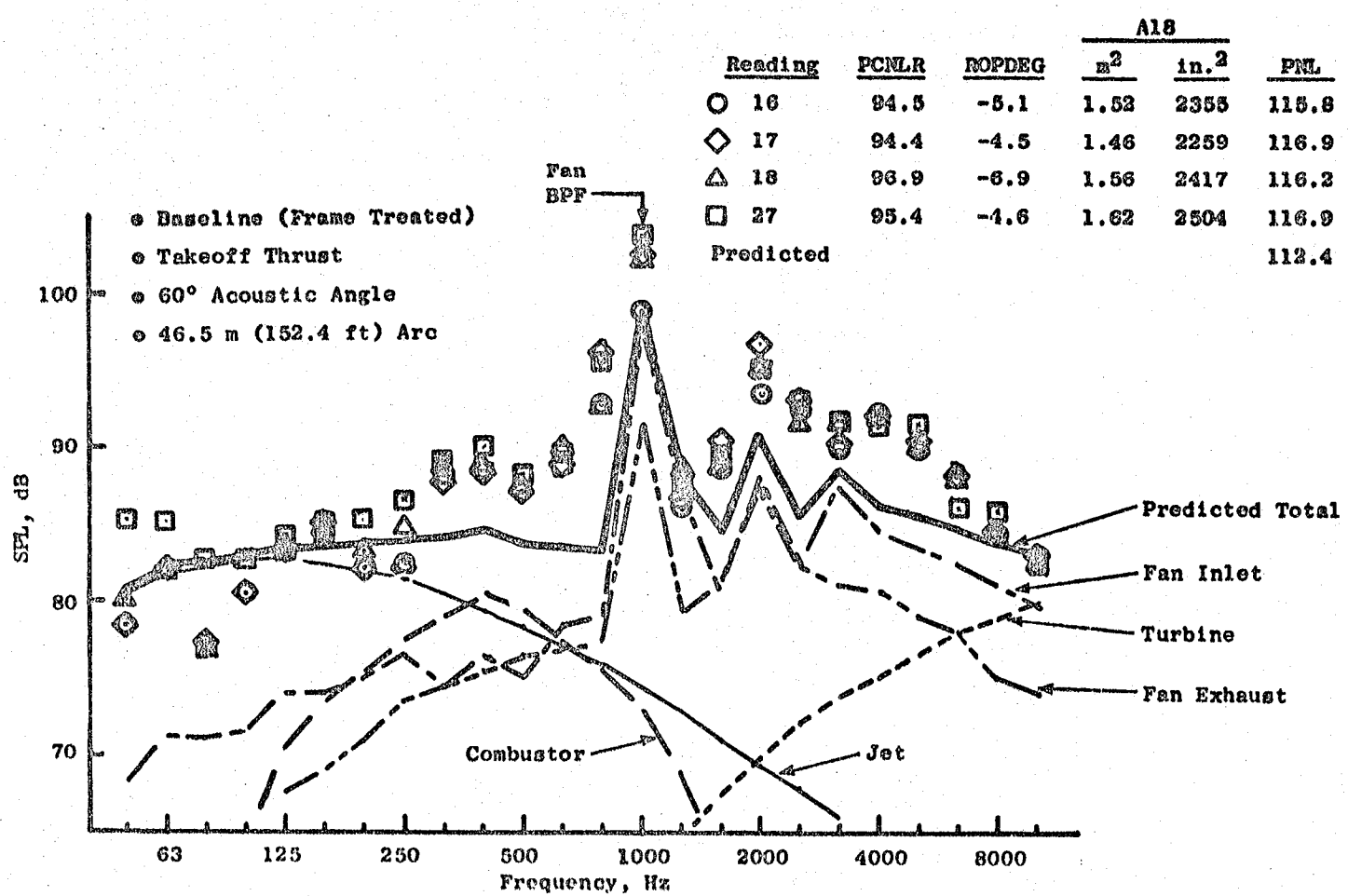

Figure 18. Measured and Predicted 60° Baseline Spectra at Takeoff.

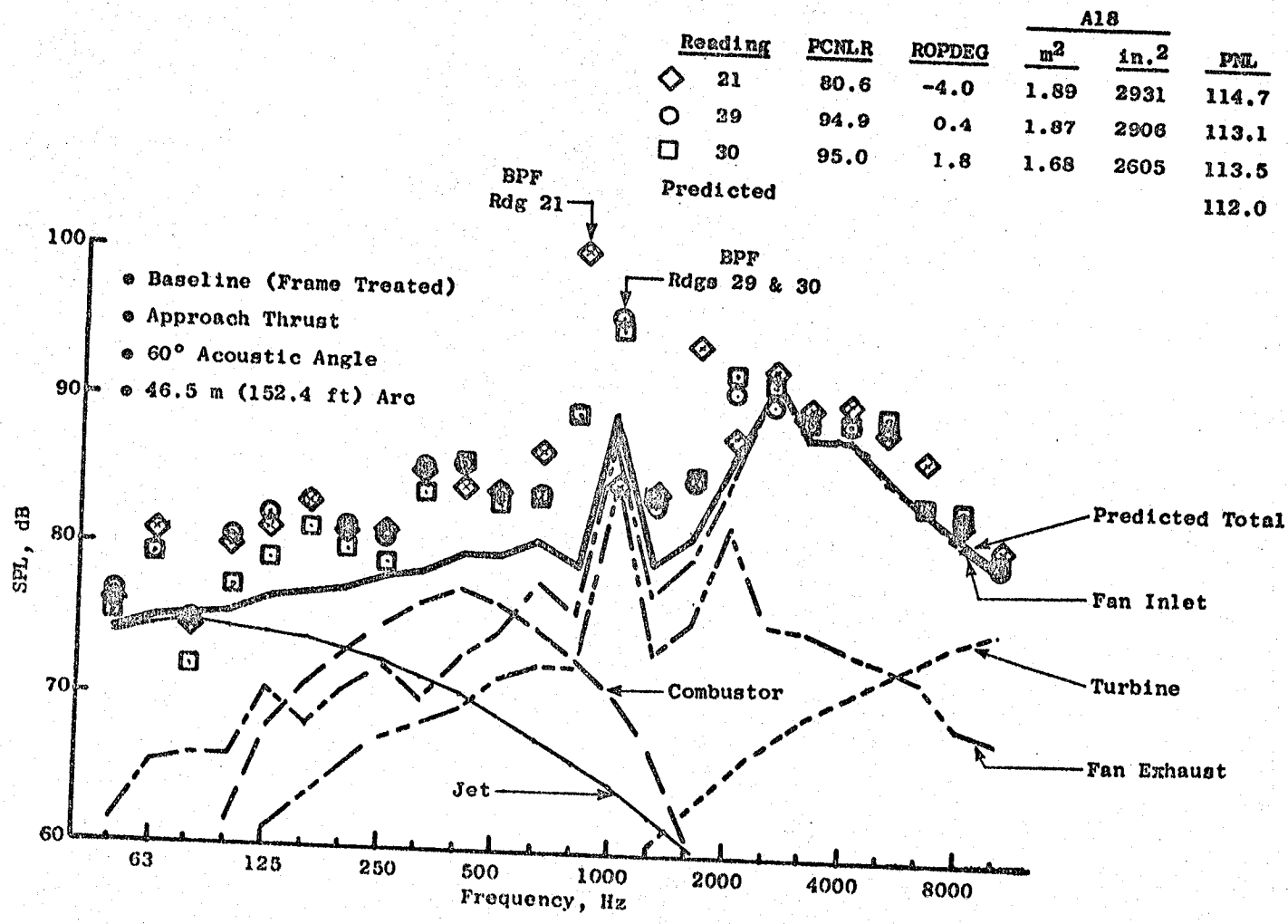

Figure 19. Measured and Predicted 60° Baseline Spectra at Approach.

A study similar to that performed at takeoff was completed for approach conditions. Five dB reductions on the BPF, second, and third harmonic individually reduced the PNL by 0.2, 0.2, and 0.3 PNdB respectively. A 5 dB reduction simultaneously on all three bands reduced the PNL by 0.7 PNdB. This indicates that higher-than-predicted tone levels do contribute to the PNL increase observed; however, there must also be a contribution from broadband noise.

Narrowband spectra for takeoff and approach are shown in Figure 20. These spectra indicate that 1/3-octave bands above 3150 Hz are controlled by broadband noise even though fan tones are present in the narrow bands. For example, examine the tone at 3720 Hz in the approach spectra. This tone would fall in the 4000 Hz 1/3-octave band. The tone level is 82 dB and the broadband level from 3560 to 4450 Hz averages 73 dB. Converting the broadband noise to 1/3-octave band level [10 Log(4450-3560)/20] adds 16.5 dB to the broadband level raising it to 89.5 dB which is 7 dB higher than the tone. Thus, the fan tones above 3150 Hz do not contribute significantly to the 1/3-octave band level.

The reason for these higher-than-predicted baseline levels is not completely understood at this time. As will be shown later, exhaust radiated baseline noise at 120° is also higher than predicted. To determine whether the exhaust radiated noise could be controlling or contributing significantly at 60°, directional array data were analyzed. Only approach data were available for the baseline at 60° and these relative noise levels are shown in Figure 21 for 1000 to 4000 Hz. Noise coming from the inlet is clearly dominant except at 1250 Hz where the exhaust constituent is down only 3 dB.

As a further aid in understanding the inlet-radiated noise measured at the far field 60° microphone, a probability density analysis was performed on the fan BPF and fan second harmonic tones. Figure 22 indicates that these signals at takeoff and approach have a random-amplitude probability distribution. This implies that a random mechanism such as rotor-turbulence-generated noise may be the source of the inlet-radiated fan BPF and second harmonic tones on the baseline UTW engine. Such a result is not unexpected for a static outdoor engine test.

One of the potential advantages of a variable pitch fan was thought to be the capability of minimizing fan noise at constant thrust, as was demonstrated in Reference 8, by continuously optimizing blade incidence angle and loading over the fan speed range. Data at approach thrust are presented in Figure 23 for several fan bypass nozzle areas. PNL is nearly constant with blade angle, with a slight trend toward lower noise at the more closed blade angles. The BPF shows a lot of scatter which is not surprising with a rotor-turbulence-generated noise source, and there is a trend for lower BPF noise at more closed blade angles. The 5000 Hz sound pressure level (SPL) which is representative of high frequency broadband noise is also relatively flat with blade angle. These data from several fan nozzle areas indicate little or no effect of fan blade stagger angle on inlet-radiated noise.

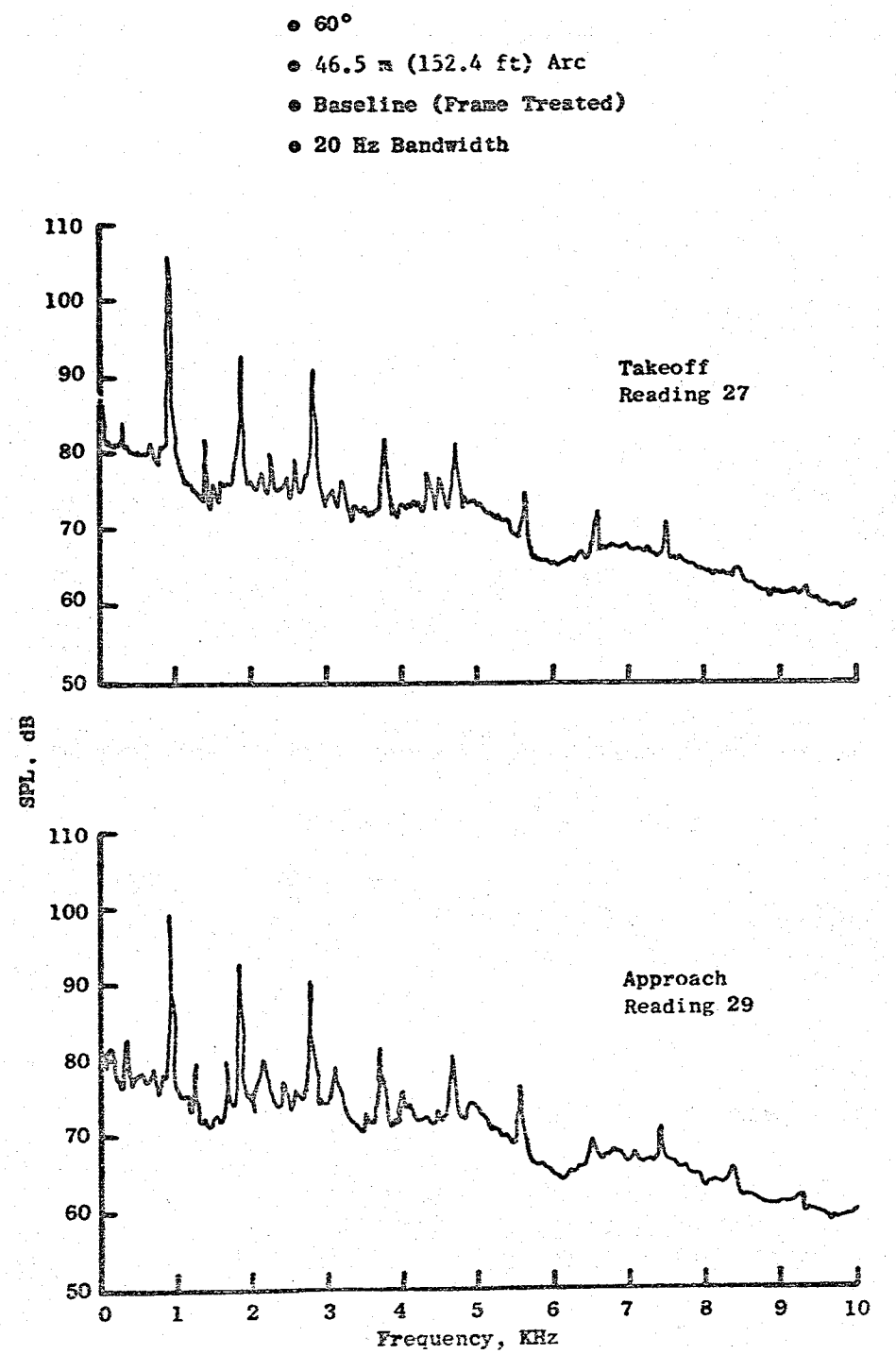

Figure 20. Narrow Band Baseline Spectra at 60°.

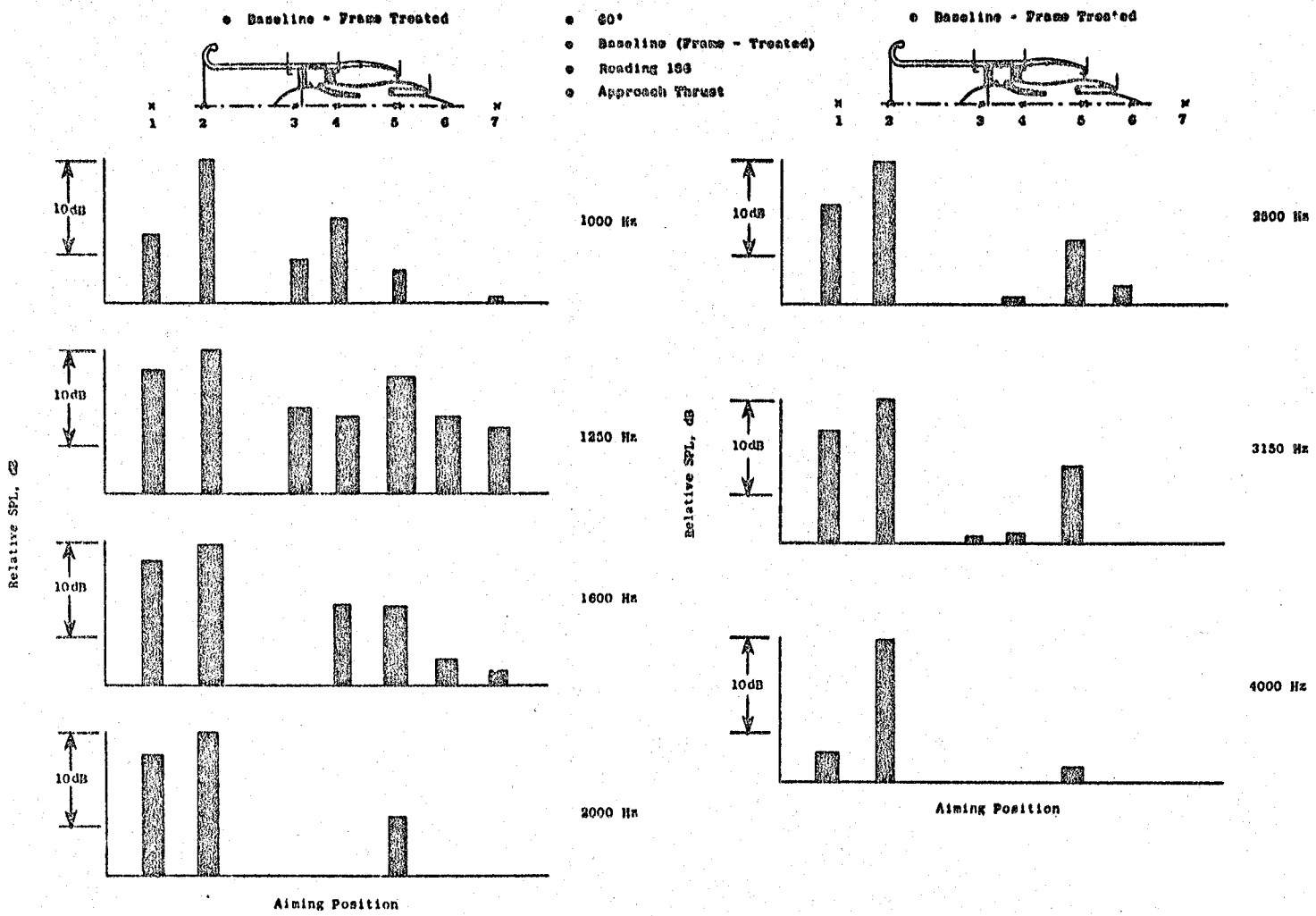

Figure 21. Baseline Directional Array Noise Levels at 60° for Approach.

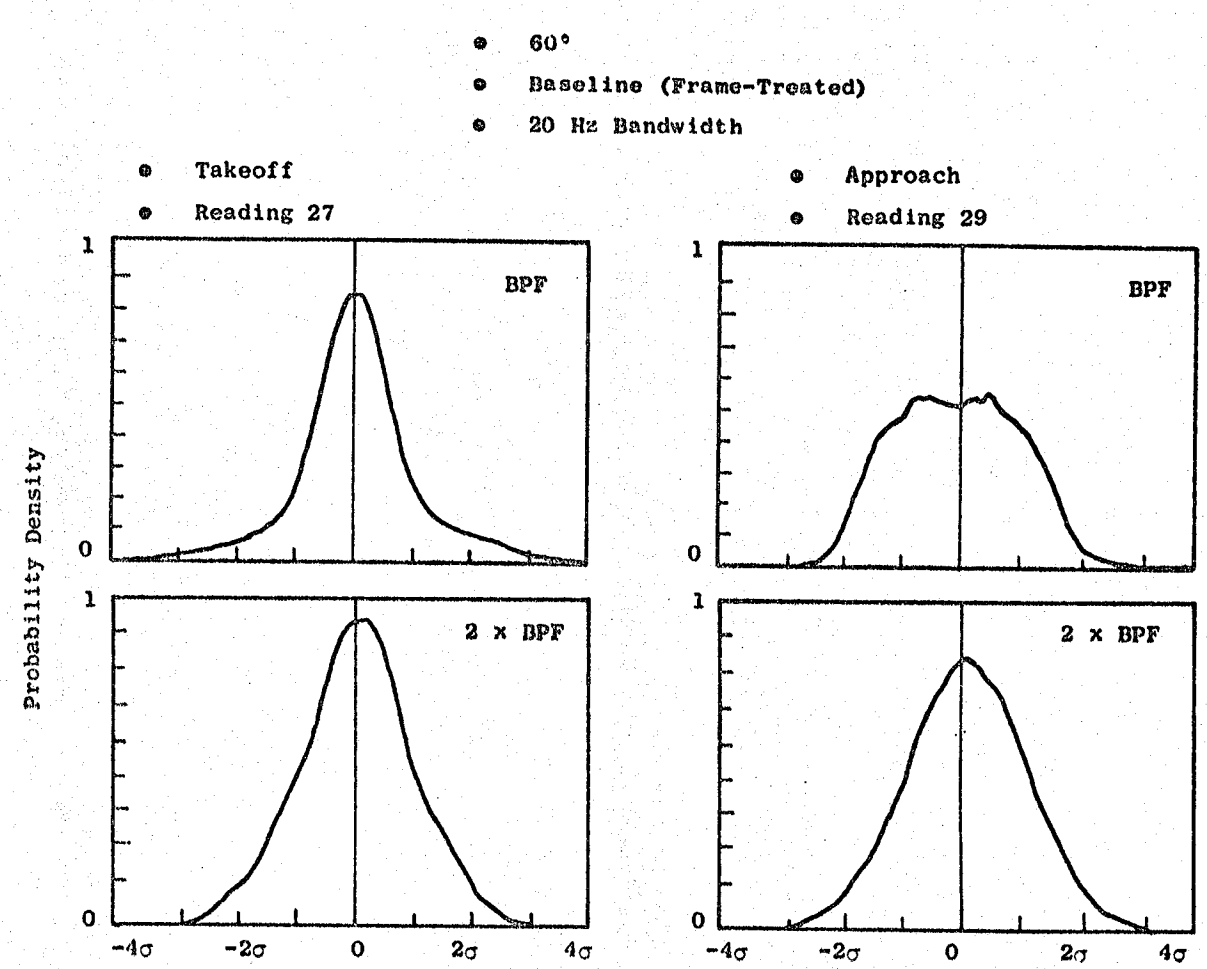

Figure 22. Baseline Inlet Radiated Source Noise Characteristics.

- 152 m (500 ft) Sideline
- 60°
- Free Field
- Baseline (Frame Treated)
- Approach Thrust

	A18	
	m^2	$in.^2$
○	1.87	2900
△	1.68	2600
□	1.52	2350

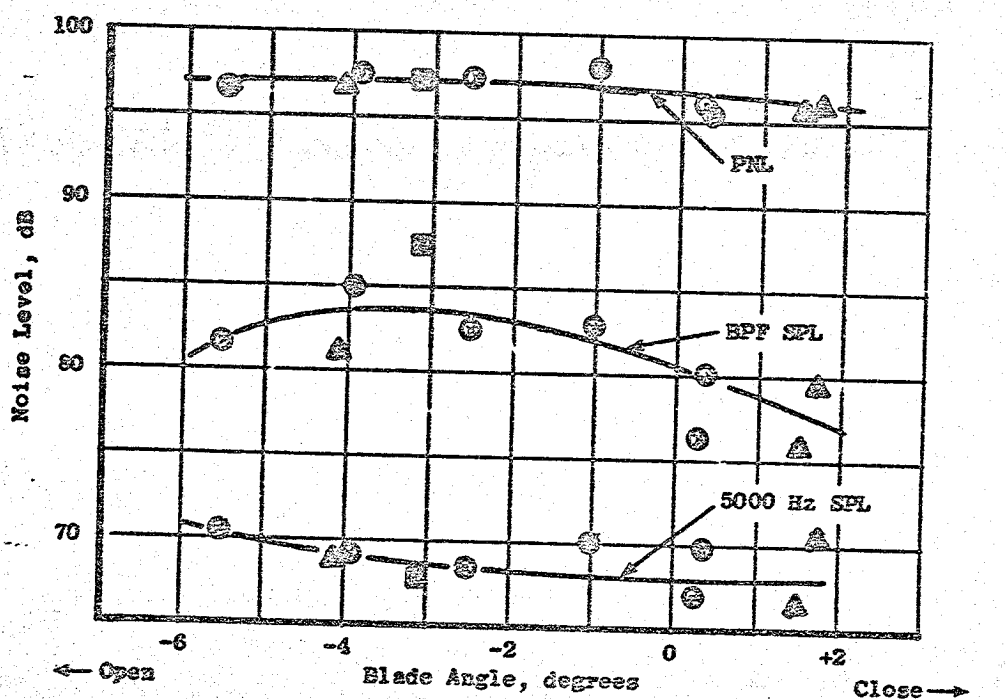

Figure 23. Approach Baseline Noise Variation with Blade Angle at 60°.

From an engine and acoustic system standpoint, the most desirable combination of blade angle, fan speed, and fan bypass nozzle area is high fan speed, open nozzle area, and closed down blade to achieve thrust. The high fan speed provides for quick response from approach to takeoff thrust in the event of a wave-off or missed approach. Large fan bypass nozzle area decreases the exhaust velocity and hence the jet/flap interaction noise. From the data in Figure 23, there is no apparent acoustic penalty for operating with high fan speed, open nozzle, and closed blade.

Figure 24 presents the variations in noise with thrust for several blade angles and for fan nozzle areas near takeoff setting. PNL and the 5000 Hz SPL show very little change with respect to blade angle. At the higher thrusts, it appears that the more open nozzle area data are slightly higher by 1 to 2 dB. The BPF SPL shows a lot of scatter but no significant trends with regard to blade angle or nozzle area.

The baseline data presented here for the QCSEE UTW variable pitch fan have indicated no optimum blade angle for minimum noise over the range of blade angles tested. Fan source mechanisms are many and varied for a static fan test. For example, one of the major noise sources is known statically to be the interaction of the rotor with inlet turbulence. This source appears to be made up of both a dipole source and a quadrupole source; one of which varies with blade loading and one independent of loading. If, for this fan design, the dipole, rotor-turbulence interaction source controls, then no change with blade angle would be expected to occur. In flight, however, the ingested turbulence is no longer affected by the contraction ratio of the static inlet and this rotor-turbulence interaction noise is reduced. In the flight case then, the effect of blade angle may be important.

5.1.2 Inlet Suppression

The UTW composite nacelle inlet acoustic design was based upon scale-model tests in the General Electric Company anechoic chamber (Reference 9). Suppression objectives for the inlet, which is shown schematically in Figure 25, were 12.8 PNdB at takeoff with a 0.79 throat Mach number and 6.3 PNdB at approach. More details of the inlet design and suppression objectives are available in Reference 1. Basically, the design was a hybrid inlet which relied on high throat Mach number suppression at takeoff and utilized single-degree of-freedom wall treatment for approach and reverse thrust suppression.

Variation in PNL as a function of inlet throat Mach number is presented in Figure 26 for acoustic angles of 50 and 60°. Data are shown from different blade angles and indicate that there is very little variation with blade angle. Baseline levels are from a hardwall cylindrical inlet with a bellmouth and have a low inlet throat Mach number. For comparison purposes, these baseline data are plotted at an equivalent Mach number which the same engine setting would give with the high Mach number inlet. Suppressed data at both angles tend to flatten out at throat Mach numbers of 0.75 and higher. The anticipated variation in suppressed inlet PNL with throat Mach number is based on the model tests as shown at 60°.

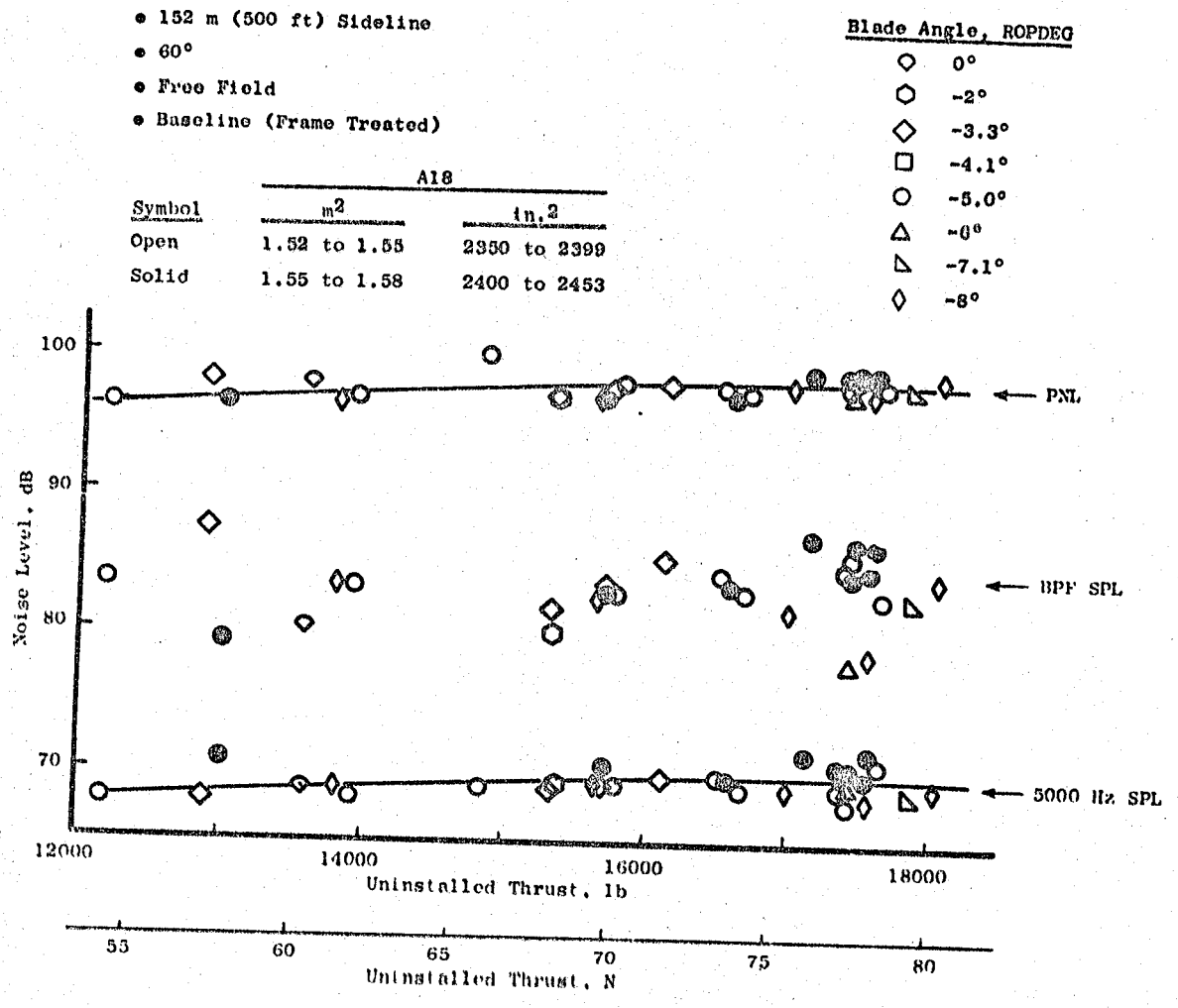

Figure 24. Baseline Noise Variation with Thrust at 60°.

- Treated $L_T/D_F = 0.74$

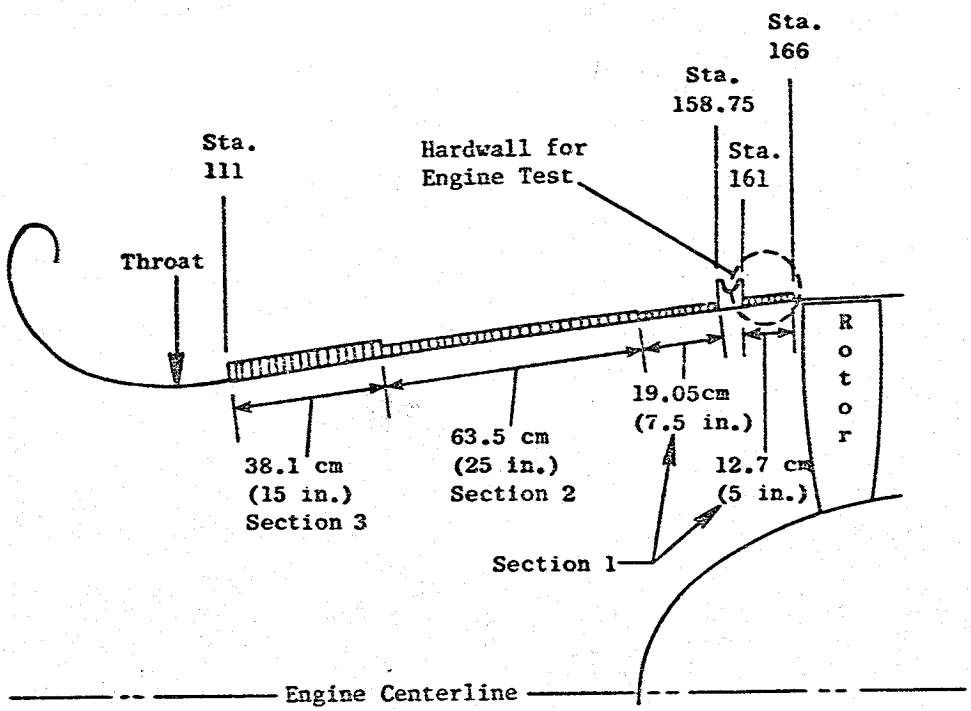

Section	Hole Size	Porosity	Cavity Depth	Faceplate Thickness
1	0.1589 cm (0.0625 in.)	9.89%	1.27 cm (0.50 in.)	0.0813 cm (0.032 in.)
2	0.1589 cm (0.0625 in.)	9.89%	1.91 cm (0.75 in.)	0.0813 cm (0.032 in.)
3	0.1589 cm (0.0625 in.)	9.89%	3.82 cm (1.50 in.)	0.0813 cm (0.032 in.)

Design Frequencies

Section	Reverse Thrust	Forward Thrust
1	3150 Hz	2000 Hz
2	2500 Hz	1600 Hz
3	1600 Hz	1000 Hz

Figure 25. Inlet Schematic and Design Details.

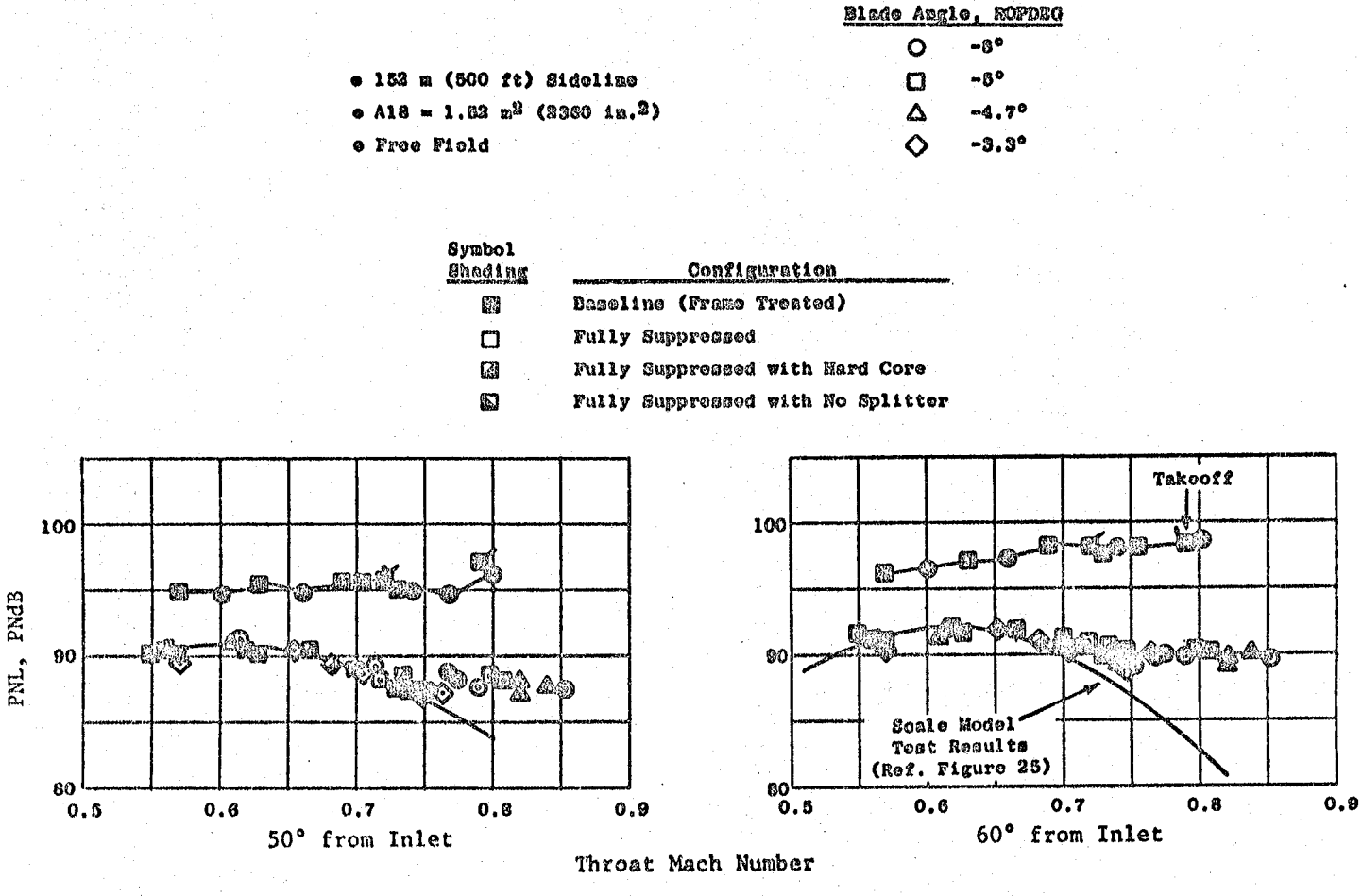

Figure 26. PNL Variation with Throat Mach Number.

Analysis of directional array data at a throat Mach number of 0.73 indicated that exhaust radiated fan noise was a major contributor to the forward quadrant noise levels in the frequency range of 1250 to 4000 Hz (operating frequency range of the directional array). Figure 27 indicates the relative SPL's from various aiming points on the engine at an acoustic angle of 60°. For the frequencies shown, exhaust radiated noise from the last three aiming points is a major noise source at 60°. On a spectral basis in Figure 28, correcting the noise levels at 60° to inlet radiated noise only results in the revised SPL spectrum and suppression spectrum shown which results in 2 PNdB more suppression. This is in agreement with the scale-model inlet radiated curve superimposed on the data in Figure 26. This scale-model curve indicates that the inlet suppression is 14 to 15 PNdB at 0.79 throat Mach number - well above the goal of 12.8 PNdB. Earlier tests of a similar inlet on the QCSEE OTW engine, as reported in Reference 10, produced inlet suppression of 14 PNdB at 0.79 throat Mach number.

As mentioned earlier, one of the unique features of a variable pitch fan is its capability to hold constant approach thrust at a variety of blade angle and nozzle combinations. A desirable combination is high fan speed (to reduce engine response time in the event of a wave off) and open fan nozzle (for lowered jet velocity and therefore jet/flap noise). This desirable combination was tested along with several other combinations, as shown in Figure 29. Here the fully suppressed PNL is nearly constant with blade angle. At the closed blade angles and high fan speeds, inlet suppression is about 4.0 dB. It was anticipated that 6.3 PNdB inlet suppression would be achieved with the SDOF treatment of the hybrid inlet at the low inlet Mach numbers associated with approach. While the design (on which acoustic predictions were based) called for a treated inlet length to fan diameter ratio (L/D) of 0.74, the inlet actually had a treated L/D of 0.67, as noted in Figure 25. On a linear basis, the suppression would be less by 0.6 PNdB; therefore, the estimated suppression for this inlet is 5.7 PNdB compared to 4.0 measured at the approach points with closed blade angle.

It is apparent in Figure 29 that a slightly higher level of PNL suppression of about 6 PNdB could be achieved at blade angles that were opened several degrees from the closed blade angles associated with the high fan speed, low nozzle area point discussed above. Predicted suppression levels were not calculated for this condition.

Figure 30 compares inlet suppression spectra observed with the wall-treated high throat Mach number (hybrid) inlet at approach thrust. Data are presented for three exhaust configurations. In the low frequency region from 315 to 630 Hz, suppression is increased by the presence of the stacked treatment in the core, indicating that these frequencies are exhaust-radiated core noise controlled, and not inlet-radiated fan noise. Above 1000 Hz, the suppression spectra are generally independent of exhaust configuration indicating that these frequencies are inlet radiated. The directional array results shown in Figure 31 confirm that the approach SPL's at 2000 to 4000 Hz are inlet radiated. At 1250 and 1600 Hz, there appears to be some contribution from the exhaust quadrant. At these lower frequencies, core noise may be the contributor; because, for the configuration on which these array results were measured,

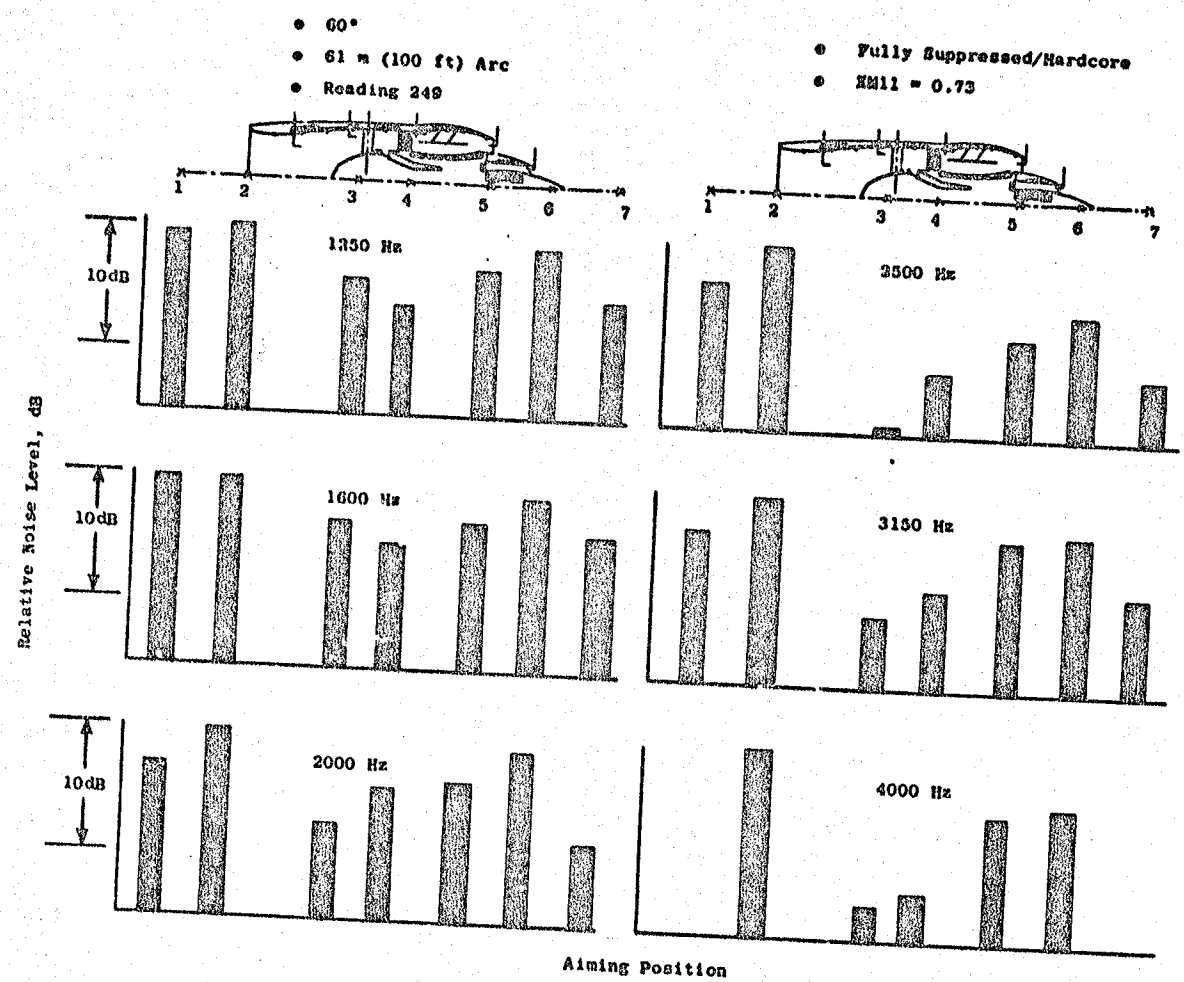

Figure 27. Fully Suppressed Directional Array Noise Levels for Takeoff at 60°.

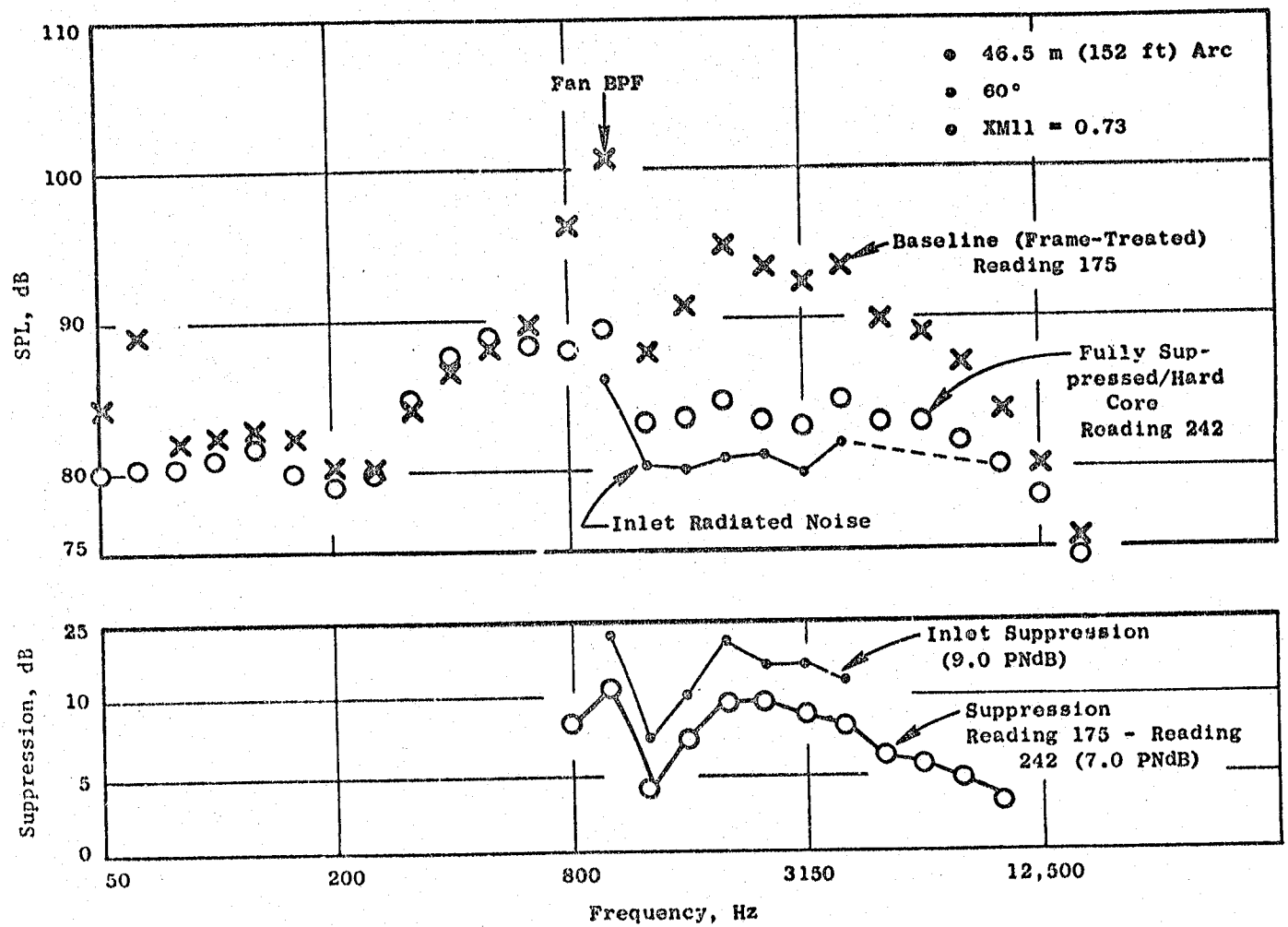

Figure 28. 60° Spectra at 0.73 Throat Mach Number.

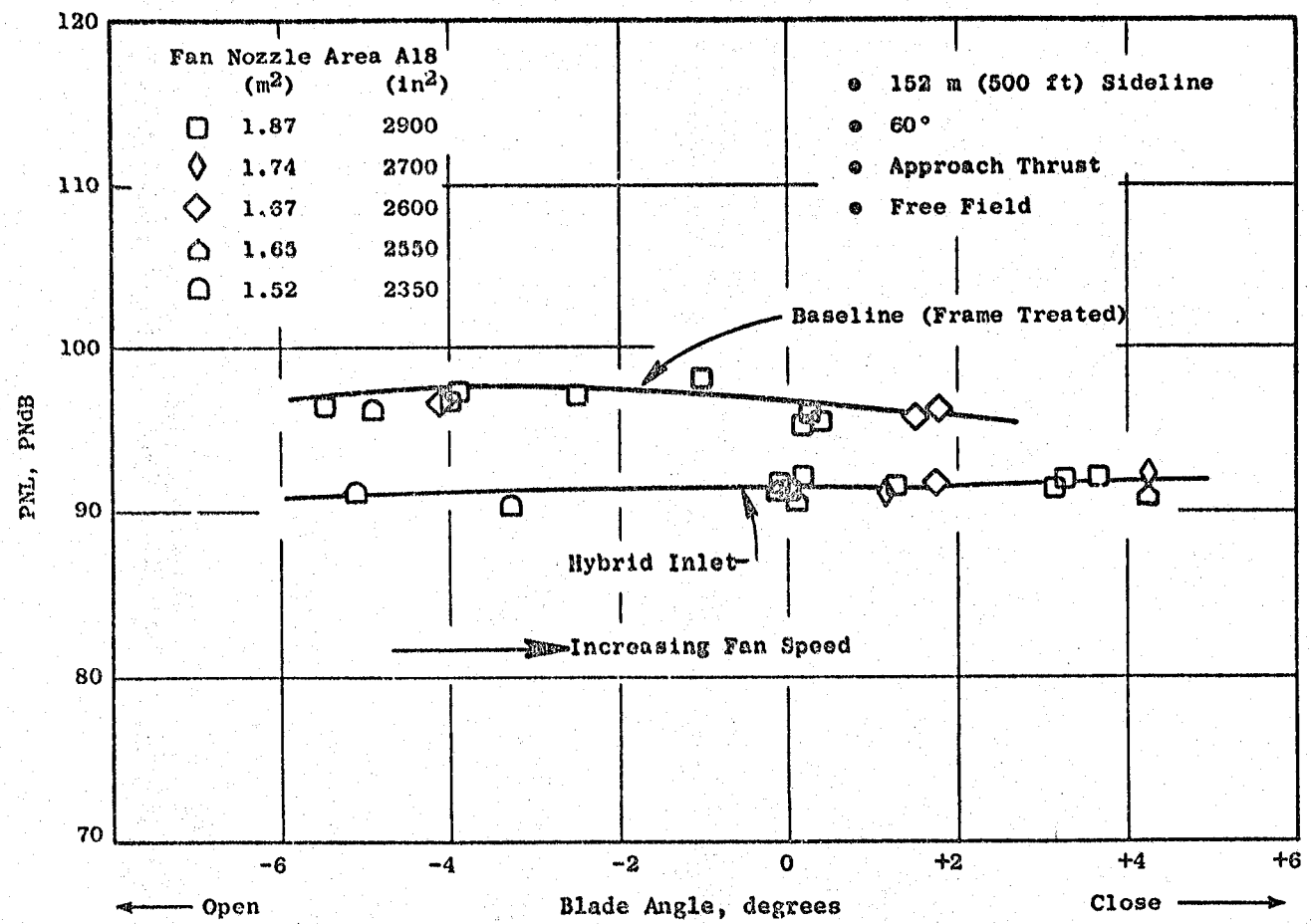

Figure 29. Approach PNL Variation With Blade Angle.

- Approach Thrust
- 1.87 m^2 (2900 in.^{2}) A18
- Hybrid Inlet

Exhaust Configuration			
Symbol	Wall Treatment	Splitter	Core Treatment
□	Yes	Yes	Yes
△	Yes	No	Yes
○	Yes	Yes	Hardwall

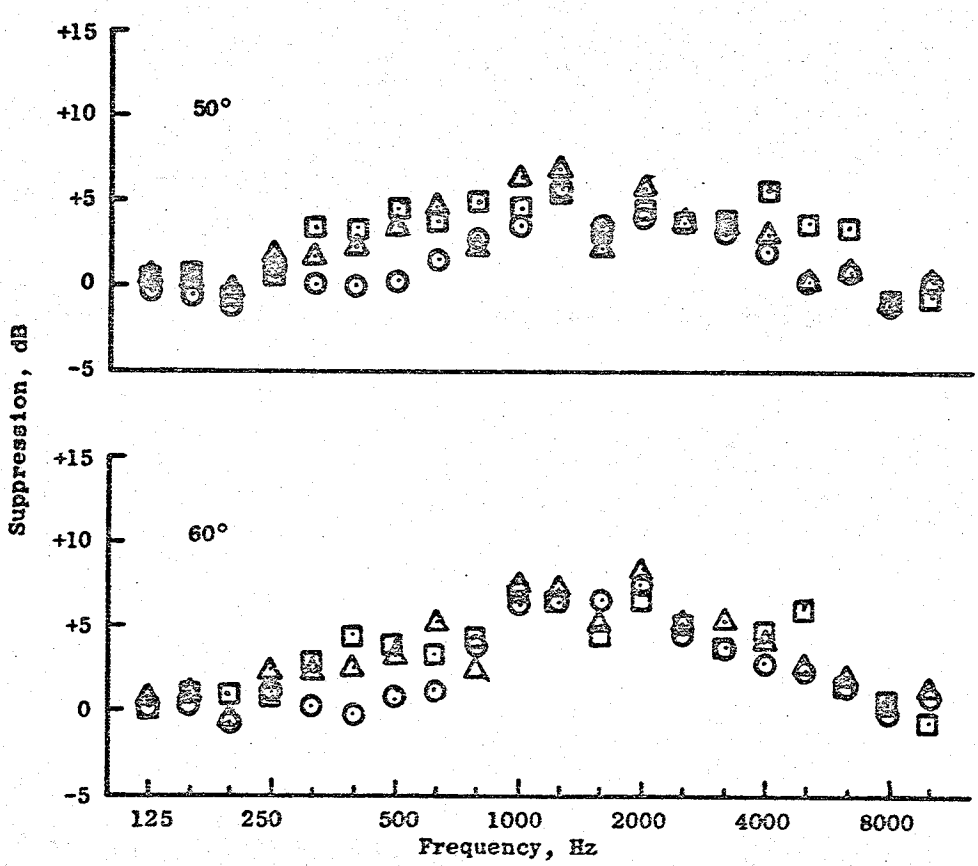

Figure 30. Inlet Suppression Spectra at Approach.

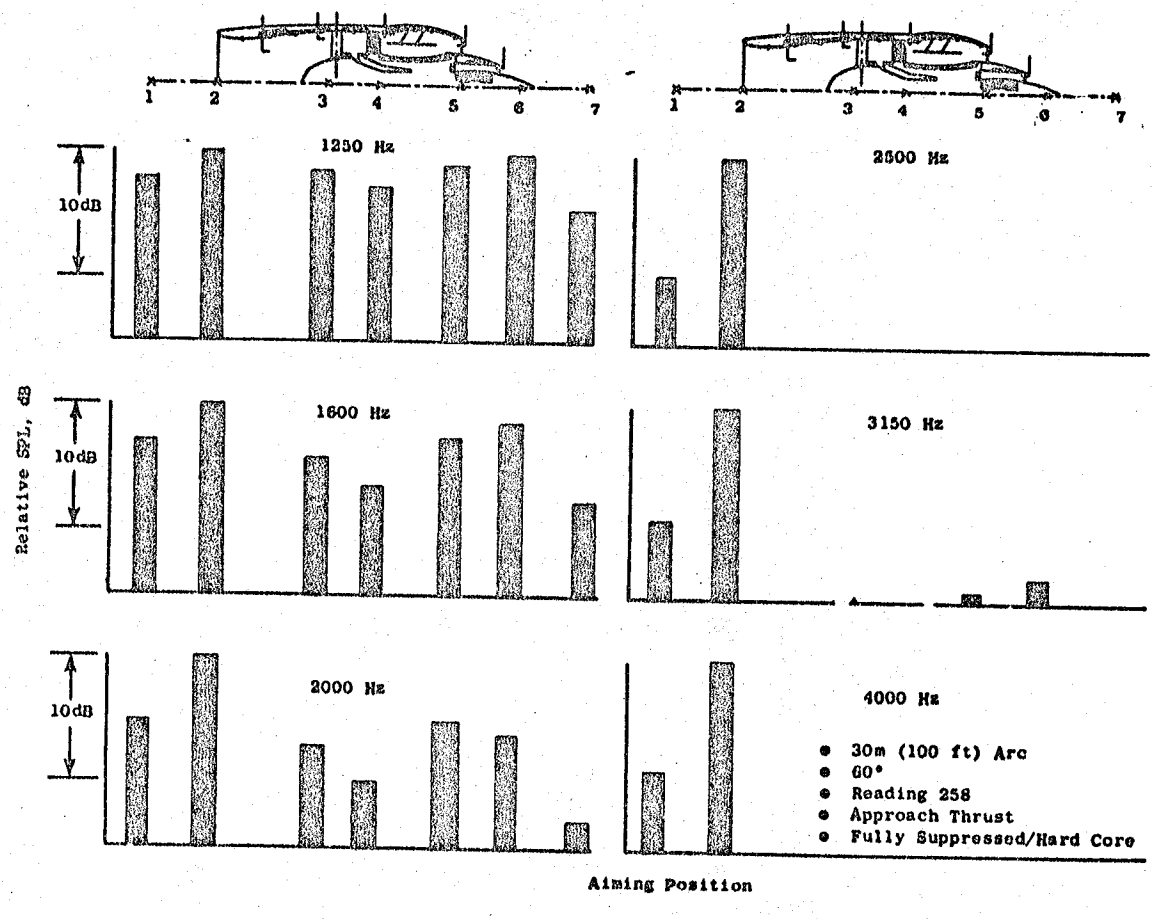

Figure 31. Fully Suppressed/Hard Core Directional Array Noise Levels for Approach at 60°.

the core was hardwall. The exhaust radiated noise had only a small effect on the forward radiated noise levels. PNL calculations made with the exhaust radiated components removed from the 800, 1000, and 1250 Hz band only increased suppression by 0.2 PNdB.

5.2 EXHAUST-RADIATED NOISE

The UTW engine, as shown schematically in Figure 1, incorporated many low noise features in the fan and core exhaust to lower exhaust-radiated noise. Baseline levels of the fan will be compared with pretest predictions and the performance of the low noise features will be discussed in the following sections.

5.2.1 Baseline Noise Levels

Prior to testing the UTW engine, estimates were made of the individual exhaust-radiated components for static tests at takeoff and approach. Comparisons of the predicted and measured baseline spectra are presented in Figures 32 and 33 at takeoff and approach, respectively. At low frequencies, the system noise level, composed primarily of jet noise, is either as predicted or lower. At higher frequencies, however, the measured spectra are consistently higher than predicted resulting in the measured PNL being 2.6 to 5.5 PNdB higher than predicted. As was the case for the inlet-radiated spectra, the 1/3-octave bands include both fan tones and broadband noise. As indicated in the narrow band spectra of Figure 34, these tones control the 1/3-octave bands of 1000, 2000, and contribute significantly to 2500 Hz. At frequencies above 3000 Hz, the fan tones do not contribute significantly to the 1/3-octave band level. To determine if higher-than-predicted tone content heavily influenced the PNL's, a study was conducted which reduced the 1000, 2000, and 2500 Hz 1/3-octave bands by 5 dB. Such a reduction on these bands containing the first three fan tones, reduced the PNL by 0.6 PNdB at both takeoff and approach. This indicates that higher-than-predicted fan broadband noise accounts for the higher-than-predicted exhaust radiated baseline noise levels. In Figures 35 and 36, at takeoff and approach, respectively, the directional array indicates that the high frequency broadband noise reaching the far-field microphone at 120° on a 30.48 m (100 ft) arc is exhaust-radiated with the fan bypass nozzle being the main source. In Figure 36 at 1000 Hz, which contains the fan BPF, there appears to be a strong contribution from Aiming Point 4 where the fan duct attaches to the fan frame. This could indicate a leakage path; however, this high level is not observed at other angles and other speeds.

Results from a probability density analysis of the fan BPF and second harmonic tones are presented in Figure 37. These signals in the aft quadrant have a random amplitude probability distribution (as they did in the inlet) which implies that a random mechanism, such as rotor-turbulence generated noise, may be the dominant source mechanism.

At approach thrust, the inlet-radiated noise showed very little variation with blade angle. Figure 38 shows the variation in aft quadrant noise with blade angle. There is a slight tendency for the BPF to decrease as the blades are closed; however, the high frequency SPL's and the PNL's are essentially invariant with blade angle over the range tested.

Symbol	Reading	PCNLR	ROPDEG	A18 m^2	A18 $in.^2$	PNL
○	16	94.5	-5.1	1.52	2355	121.6
◇	17	94.4	-4.5	1.46	2259	121.0
△	18	96.9	-6.9	1.56	2417	121.8
□	27	95.4	-4.6	1.62	2504	123.0
	Predicted					118.4

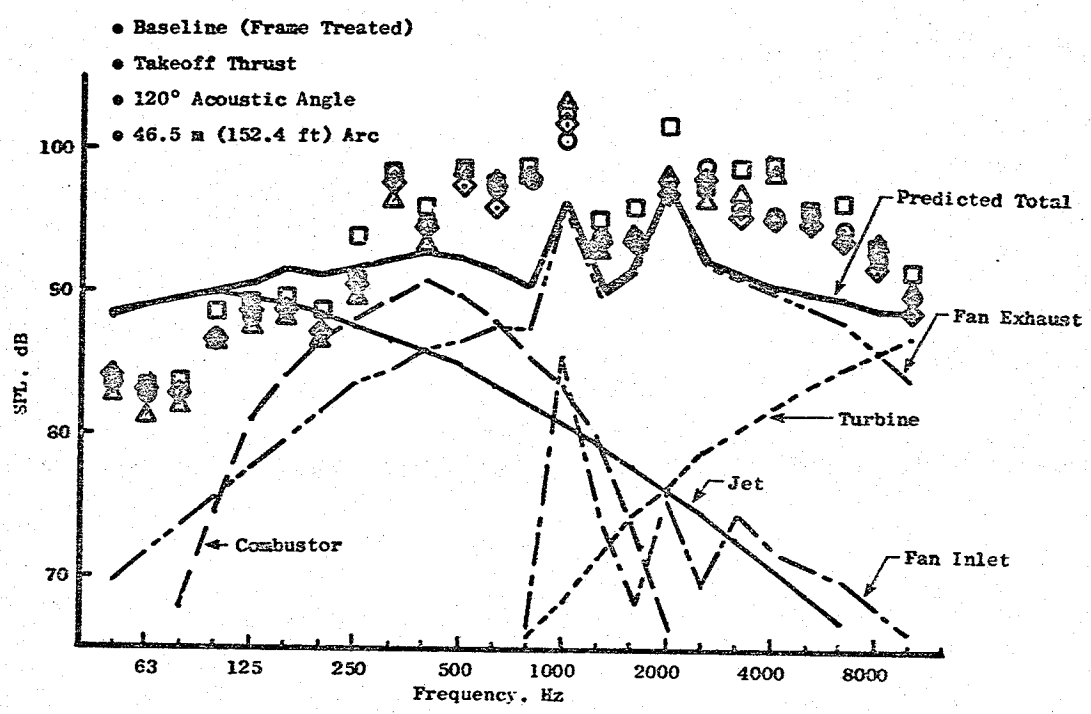

Figure 32. Measured and Predicted 120° Baseline Spectra at Takeoff.

Symbol	Reading	PCNLR	ROPDEG	A18 m^2	A18 $in.^2$	PNL
◇	21	80.6	-4.0	1.89	2931	118.0
○	29	94.9	0.4	1.87	2906	118.3
□	30	95.0	1.8	1.68	2605	118.4
	Predicted					112.9

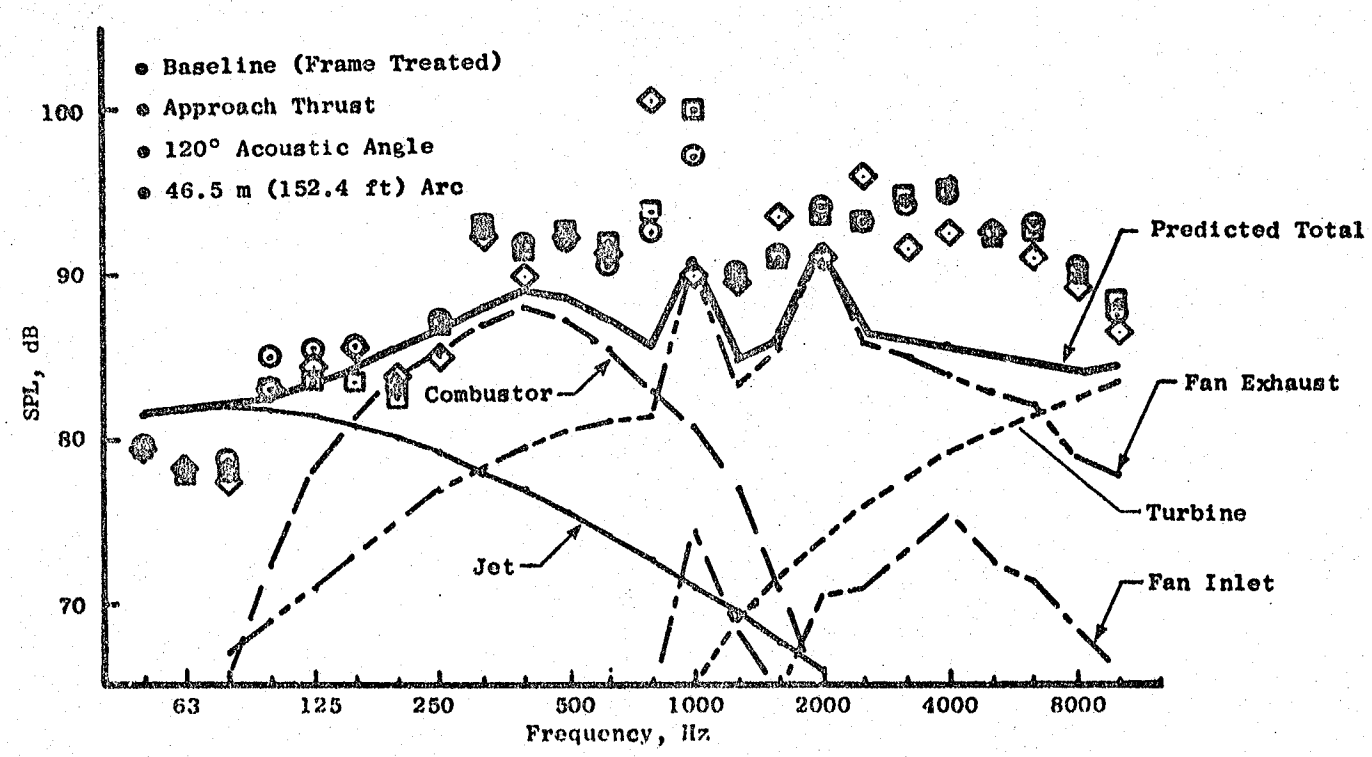

Figure 33. Measured and Predicted 120° Baseline Spectra at Approach.

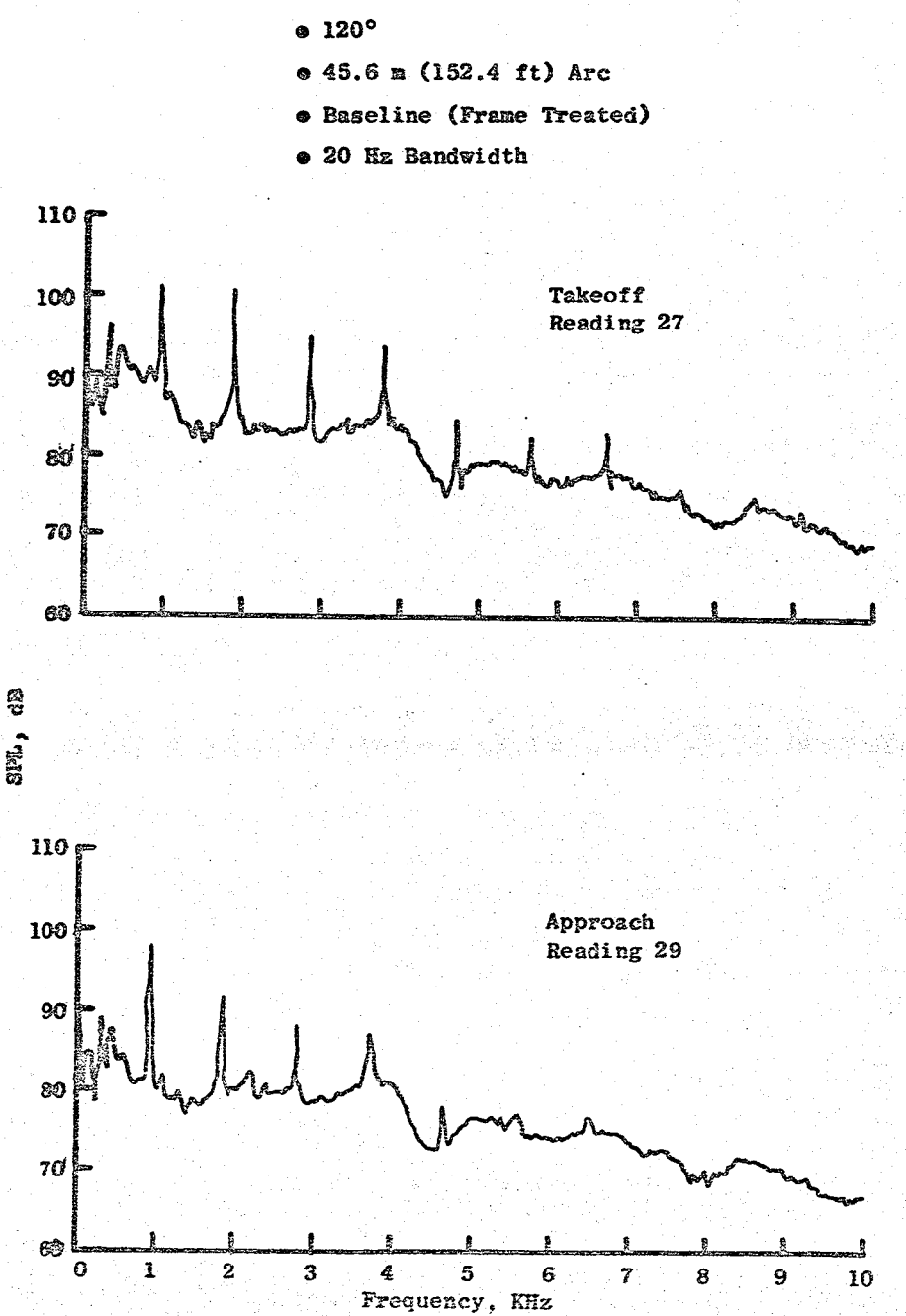

Figure 34. Narrow Band Baseline Spectra at 120°.

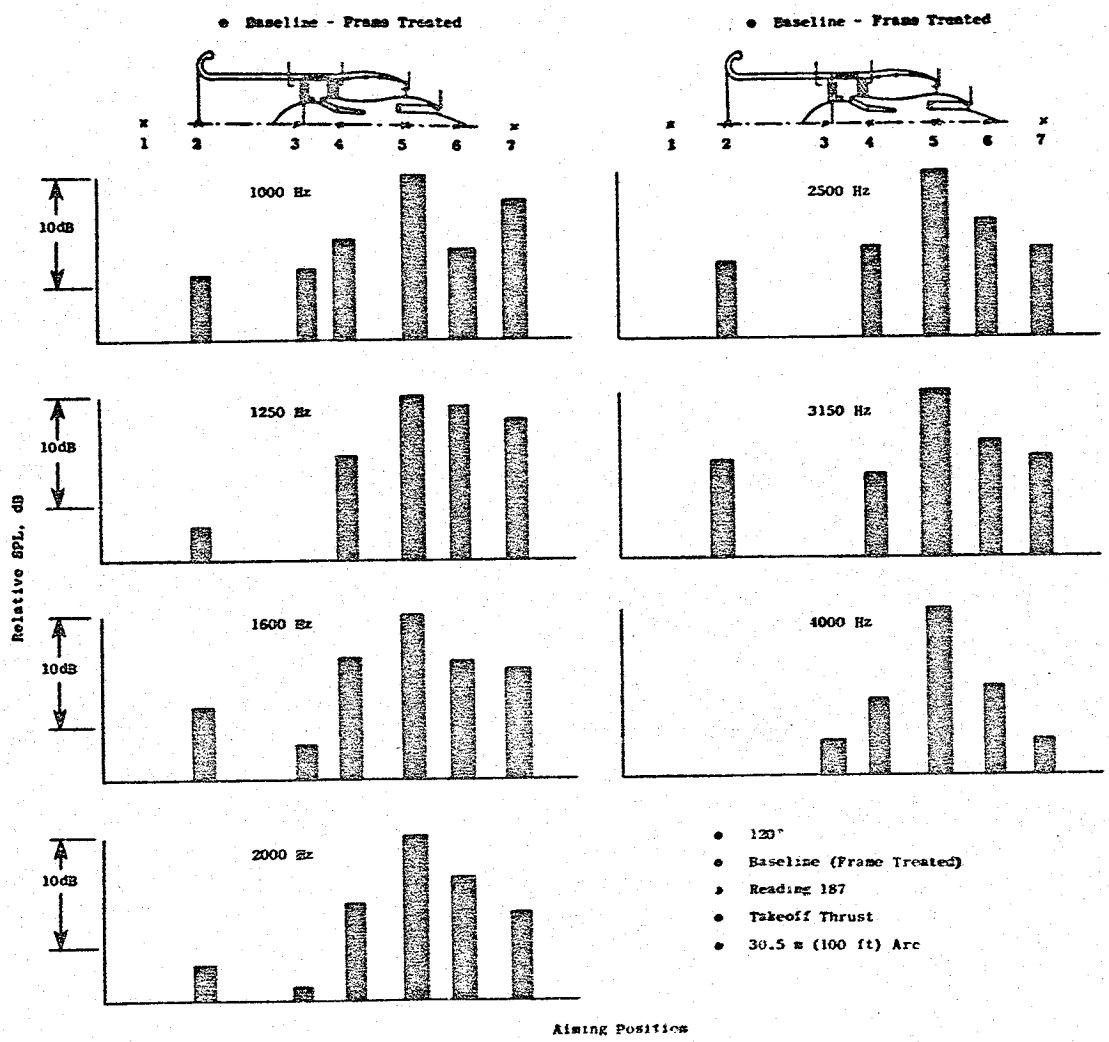

Figure 35. Baseline Directional Array Noise Levels at 120° Takeoff.

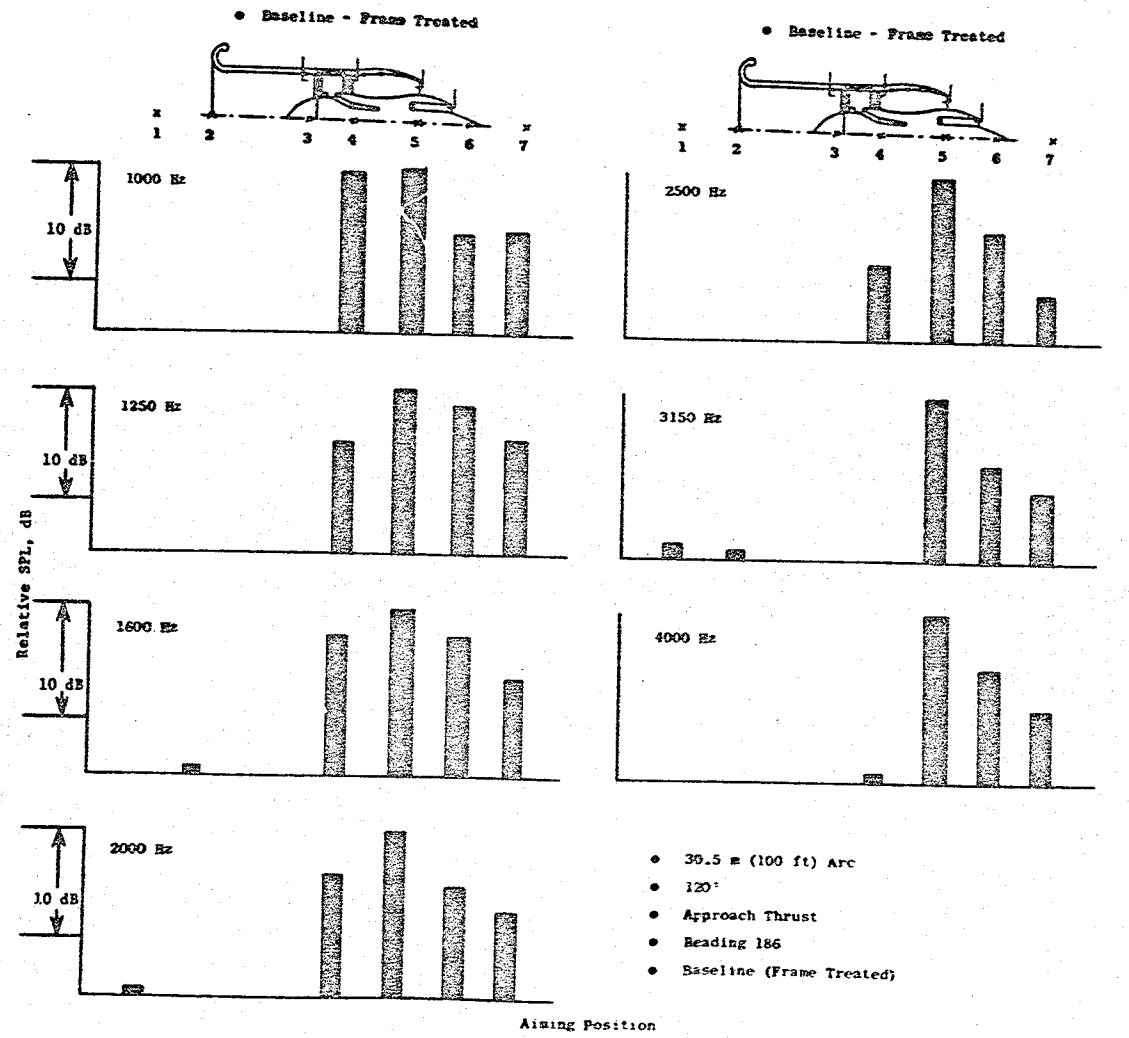

Figure 36. Baseline Directional Array Noise Levels at 120° for Approach.

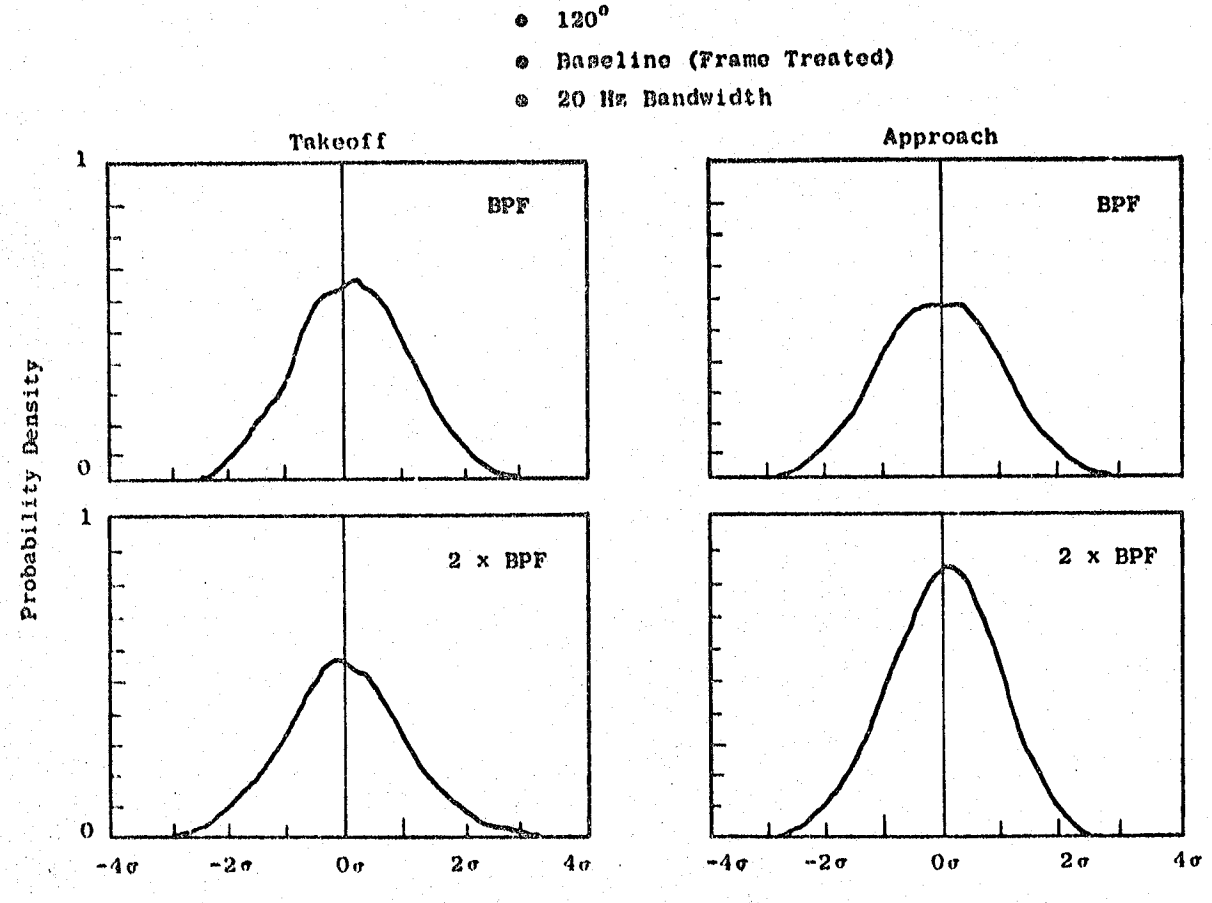

Figure 37. Baseline Exhaust Radiated Source Noise Characteristics at 120°.

- 152 m (500 ft) Sideline
- 120°
- Free Field
- Baseline (Frame Treated)
- Approach Thrust

	A18	
	m^2	$in.^2$
○	1.87	2900
△	1.68	2600
□	1.52	2350

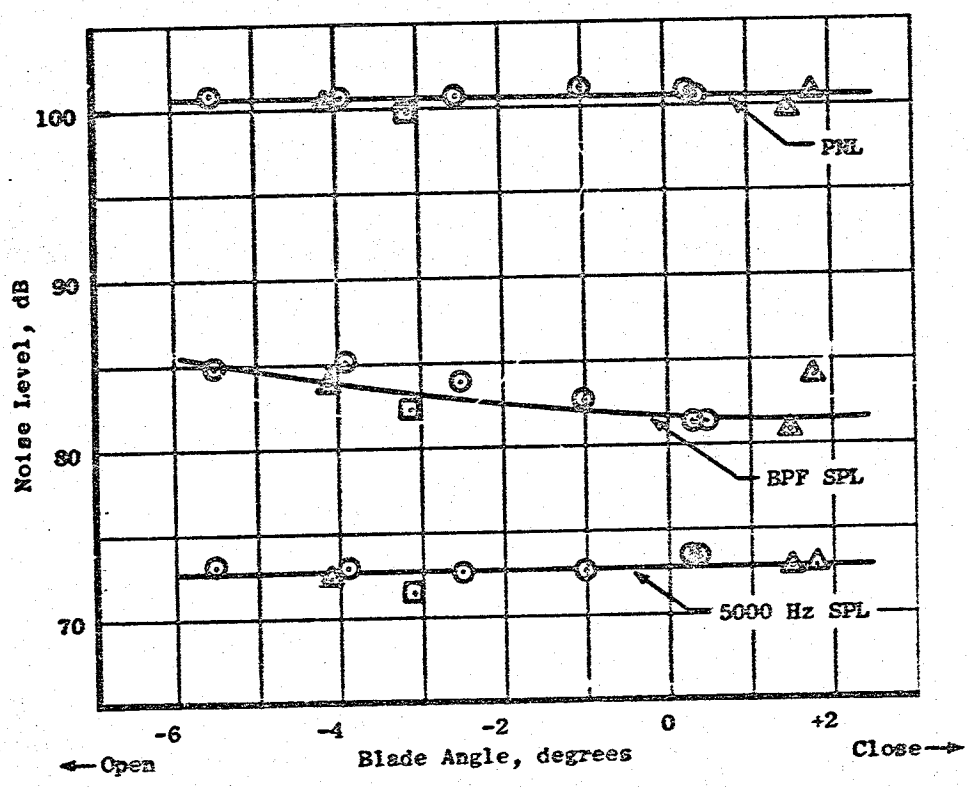

Figure 38. Approach Baseline Noise Variation with Blade Angle at 120°.

Due to the limited blade angle variation at takeoff thrust, noise levels were plotted as a function of thrust for fan bypass nozzle areas near takeoff. The data, shown in Figure 39, indicated no significant variation in noise with blade angle. As with the inlet-radiated tone noise, it appears that a fan source mechanism such as the dipole, rotor-turbulence interaction is controlling and thus no change with blade angle would be expected to occur. Under a turbulence-free environment such as in flight, the effect of blade angle could be important as a means of minimizing tone noise. Rotor turbulence generally works on tones; however, recent studies have indicated that high frequency broad band noise can also be attributed to rotor turbulence noise. This would mean that in-flight conditions could improve high frequency broad band noise.

The exhaust-radiated fan noise which controls the spectra above 800 Hz, was predicted based upon General Electric Company experience with fixed pitch fans (Reference 3). It appears that the fixed-pitch fan data base cannot be used to reliably predict a variable-pitch fan design. Variances such as fan solidity, blade number, and perhaps the vane-frame itself are possible causes of discrepancy. Additional investigations are in order to determine the exact cause of our divergence. The QCSEE UTW engine does provide an excellent data base on which future variable-pitch designs and noise estimates can be made.

5.2.2 Exhaust Suppression

5.2.2.1 Engine Treatment

Exhaust-radiated noise on the QCSEE UTW engine consists of fan noise (both tones and broad band), low frequency combustor noise, low frequency jet noise, and high frequency turbine noise. In order to meet the challenging noise goals of the QCSEE program, suppression for the fan, combustor, and turbine was incorporated into the design of the UTW composite nacelle.

Schematics showing the exhaust treatments for the fan bypass duct and the core are presented in Figures 40 and 41, respectively. Included in the fan treatment are fan frame treatment betweeen the rotor and OGV, vane treatment on the pressure surface, fan bypass duct wall treatment, and an acoustic splitter. The core incorporates a "stacked" treatment to attenuate both the low frequency combustor noise and the high frequency turbine noise.

Variation of the aft quadrant PNL's with engine thrust is shown in Figure 42. Fully suppressed levels relative to the baseline (frame treated) configuration are lower by 6 to 8 PNdB. These data are for blade angles and operating lines representative of takeoff conditions. There appears to be no significant variation present due to either blade angle or fan bypass nozzle area over the range presented. On a spectral basis, Figure 43 compares spectra from baseline and fully suppressed configurations at takeoff thrust over a range of blade angles and fan bypass nozzle areas. The average suppression from these data is compared with predicted values in Figure 44. Note that these measured and predicted suppression spectra are for the engine system as tested - not for an individual component. On a PNL basis, the average

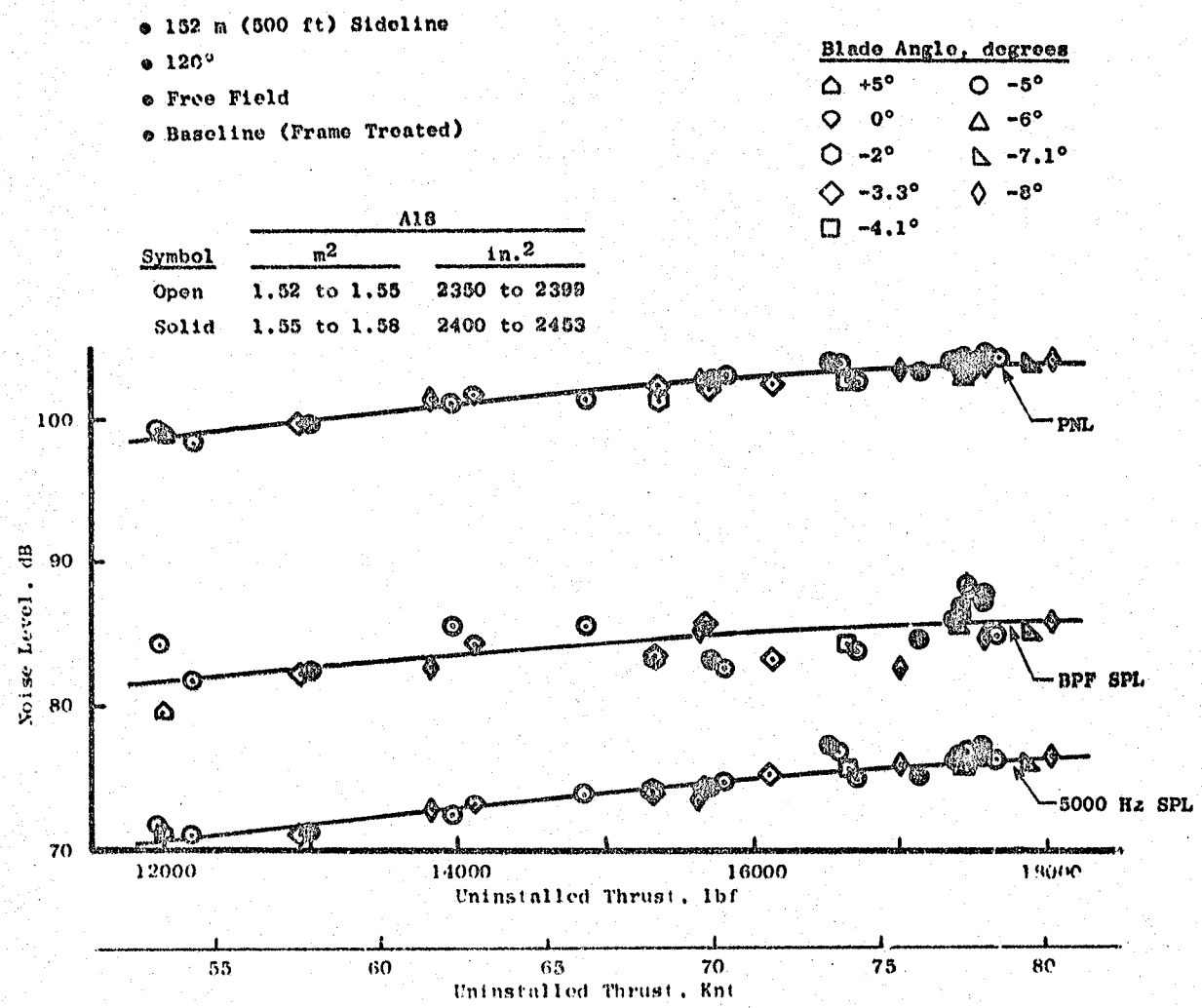

Figure 39. Baseline Noise Variation with Thrust at 120°.

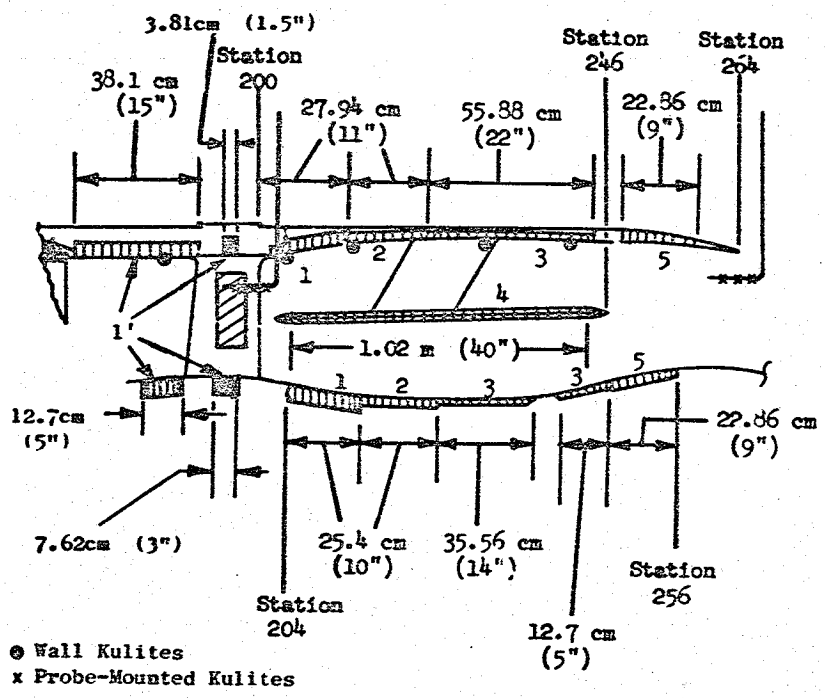

	Depth	Porosity	Hole Size	Faceplate Thickness	Frequency
Fan Frame Treatment					
Section 1	5.08 cm (2.0 in.)	10%	0.1589 cm (0.0625 in.)	0.0869 cm (0.035 in.)	1000 Hz
Treated Vanes	0.76 cm (0.3 in.)	10%	0.1589 cm (0.0625 in.)	0.127 cm (0.05 in.)	4000 Hz
Fan Exhaust Treatment					
Section 1	5.08 cm (2 in.)	22%	0.1589 cm (0.0625 in.)	0.1016 cm (0.040 in.)	1250 Hz
Section 2	2.54 cm (1 in.)	15.5%	0.1589 cm (0.0625 in.)	0.1016 cm (0.040 in.)	2000 Hz
Section 3	1.90 cm (0.75 in.)	15.5%	0.1589 cm (0.0625 in.)	0.1016 cm (0.040 in.)	2500 Hz
Section 4	1.27 cm (0.5 in.)	11.5%	0.198 cm (0.078 in.)	0.2032 cm (0.080 in.)	2500 Hz
Section 5	2.54 cm (1 in.)	15.5%	0.1589 cm (0.0625 in.)	0.1016 cm (0.040 in.)	1600 Hz

Figure 40. Composite Nacelle Fan Exhaust Duct Treatment.

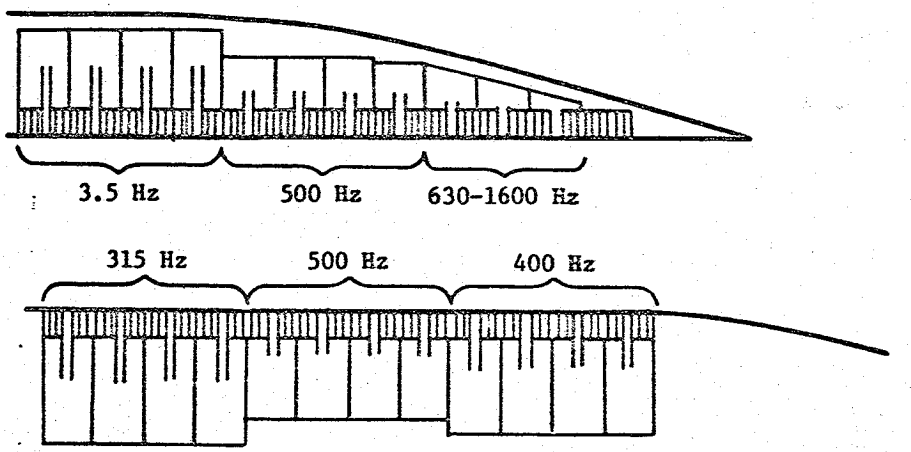

	Combustor						Turbine
	Inner Wall			Outer Wall			Both Walls
Tuning Frequency, Hz	315	400	500	315	500	630 - 1600	3150
Neck Length, cm Faceplate Thick, (in.)	6.99 (2.75)	5.72 (2.25)	4.45 (1.75)	6.99 (2.75)	4.45 (1.75)	3.56-2.54 (1.4)-(1.0)	0.08128 (0.032)
Cavity Depth, cm (in.)	10.2 (4.0)	8.89 (3.5)	7.62 (3.0)	7.62 (3.0)	4.32 &5.08 (1.7) &(2)	4.06- 0.51 (1.6)-(0.2)	1.905 (0.750)
Porosity	10%	10%	10%	7%	7%	7%	10%
Treatment Length, cm (in.)	20.32 (8.0)	20.32 (8.0)	20.32 (8.0)	20.32 (8.0)	15.24 &5.08 (6.0) &(2.0)	20.32 (8.0)	60.96 (24.0)
Hole Diameter, cm (in.)	1.52 (0.6)	1.52 (0.6)	1.52 (0.6)	1.52 (0.6)	1.52 (0.6)	1.52 (0.6)	0.1575 (0.062)

Figure 41. Core Exhaust Treatment.

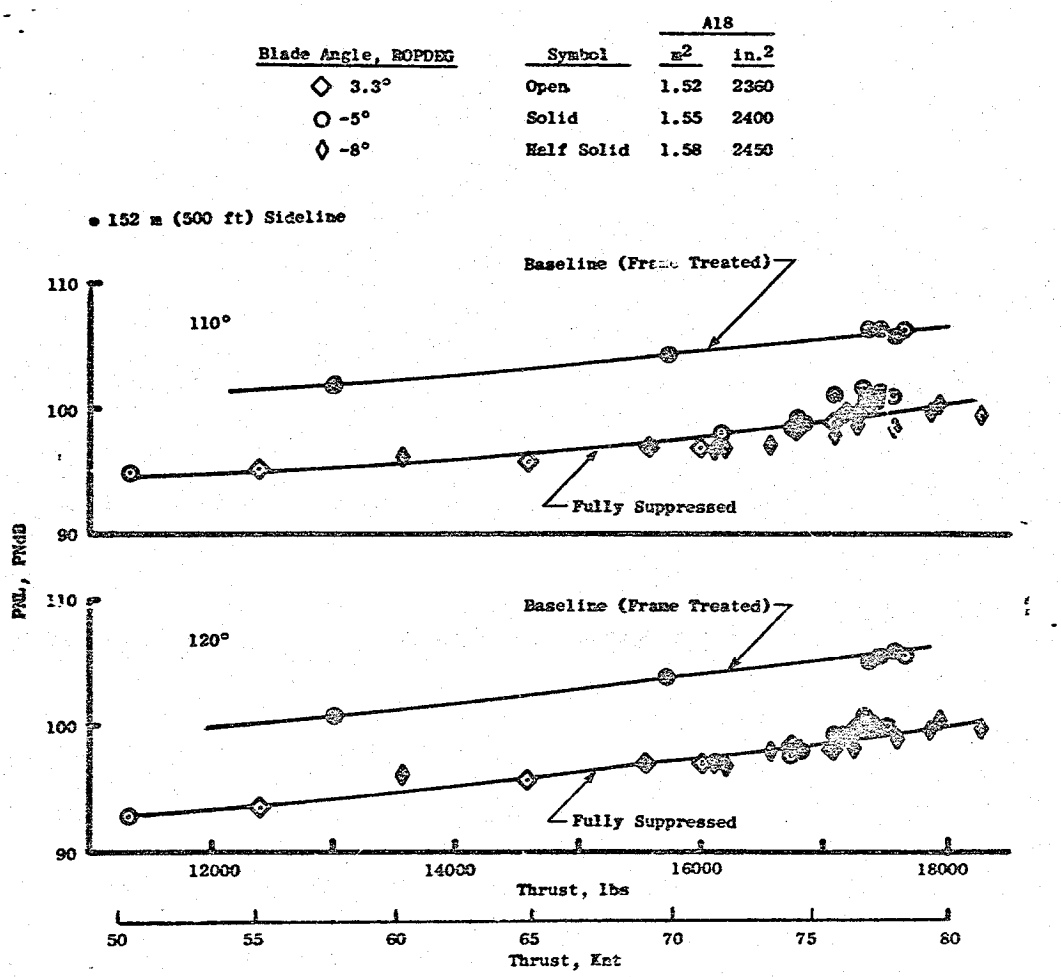

Figure 42. Exhaust Radiated PNL Variation with Thrust.

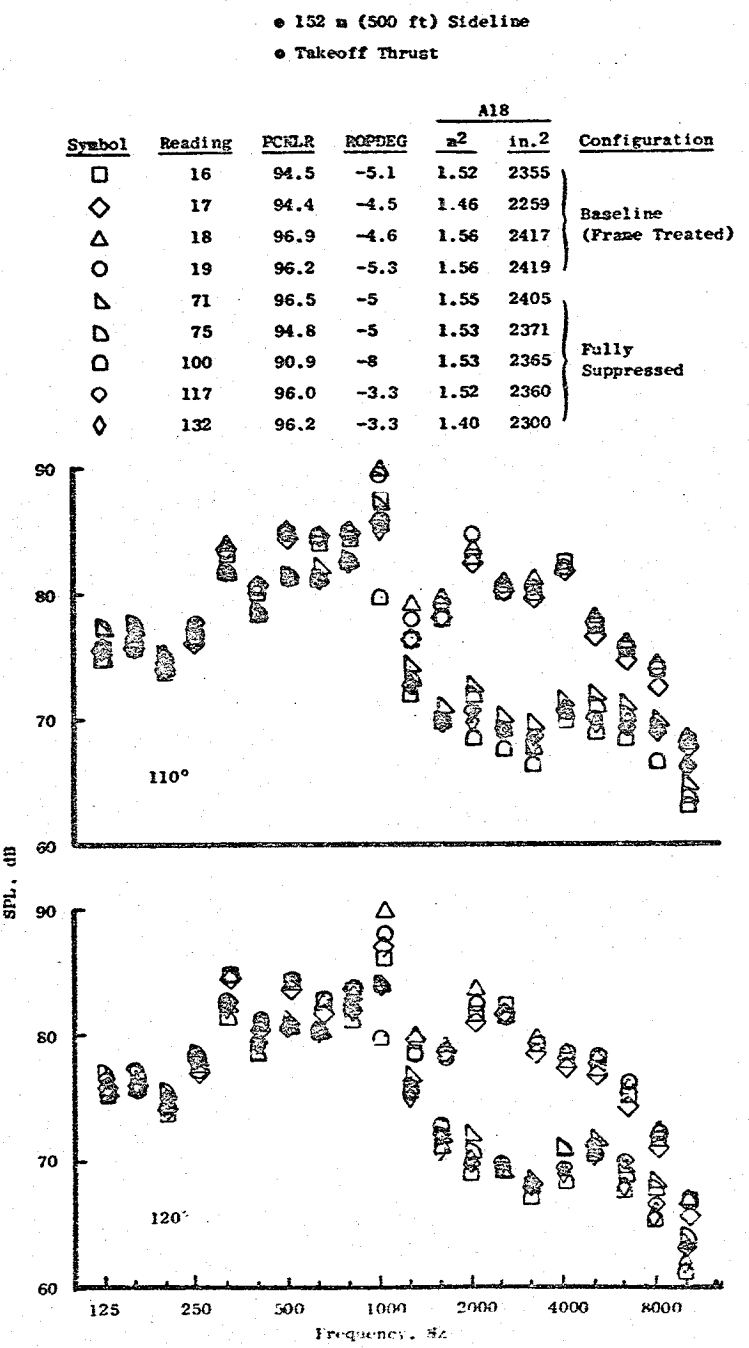

Figure 43. Exhaust Radiated Baseline and Fully Suppressed Spectra at Takeoff.

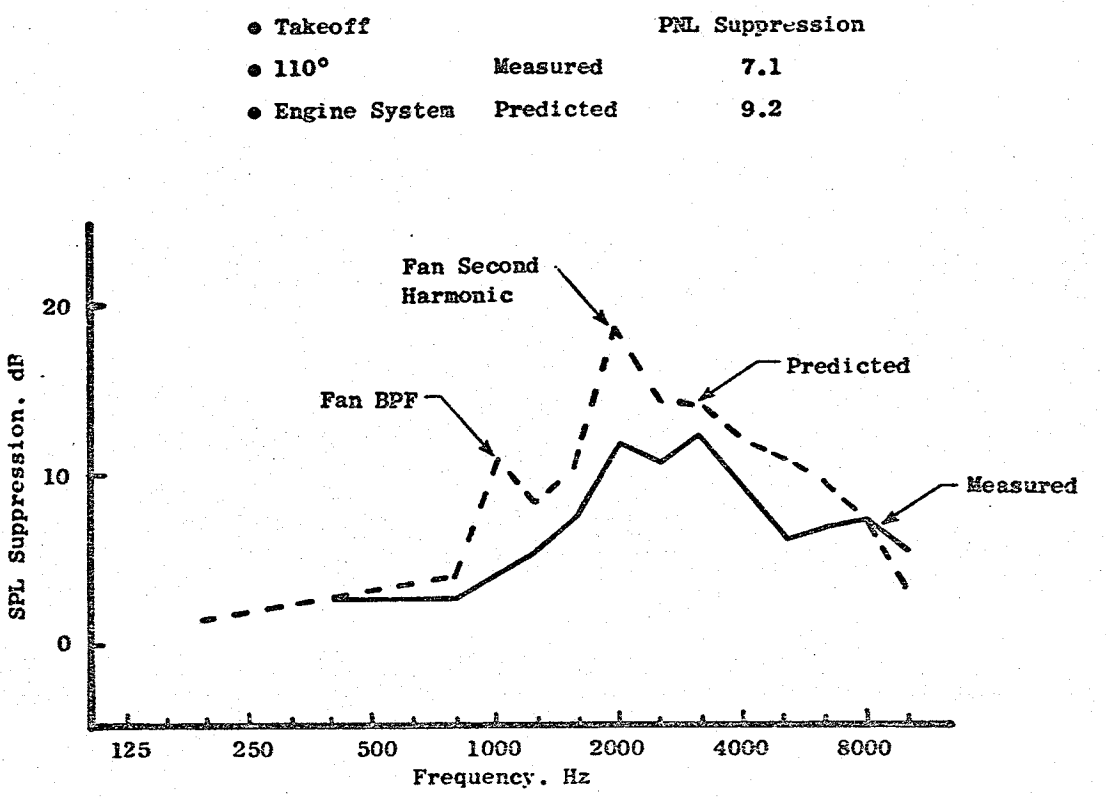

Figure 44. Measured and Predicted Engine Exhaust Suppression Spectra at Takeoff.

measured PNL suppression is 7.1 PNdB compared to a predicted 9.2 PNdB. Suppression of the BPF and its second harmonic were less than anticipated and this is the primary reason for not meeting the predicted suppression.

Directional array data at near takeoff thrust are presented in Figure 45. At 1000, 1250, and 1600 Hz, there is a significant contribution from the core region. This is not surprising since, for the directional array study, the engine was fully suppressed except for the core which was hardwall. At higher frequencies, the noise is radiated from the fan exhaust.

Approach baseline and fully suppressed spectra are presented in Figure 46. Suppression is evident at low frequencies near 500 Hz, which is combustor noise, and at the higher frequencies associated with fan noise. The average suppression spectra from these data is compared to predicted in Figure 47. The average PNL suppression is 7.5 PNdB compared with a predicted value of 9.6 PNdB.

As did the takeoff directional array data, the fully suppressed/hardwall core configuration at approach in Figure 48 indicates a strong contribution of core noise at all frequencies. The 2500 and 3150 Hz bands indicated that inlet-radiated noise is contributing to the far field 120° levels. At 4000 Hz, the noise is all exhaust-radiated.

Due to the high bypass ratio and fan diameter of the QCSEE UTW engine, the fan bypass duct height was very large, on the order of 0.51 m (20 in.). The desired level of fan exhaust suppression required the use of an acoustic splitter in this large duct. This splitter was removable and the exhaust suppression with the splitter removed is shown in Figure 49 for takeoff and approach. The measured suppression spectra for the splitter-out case are in good agreement with predicted for wall-treatment-only, except at 2000 Hz and the high frequencies near 6300 Hz. As a result, the measured PNL suppression is about 1 to 1.5 PNdB less than predicted. These results indicate that the use of the acoustic splitter in the fan bypass duct increased suppression by about 4 PNdB.

In-duct instrumentation in the fan bypass duct consisted of flush-mounted wall Kulites and radially traversible sound separation probes. Figures 50 and 51 show the axial decay of the fan BPF and fan second harmonic for approach and takeoff, respectively. At approach, the loss down the duct is on the order of about 10 dB on the tones. At takeoff, the fully suppressed configurations show some scatter but generally also give about 10 dB tone suppression. Narrow band spectra at takeoff in Figure 52 indicate that the BPF tone decreases down the duct; however, there is still a tone remaining. The second harmonic has been generally suppressed to the broadband by Station 242. Higher fan harmonics still remain even at Station 242. Similar spectral results are evident at approach in Figure 53. Fan second harmonic tone suppression is evident to the broadband floor while higher fan harmonics are still visible in the spectra. Note that there is an identifiable tone at 7600 Hz which is the BPF of the core compressor first stage.

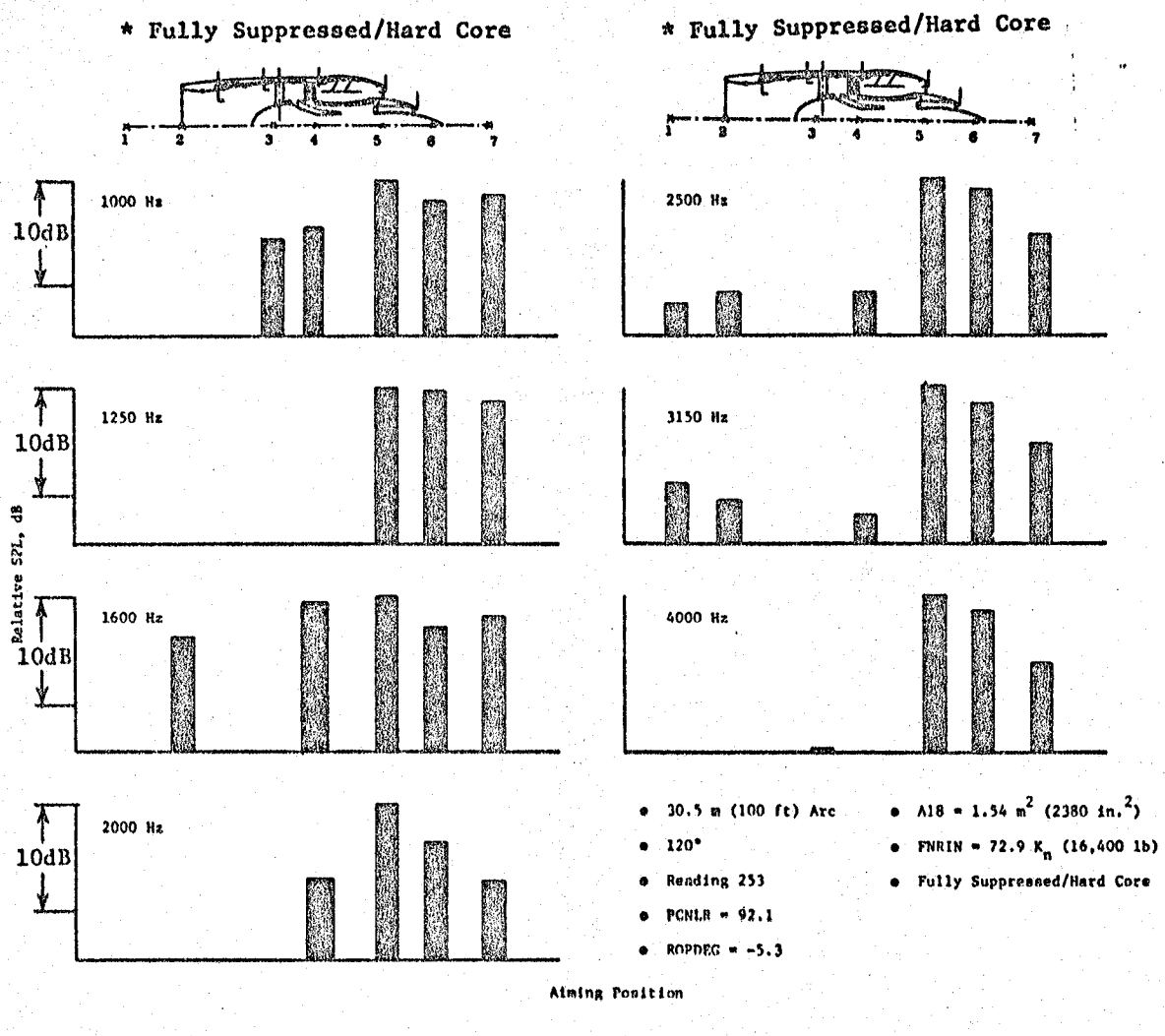

Figure 45. Fully Suppressed/Hard Core Directional Array Data at 120° for Takeoff.

● 152 m (500 ft) Sideline

● Approach Thrust

Symbol	Reading	PCNLR	ROPDEG	A18 m^2	A18 $in.^2$	Configuration
○	29	95.0	+0.4	1.87	2906	Baseline (Frame-Treated)
□	30	94.9	+1.8	1.68	2605	
◇	51	96.7	+3.7	1.86	2882	Fully Suppressed
△	54	94.4	+4.2	1.65	2550	
◺	58	89.4	+1.3	1.86	2885	

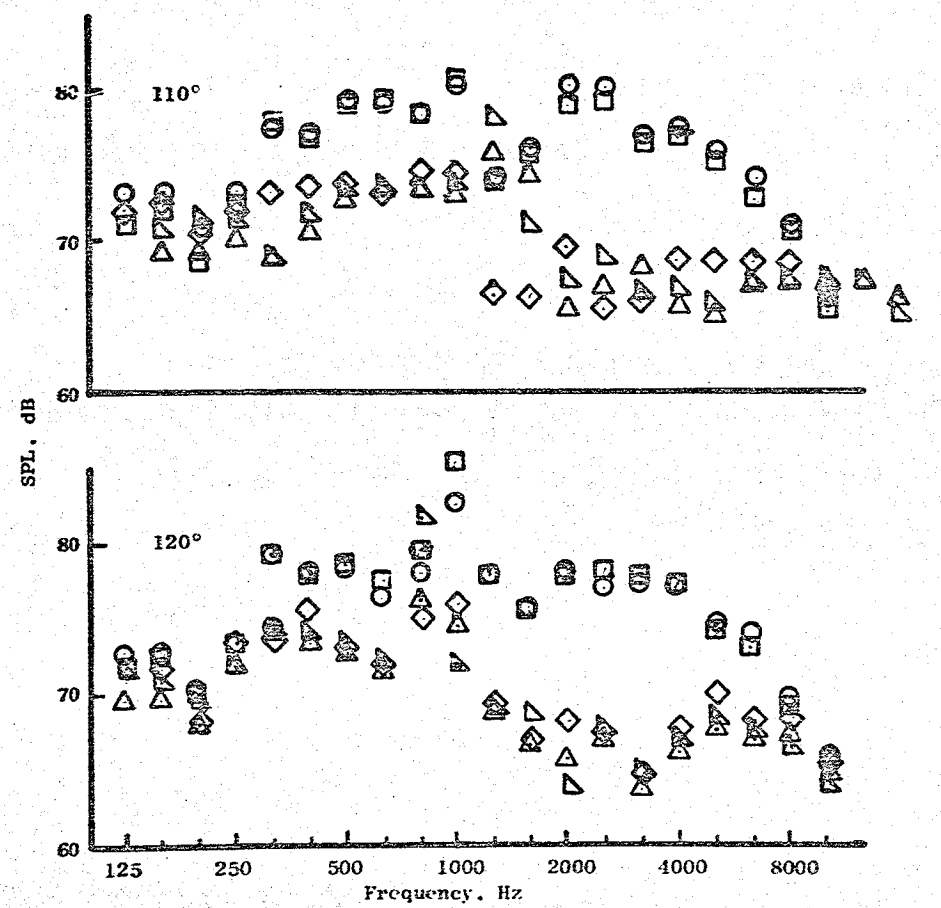

Figure 46. Exhaust Radiated Baseline and Fully Suppressed Spectra at Approach.

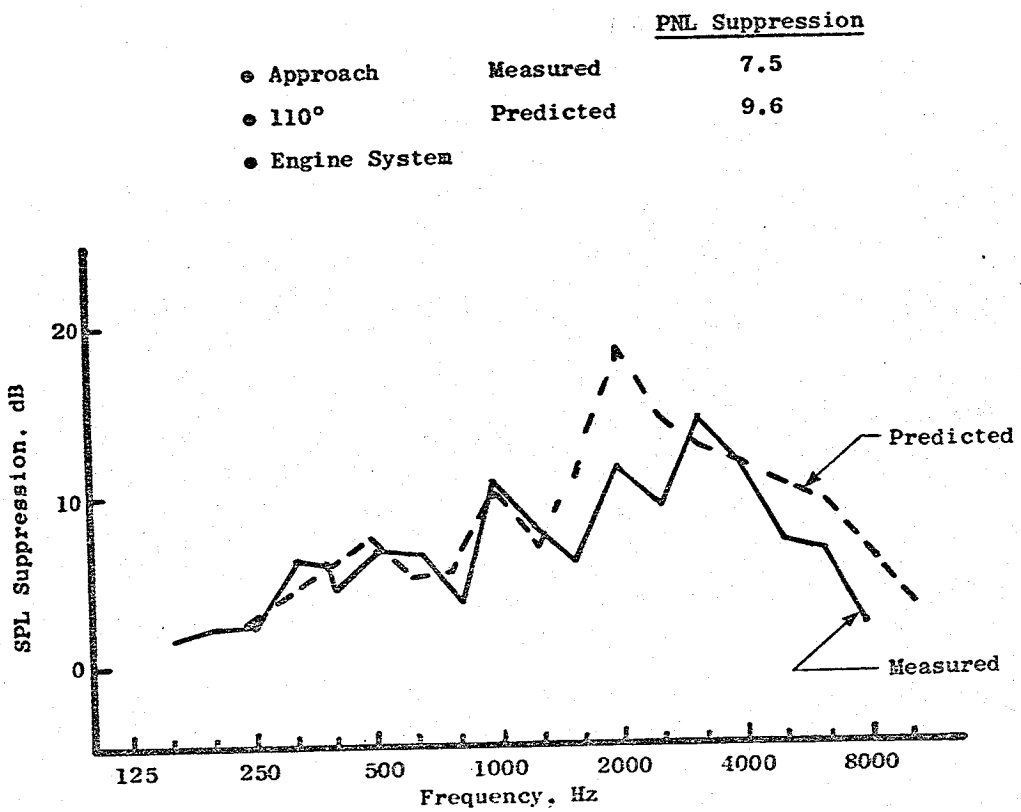

Figure 47. Measured and Predicted Engine Exhaust Suppression Spectra at Approach.

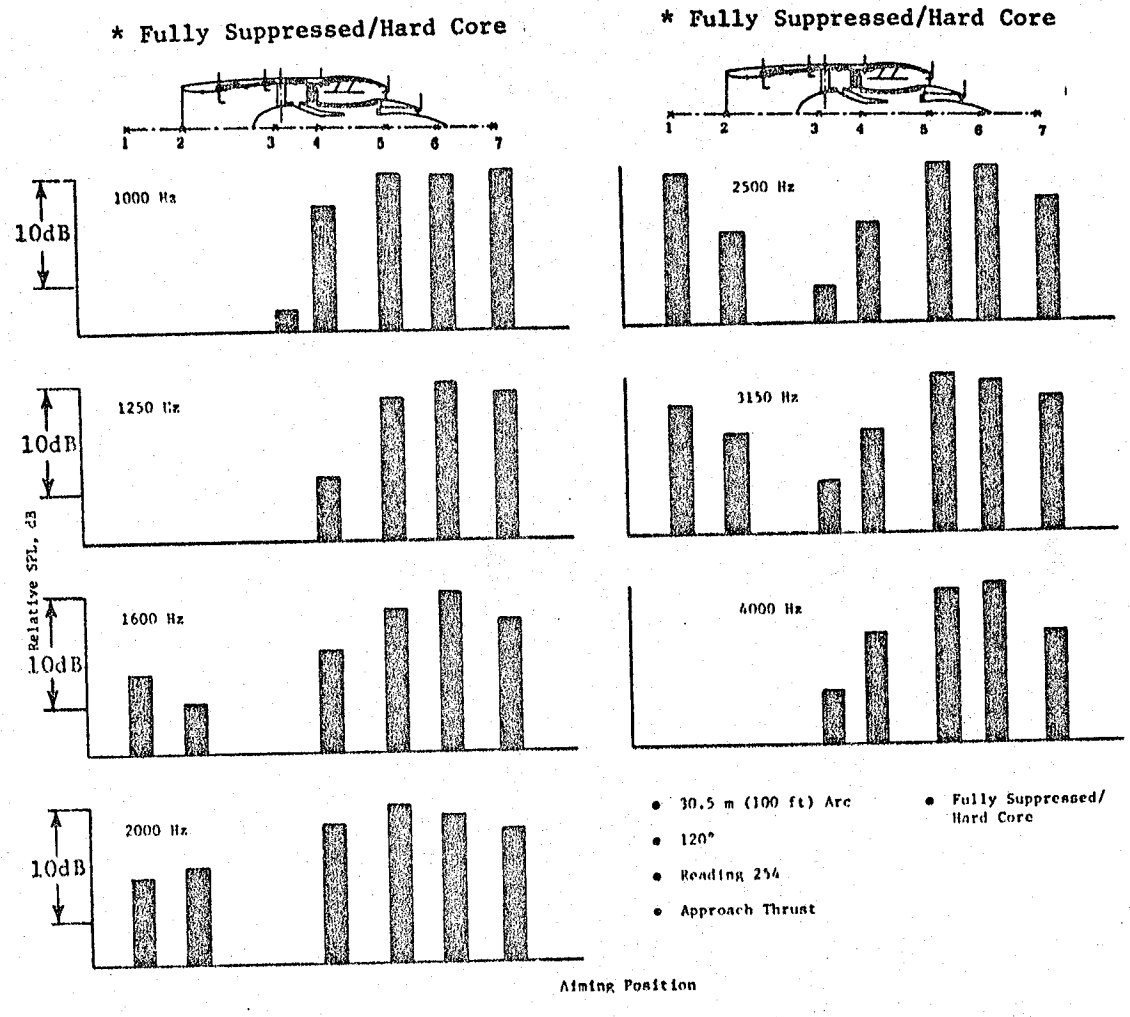

Figure 48. Fully Suppressed/Hard Core Directional Array Data for 120° at Approach.

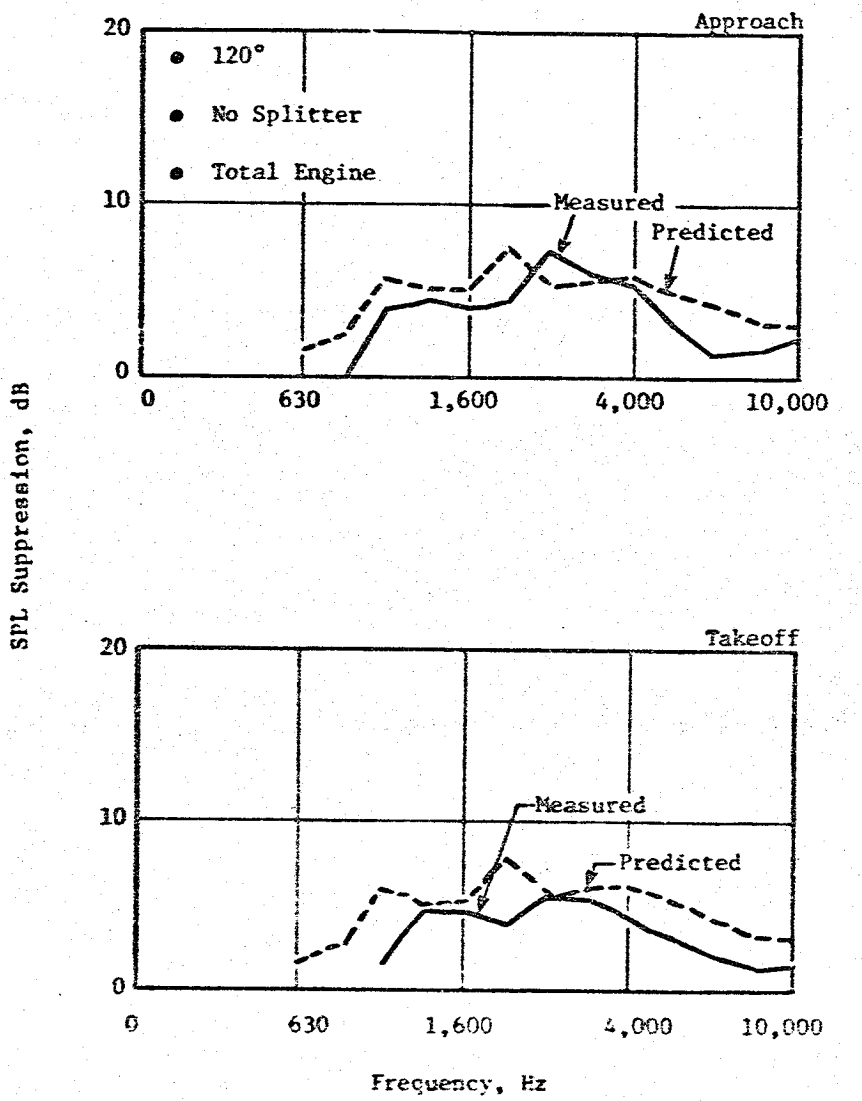

Figure 49. Measured and Predicted Engine Exhaust Suppression Spectra Without Splitter.

Exhaust Kulite Levels at Approach

- Approach Thrust
- A18 = 1.87 m^2 (2900 $in.^2$)
- 20 Hz Bandwidth

Symbol	Reading	PCNLR	ROPDEG	Configuration
◍	29	95.0	+0.4	Baseline (Frame Treated)
△	57	91.8	+3.2	Fully Suppressed

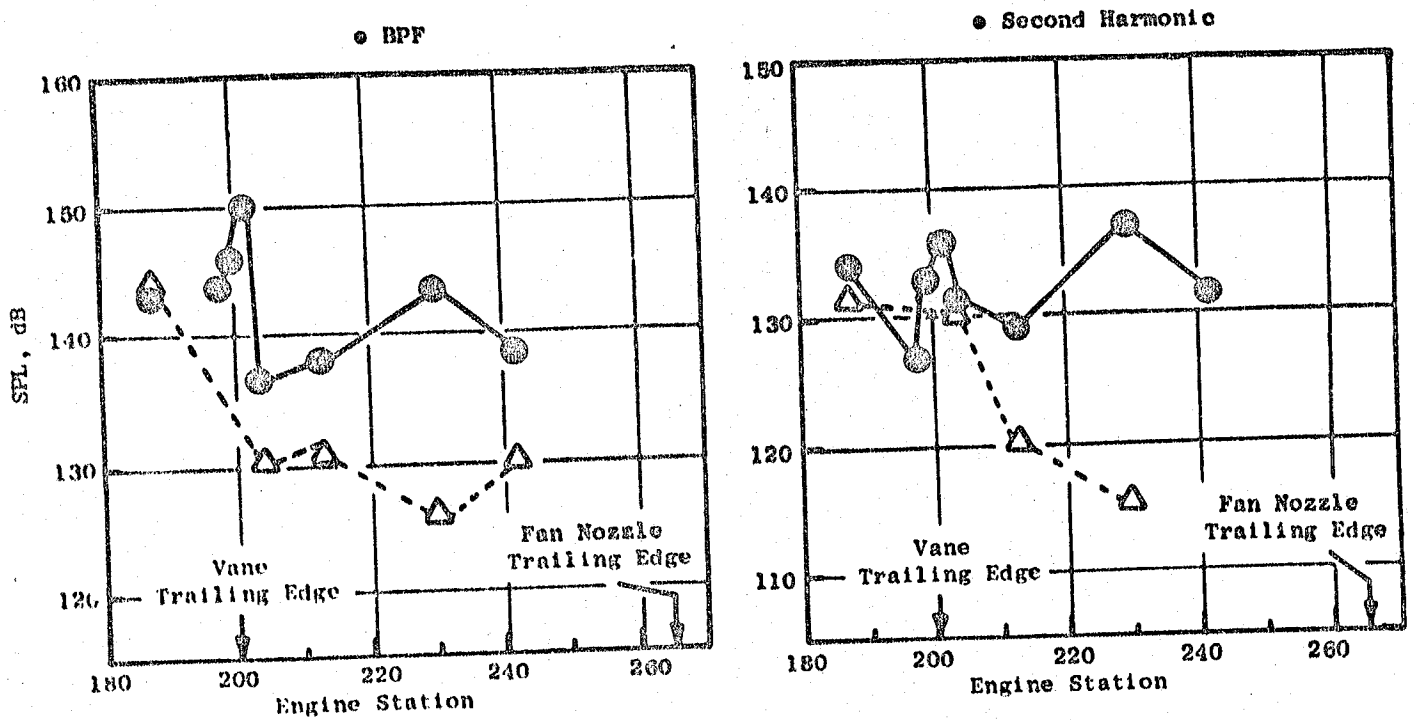

Figure 50. Axial Distribution of Tones in the Fan Bypass Duct at Approach.

Exhaust Kulite Levels at Takeoff

- Takeoff Thrust
- A18 = 1.53 m^2 (2371 $in.^2$)
- 20 Hz Bandwidth

Symbol	Reading	PCNLR	ROPDEG	Configuration
●	27	95.4	-6.9	Baseline
X	46	94.6	-4.6	Fully Suppressed
△	75	94.8	-5	
◇	100	90.9	-8	
◊	117	96.0	-3.3	

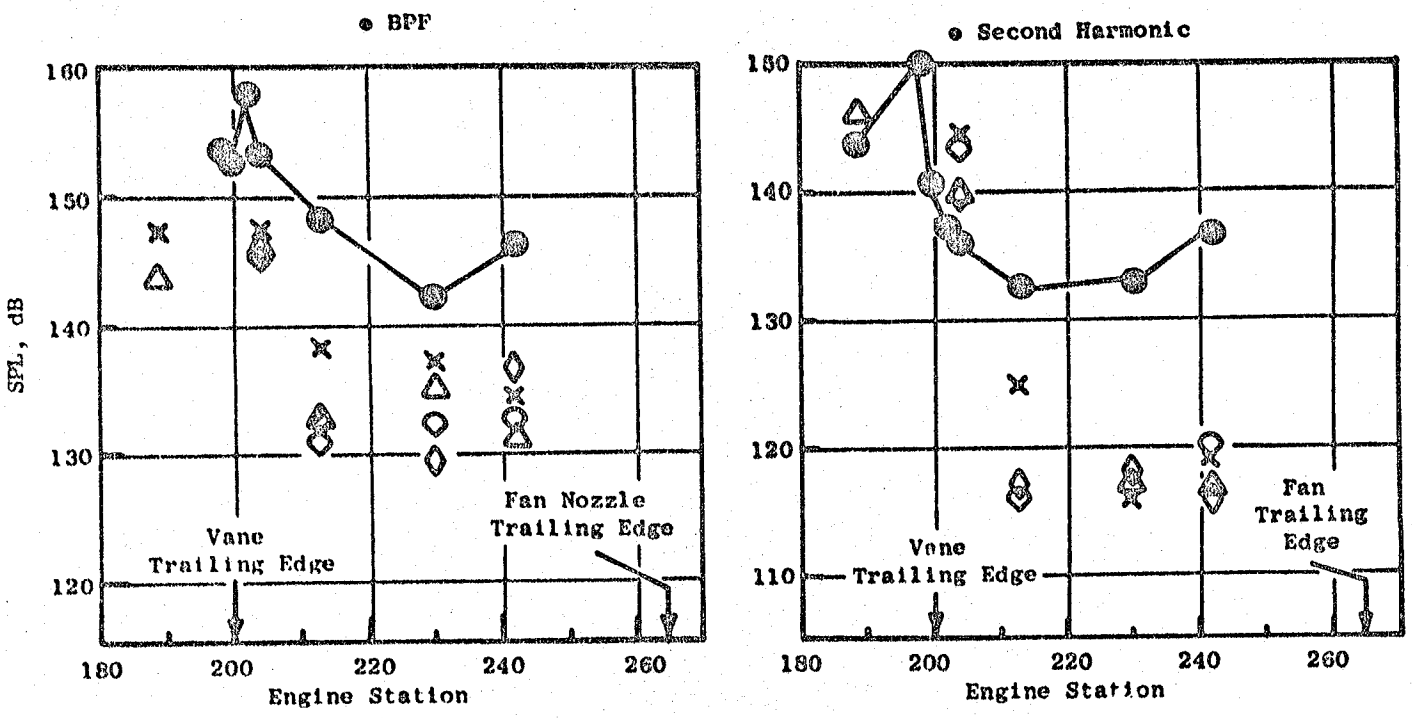

Figure 51. Axial Distribution of Tones in the Fan Bypass Duct at Takeoff.

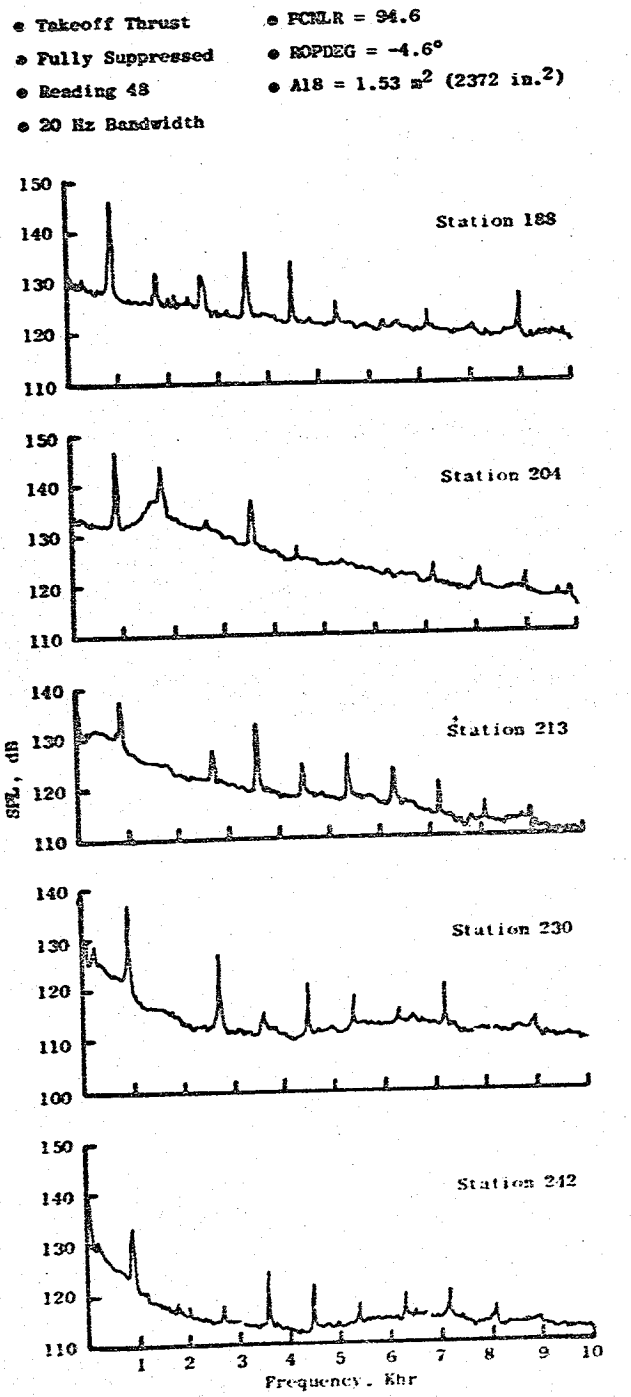

Figure 52. Fan Bypass Duct Wall Kulite Narrow Band Spectra at Takeoff.

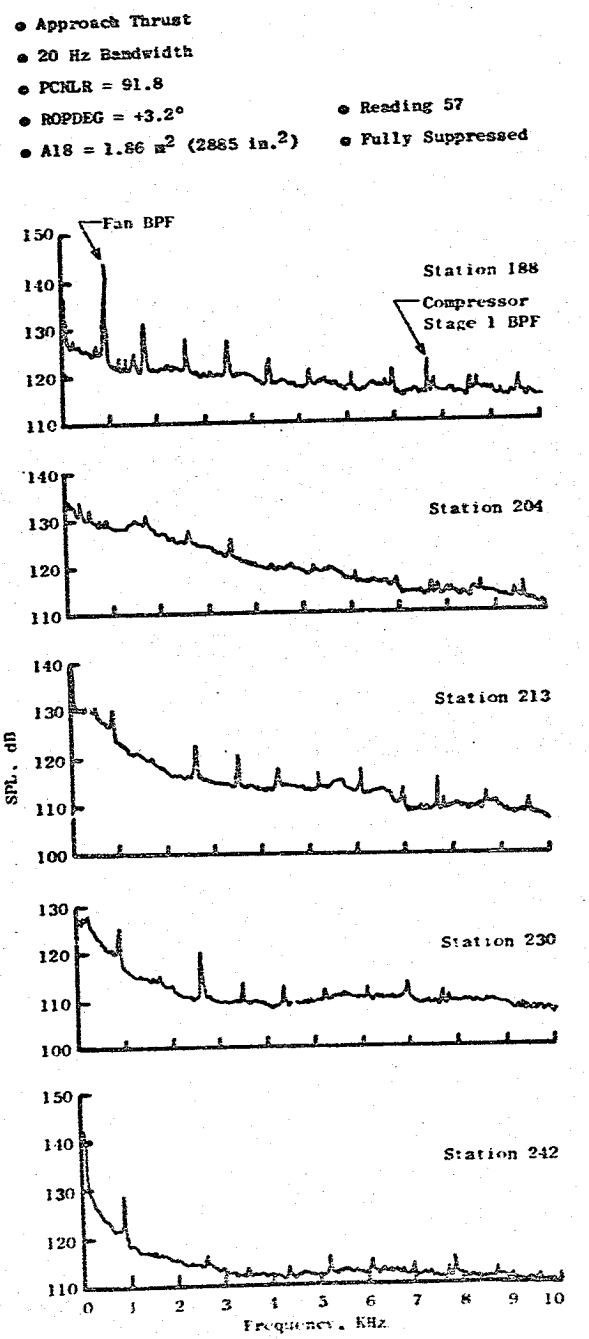

Figure 53. Fan Bypass Duct Wall Kulite Narrow Band Spectra at Approach.

Sound separation probe data were acquired at approach for several radial immersions at two stations - the OGV trailing edge and the fan bypass nozzle flap trailing edge. Results are presented in Figure 54 and show that the narrow band tone PWL transmission losses were 21 and 15 dB, respectively, at the fan BPF and fan second harmonic.

5.2.2.2 Vane Suppression

One of the advanced technology items in the QCSEE program was the incorporation of treatment on the pressure surface of the outlet guide vanes (OGV'S). Although no model testing was conducted, it was felt that this treatment would demonstrate high frequency broad band suppression that could be useful on engines with marginal suppression designs. Acoustic design parameters are as follows:

- Pressure side only treated with SDOF treatment
- Facesheet thickness - 1.27 mm (0.05 in.)
- 10% porosity
- Hole diameter - 1.52 mm (0.06 in.)
- Cavity depth - 6.35 to 12.7 mm (0.25 to 0.5 in.)
- Treated length to duct height (L/H) ~ 0.33
- Tuning frequency ~ 4000 Hz
- Treated area per vane - 203 cm^2 (31.5 $in.^2$)

The treated L/H for the vane was based on the axial treated length of the vane divided by two times the average circumferential spacing between the vanes.

As discussed earlier in Section 3.0, vane treatment was evaluated by taping the OGV's with a metal duct tape to simulate a hardwall vane. This was done with the rest of the engine in a baseline configuration. Vane treatment suppression spectra for 110, 120, and 130° are shown in Figure 55. These curves are an average suppression based on 10 pairs of treated and untreated vane data points covering a range of fan speeds, blade angle, and fan bypass nozzle areas. Suppression of nearly 2 dB was achieved with the vane treatment in the frequency region of 5 to 10 kHz. Not only is suppression evident in the aft quadrant, but it is also present in the inlet quadrant as shown in Figure 56 which presents suppression directivity at 1/3-octave band frequencies of 4000 to 8000 Hz.

5.2.2.3 Core Noise

The core suppressor shown schematically in Figure 41 was designed (Reference 2) to suppress both high frequency turbine noise and low frequency combustor noise. Since both of these components are marginal in terms of contribution to the total UTW system noise (Reference 1), it was recognized early

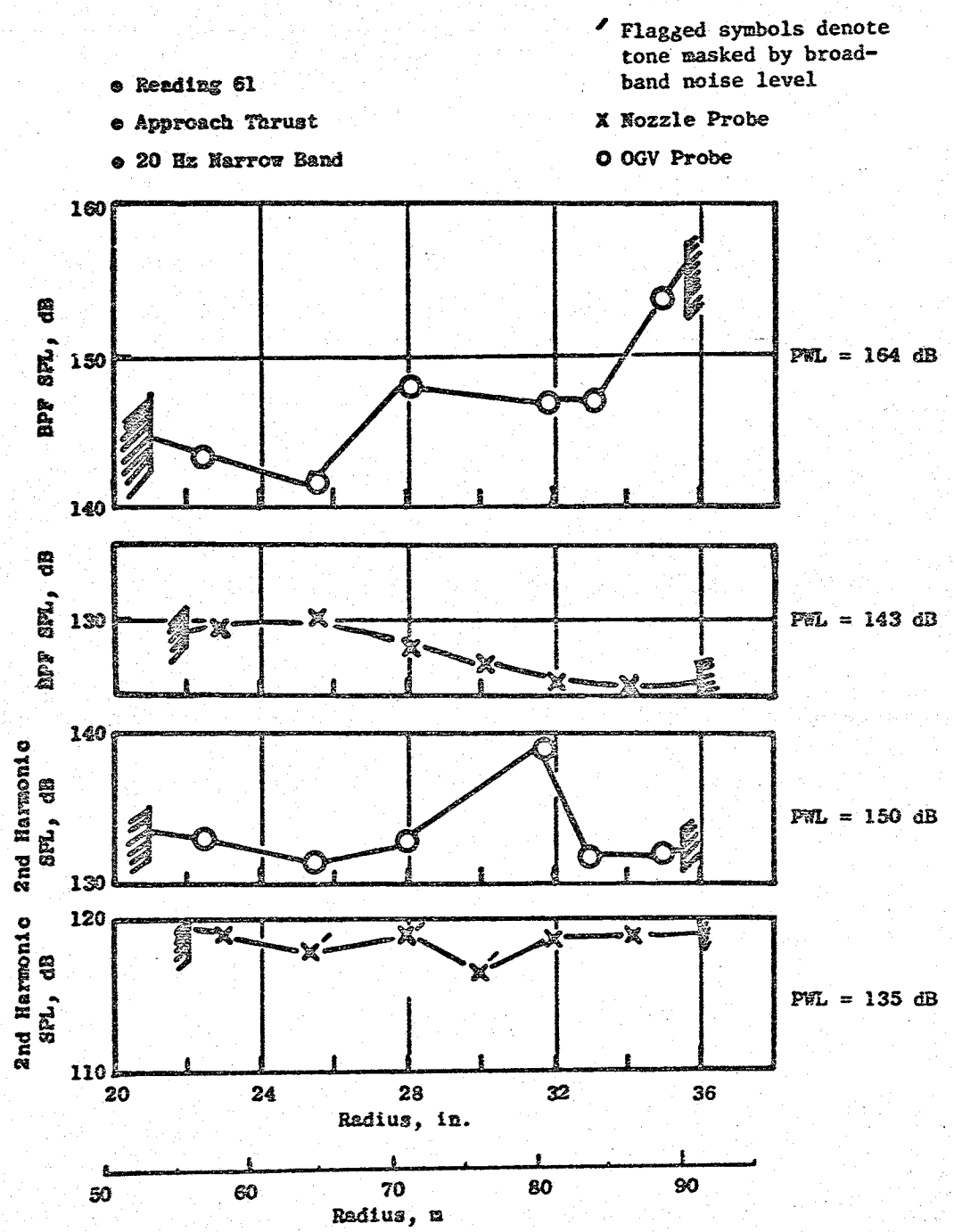

Figure 54. Fan Bypass Duct Tone Radial Profiles at Approach.

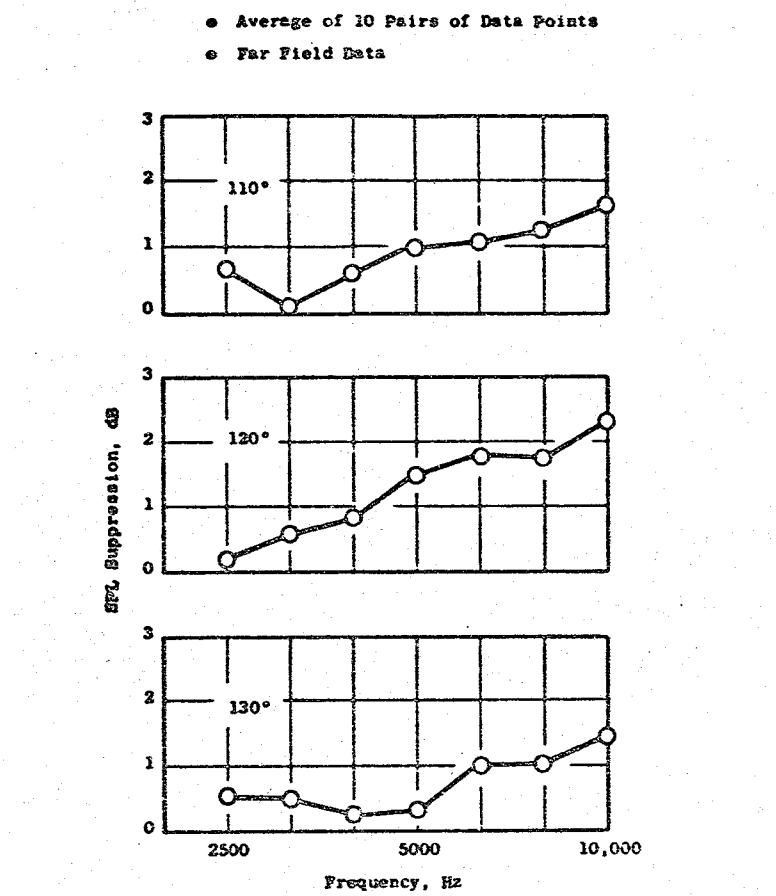

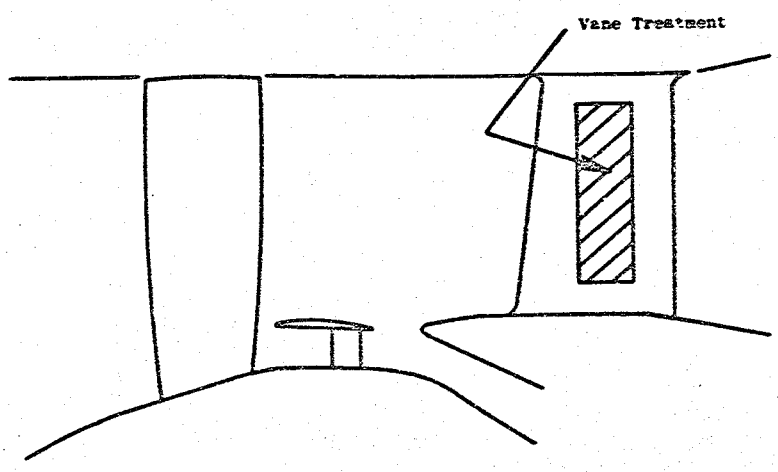

Figure 55. Treated Vane Suppression Spectra.

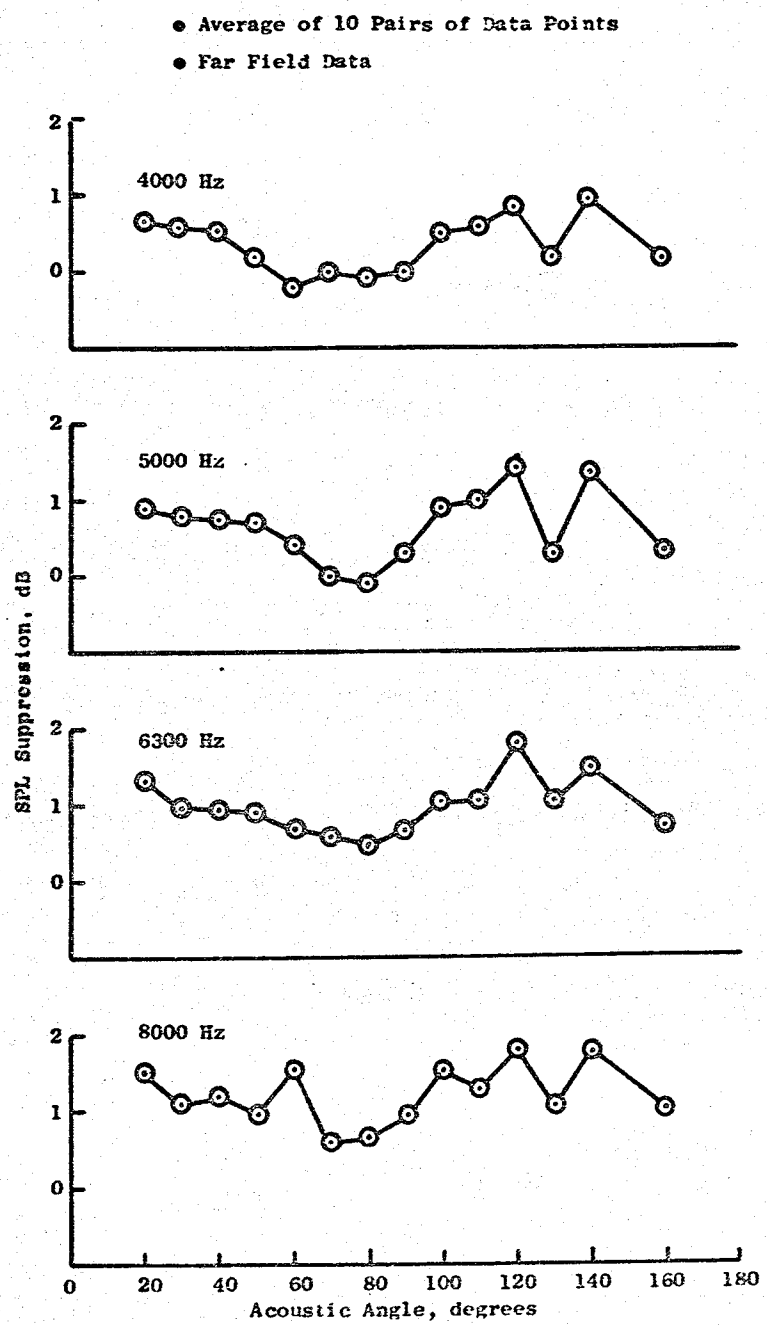

Figure 56. Treated Vane Suppression Directivity.

in the program that it would be extremely difficult to measure the unsuppressed and suppressed levels of these components. The difficulty in measurement of the core suppression has been compounded by the fan source noise increase of about 5 dB which results in aft fan noise levels high enough to completely mask the high frequency turbine noise.

Spectral comparisons with a hardwall core and the treated core suppressor are shown in Figure 57. The comparisons are made at a large fan bypass nozzle area to keep jet noise low. Low frequency suppression is evident in the frequencies where combustor noise is expected to occur, i.e., 315 to 630 Hz. The resulting suppressions which are evident in the far field are shown in Figure 58 and compared to the predicted combustor suppression spectra. Broad band suppression in the band containing the fan BPF was determined by fairing out the BPF in the 1/3-octave band spectra. This comparison reflects the measurement difficulties associated with noise masked by other sources, rather than poor performance of the core suppressor. Additional testing to isolate the core noise and core noise suppression is needed and should be considered in future tests of the UTW engine.

An interesting observation can be made with regard to the low frequency stacked treatment, as shown in Figure 59. Suppression is evident at all angles indicating that low frequency combustion noise is present even in the forward quadrant.

5.2.3 UTW Radial Modes

Measurements of radial mode content were made for an untreated (hardwall) duct configuration at two planes of the exhaust duct, using the OGV exit probe at Station 204.5 and the fan nozzle probe at Station 267.4, as shown in Figures 3 and 40. Data were taken at takeoff and approach conditions.

A radial modal measurement consists of the determination of the spatial variation of the complex acoustic pressure profile across the duct, which is then expanded into characteristic duct modes. For the exhaust duct, it is assumed that the modal expansion can be made in terms of the modes of a rectangular duct. This approximation will be true for high radius ratio annular ducts in the presence of low spinning mode orders. The complex acoustic pressure profile is obtained by computing the cross spectrum of the traversing probe signal with a wall-mounted reference microphone located close to the traverse plane. The data were reduced at the pure tone frequencies, where coherence between the traversing probe and the wall Kulite was sufficiently high to provide validity to the measurement. Figures 60 to 63 are plots of the modal content in terms of relative mode magnitudes for 50 Hz bandwidth narrow bands which contain energy from pure tone generation by the source. The modal participation, in almost all cases, is noted to be rich in higher order mode content, a condition which should be advantageous to treatment suppression. The modal participation could be used to predict suppression for any given configuration of treatment panels. This procedure has the potential of increasing suppression well above that of current design techniques.

- 152 m (500 ft) Sideline
- 120°
- A18 = 1.87 m^2 (2900 $in.^2$)
- ROPDEG = 0°
- Ground Microphones

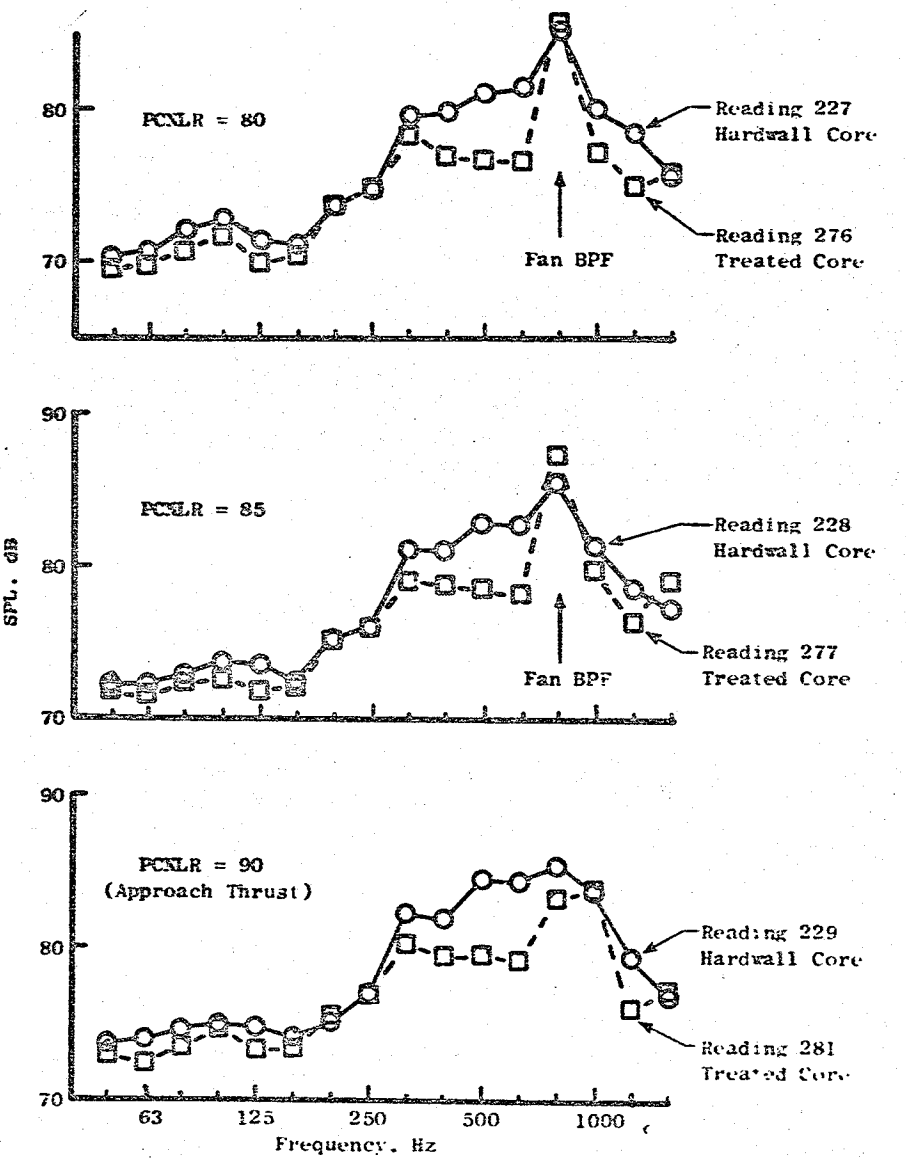

Figure 57. Comparison of 120° Spectra with Hardwall and Treated Core Suppressor.

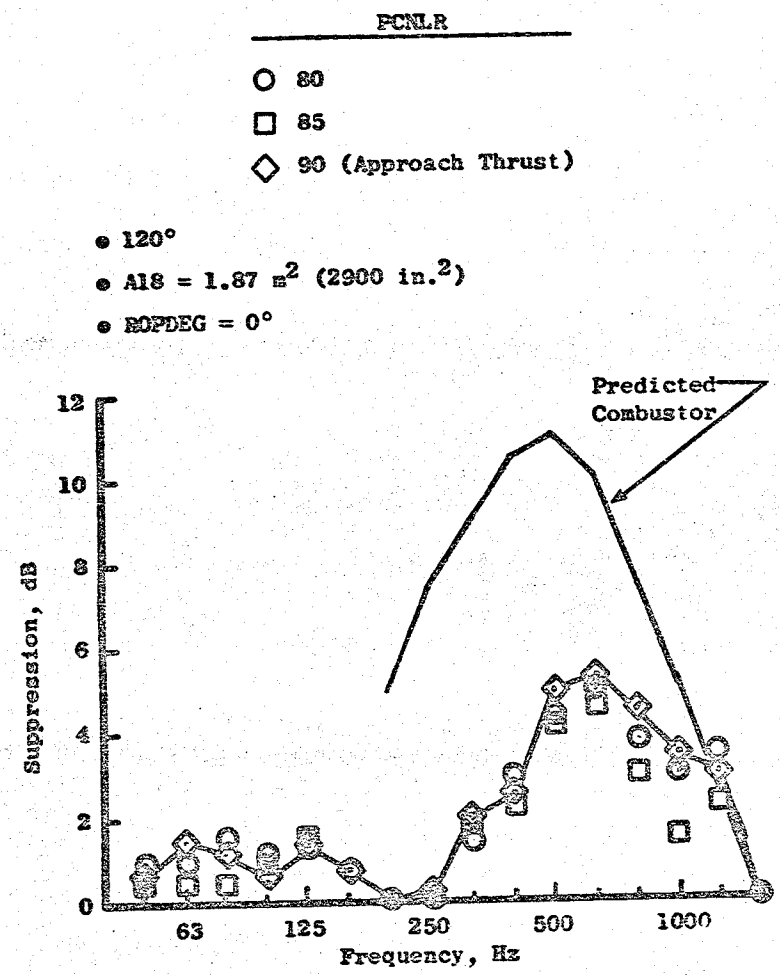

Figure 58. Comparison of Predicted and Measured Combustor Suppression.

- Approach Thrust
- PCNLR = 90
- ROPDEG = 0°
- A18 = 1.87 m^2 (2900 $in.^2$)
- 152 m (500 ft) Sideline

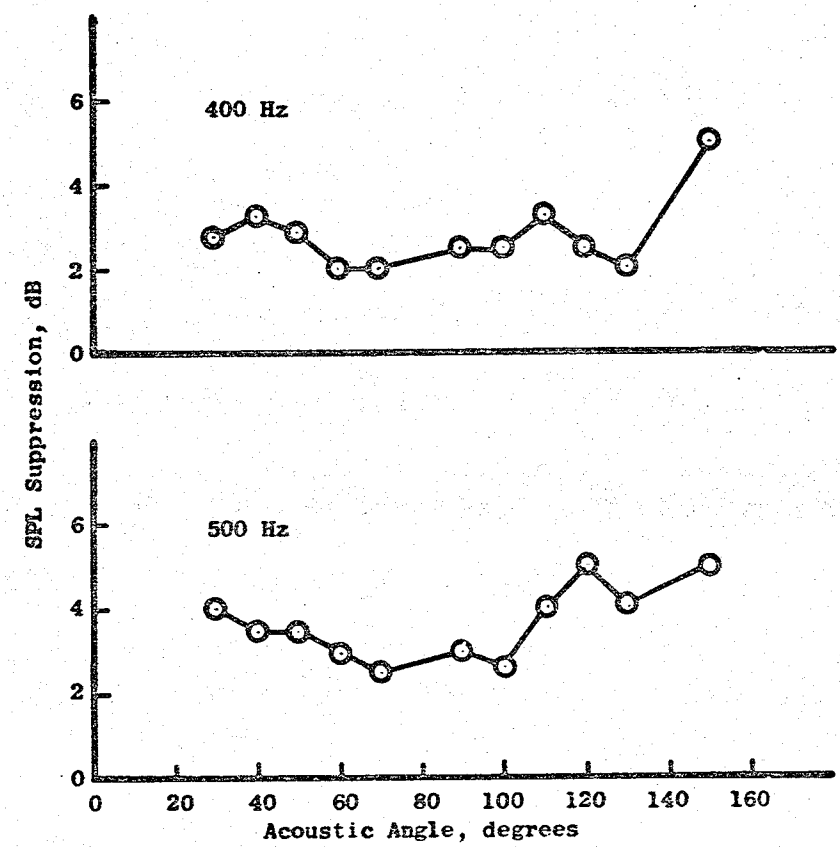

Figure 59. Low Frequency Suppression Directivity.

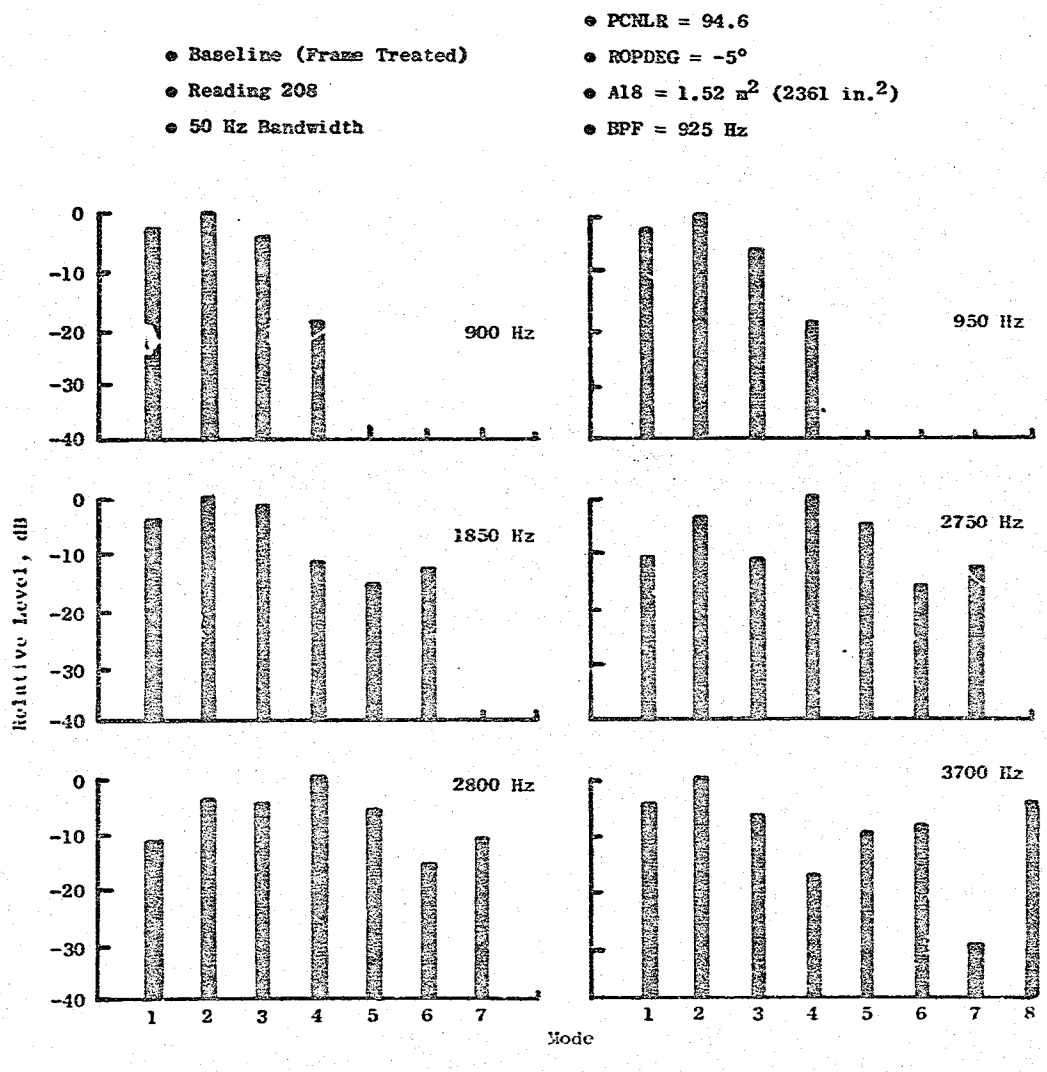

Figure 60. Radial Mode Content at Takeoff - OGV Probe.

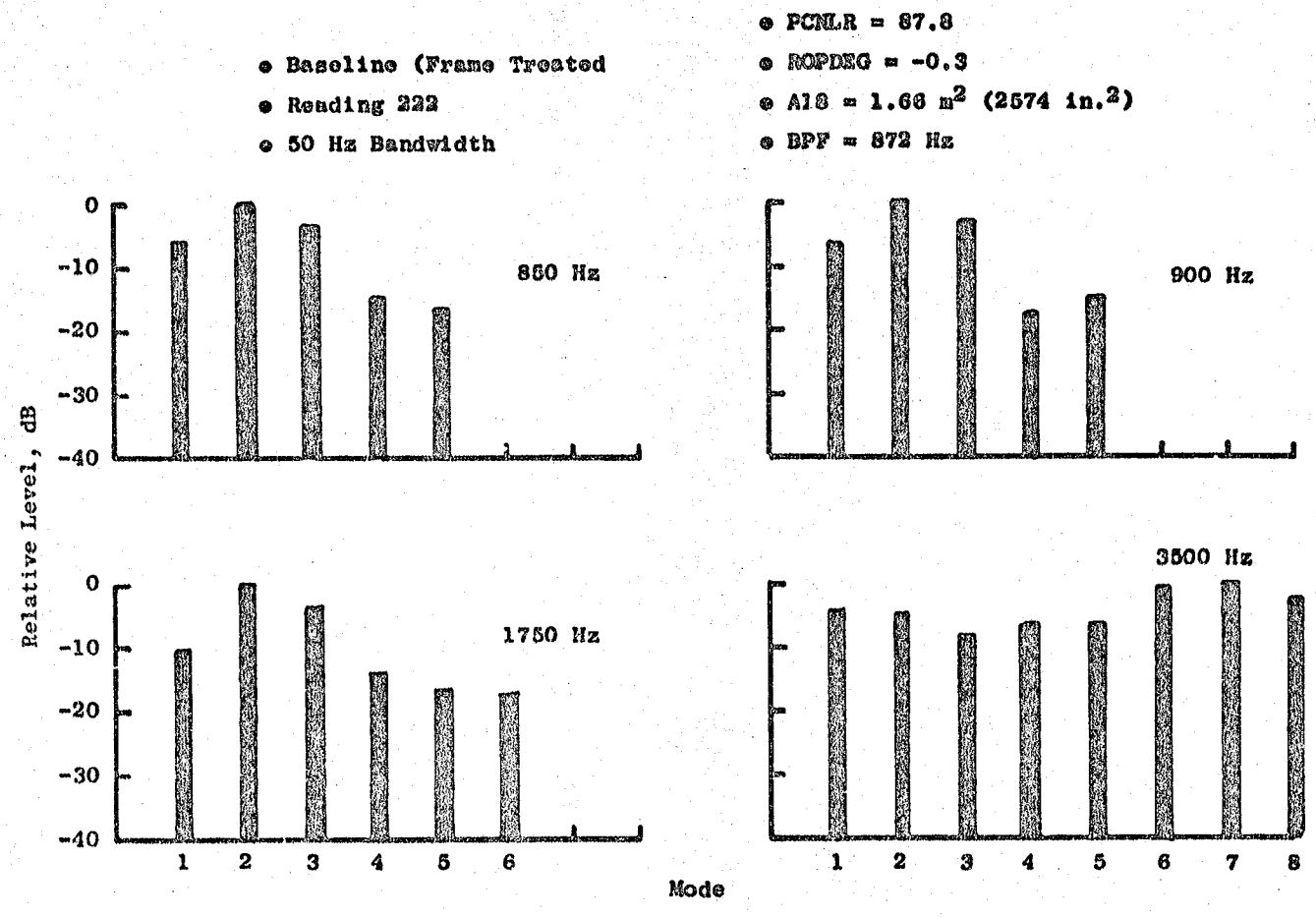

Figure 61. Radial Mode Content at Approach - OGV Probe.

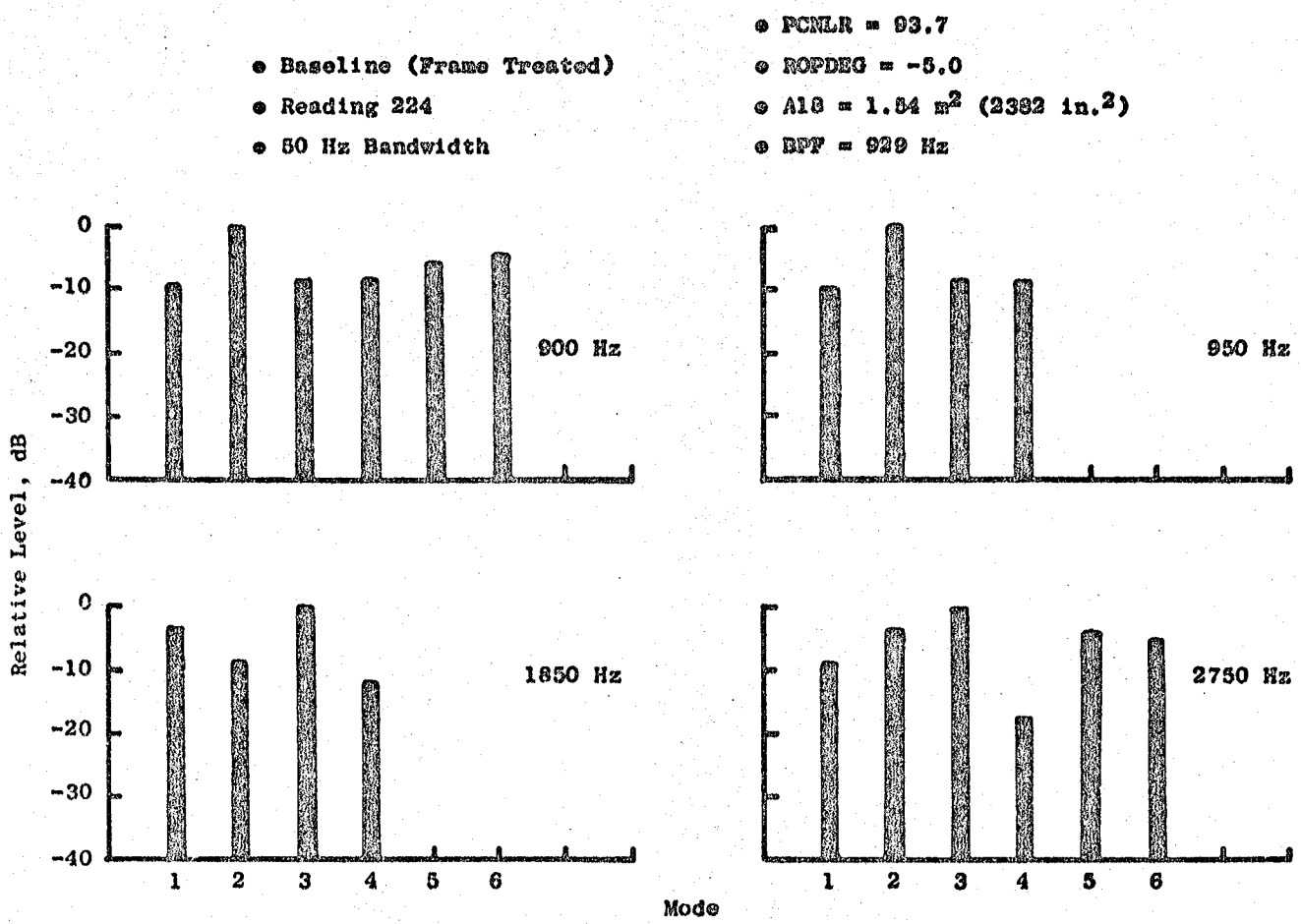

Figure 62. Radial Mode Content at Takeoff - Fan Nozzle Probe.

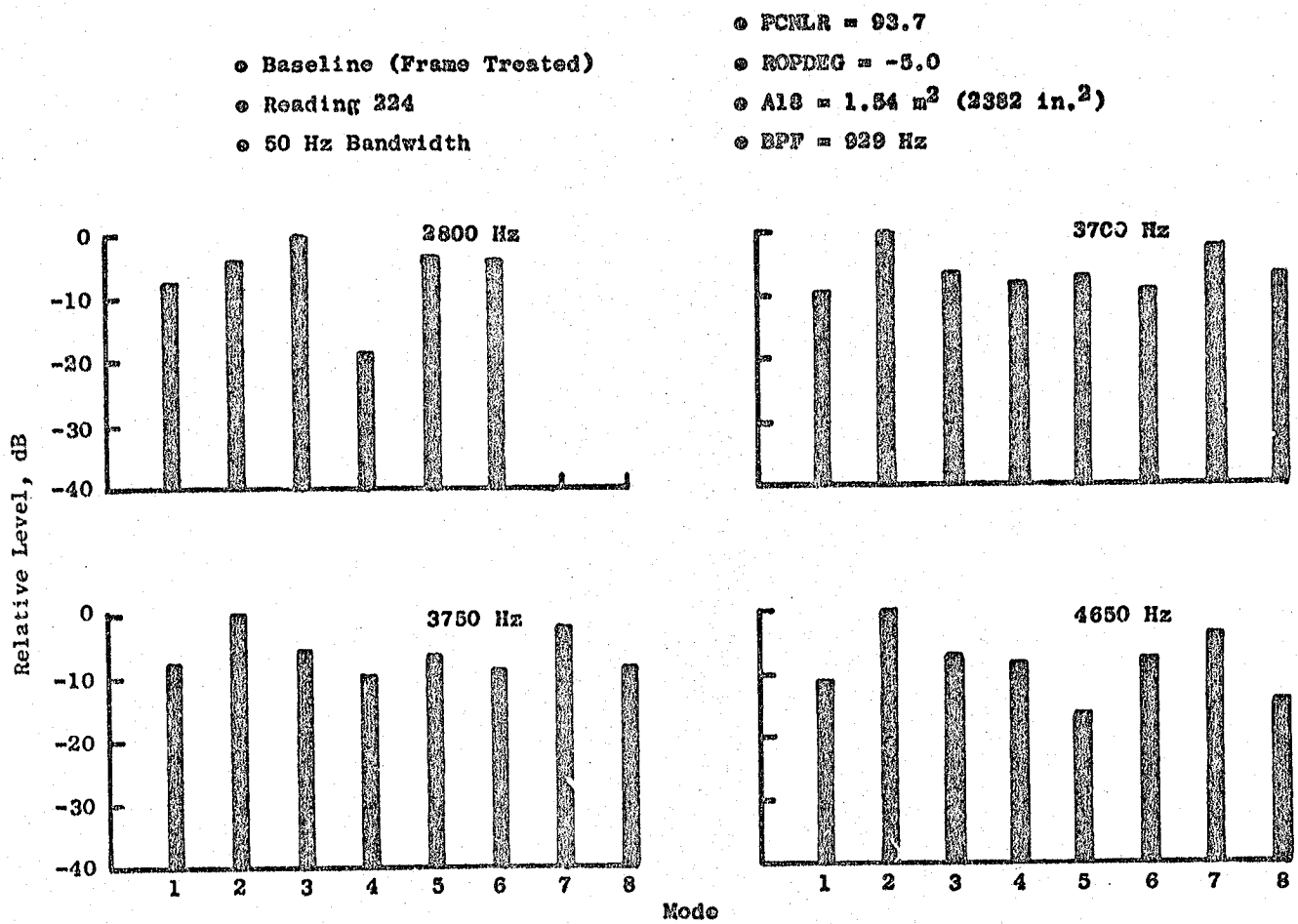

Figure 62. Radial Mode Content at Takeoff - Fan Nozzle Probe (Concluded).

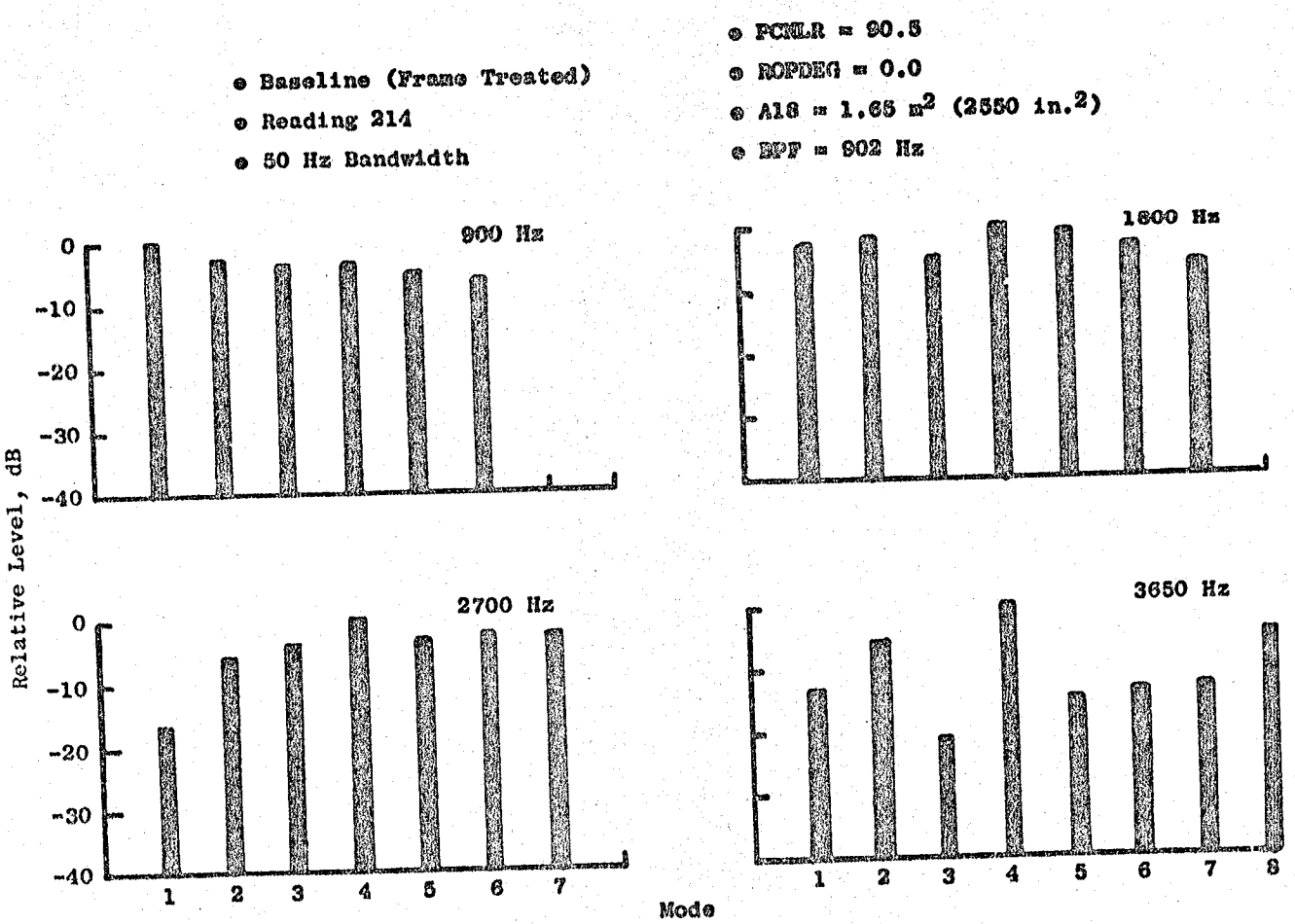

Figure 63. Radial Mode Content at Approach - Fan Nozzle Probe.

5.3 NOISE DIRECTIVITY COMPARISONS

PNL directivity comparisons for the five engine configurations are presented in Figures 64 and 65 for takeoff and approach thrust, respectively. These comparisons are on a 61 m (200 ft) sideline and indicate that the peak angle - both suppressed and unsuppressed - is in the aft quadrant near 110°.

Comparisons are made for two different builds of the QCSEE UTW over two different sound field surfaces and are for data that have been corrected to standard day conditions (298 K [77° F] and 70% relative humidity) but not to free-field conditions.

In the aft quadrant, the fully suppressed no-splitter configuration is about 1 PNdB higher than the fully suppressed/hard core configuration at both takeoff and approach.

5.4 SYSTEM NOISE LEVELS

The noise objectives for the UTW engine are depicted schematically in Figure 66. They are based upon the total system noise levels that would be heard by an observer on a 152.4 m (500 ft) sideline. At takeoff and approach, the noise levels include not only the engine noise (less static jet noise) but also the jet/flap noise associated with the interaction of the exhaust gases with the powered-lift flap system. Specific aircraft operating requirements are given in Table IX.

At takeoff, the noise goal is a maximum of 95 EPNdB. At approach, with the engines developing 65% of takeoff thrust, the goal is also 95 EPNdB.

Since the engine noise levels are to be measured during static testing, a procedure for determining in-flight noise levels from static data has been established as part of the contract. This procedure establishes the following (See Appendix A of Reference 3):

1. Jet/flap noise calculation procedure
2. Extrapolation procedures including air attenuation and extra ground attenuation
3. Doppler shift correction
4. Dynamic effect correction
5. Size correction
6. In-flight cleanup and upwash angle correction
7. Number of engine correction
8. Relative velocity correction for jet/flap noise

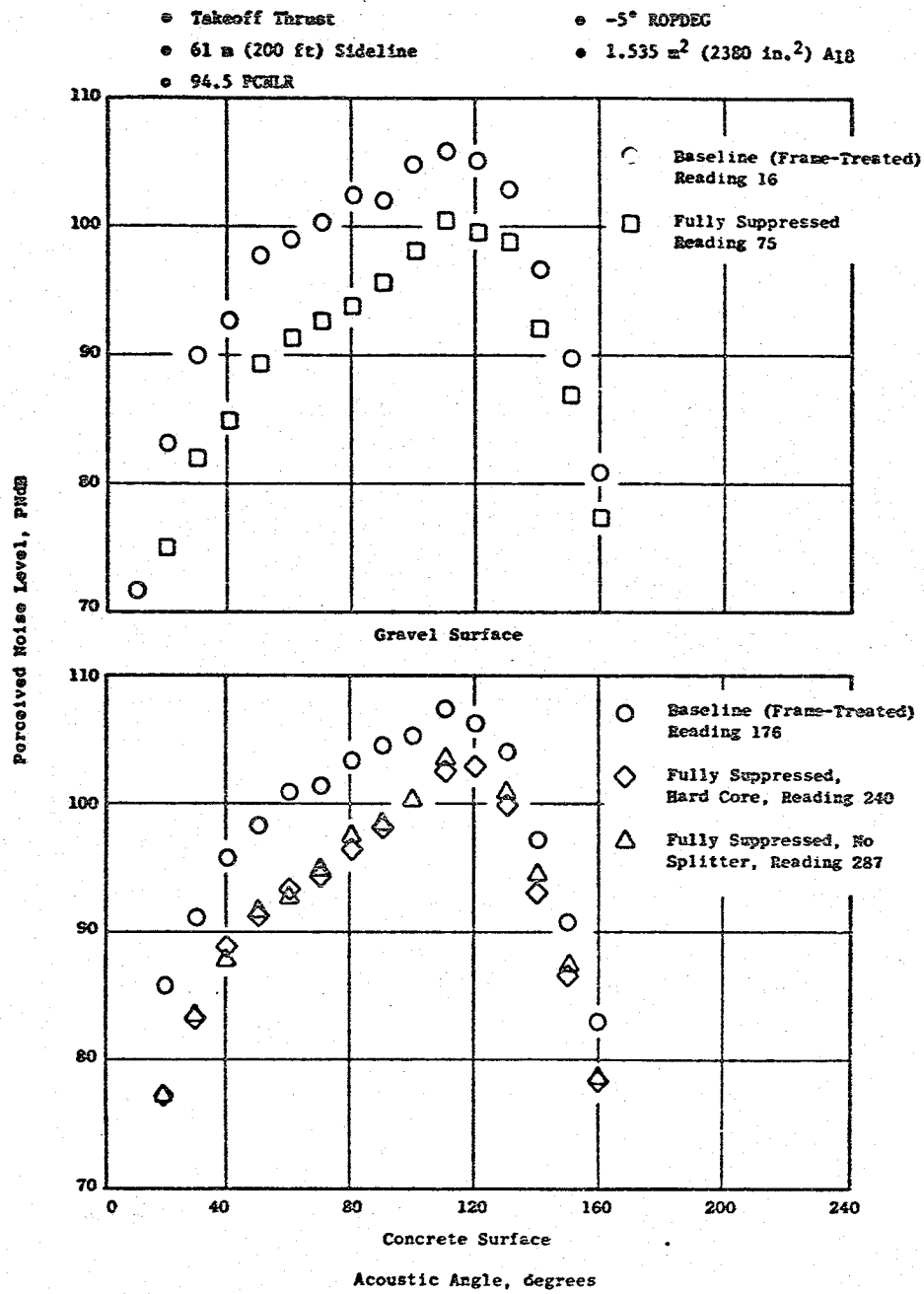

Figure 64. Takeoff PNL Directivity Comparison.

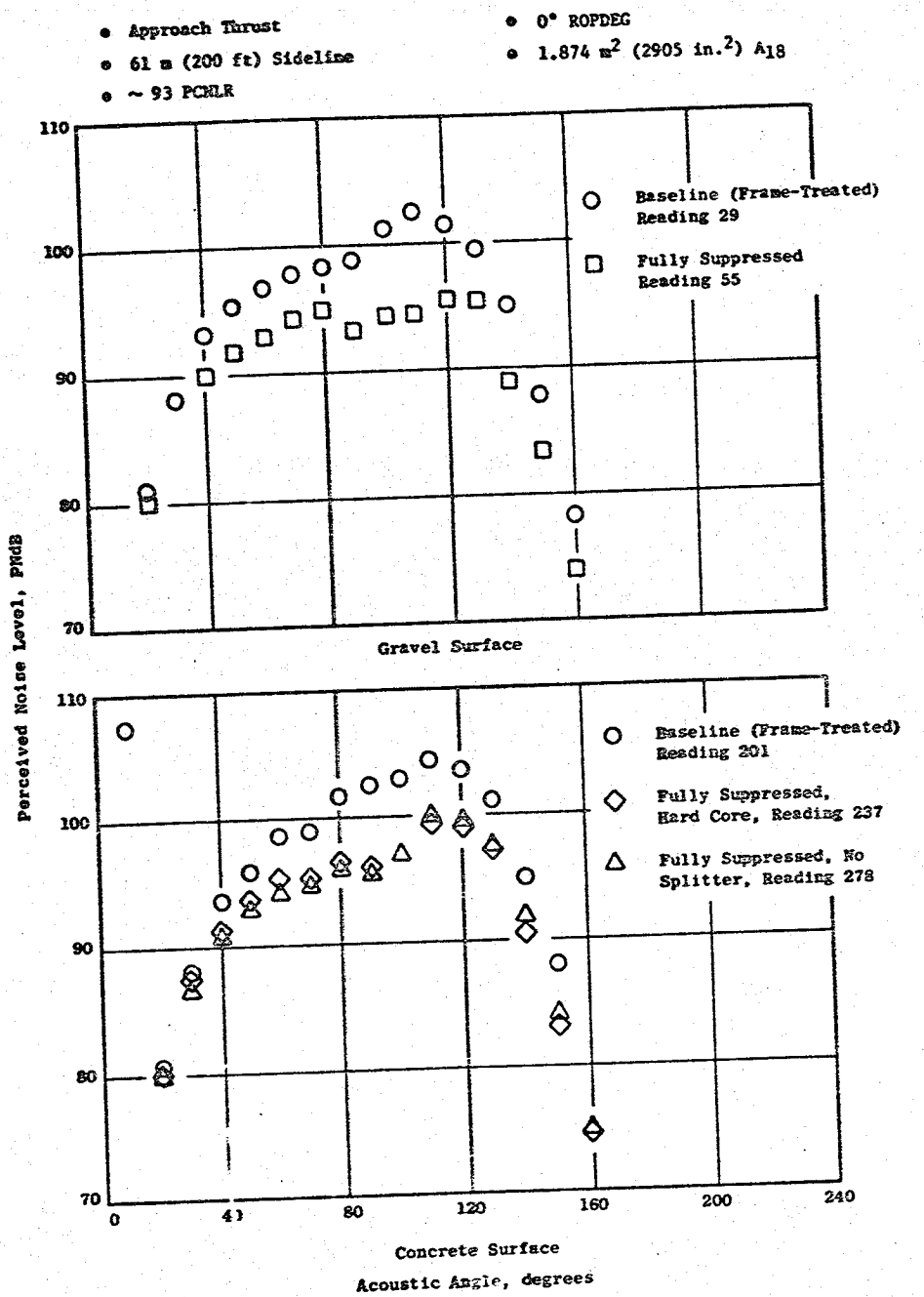

Figure 65. Approach PNL Directivity Comparison.

- Four Engines
- F_N = 400 kilonewtons (90,000 lb) Total SLS Thrust

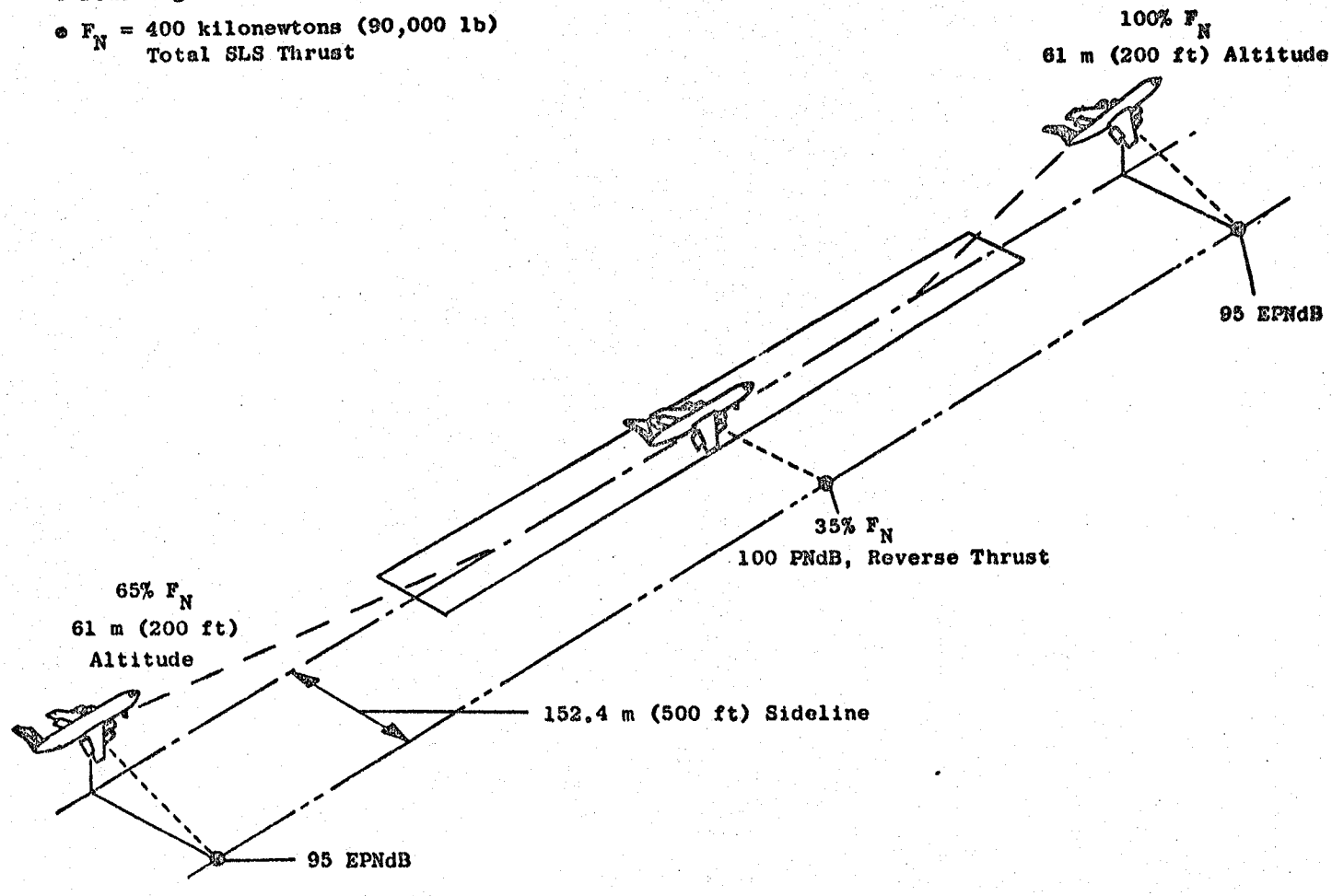

Figure 66. Acoustic Requirements.

Table IX. UTW Engine and Aircraft Flight Characteristics for Acoustic Calculations.

Flight Conditions	Takeoff	Landing
Aircraft Speed, m/sec (knots)	41 (80)	41 (80)
Flap Angle, degrees	30	60
Climb or Glide Angle, degrees	12.5	6
Angle of Attack, degrees	6	2
Upwash Angle, degrees	15	11
Installed Net Thrust, percent	100	65

9. Fuselage shielding
10. PNL to EPNL calculation
11. Dirt/grass ground absorption correction

These calculations are performed on the peak forward and peak aft angles.

Using the contract procedure specified above, the takeoff noise level for an aircraft powered by four QCSEE UTW composite nacelle engines would be 97.2 EPNdB on a 152 m (500 ft) sideline. Table X presents the forward and aft quadrant summaries for this system. It is evident that exhaust-radiated noise of 99 PNdB is a major contributor to the total system noise level. This results from the higher-than-predicted high frequency fan broad band noise levels which were measured on the UTW engine.

At approach, the total system noise level is 95.7 EPNdB - just 0.7 EPNdB over the goal of 95.0 EPNdB. Table XI shows that the suppressed engine noise is the dominant noise source in both quadrants and that any reduction to the noise goal must include fan noise source reduction and/or suppression.

The noise goals for the QCSEE program were very challenging, representing a noise reduction step of about 10 EPNdB below current wide-body aircraft. UTW noise levels were within 2.2 EPNdB of these goals and, thus, still represent a major reduction in noise.

Table X. Takeoff System Noise.

- 90.8% corrected fan speed, PCNLR
- 0.79 throat Mach number, XMII
- 1.58 m^2 (2451 $in.^2$) fan exhaust nozzle area, A_{18}
- -8.0 Fan blade angle, ROPDEG
- 152 m (500 ft) sideline
- 61 m (200 ft) altitude
- Fully suppressed (Reading 103)

Maximum Noise

	Forward Quadrant		Aft Quadrant	
	Engine	Jet/Flap	Engine	Jet/Flap
PNL	91.7	94.6	99.0	90.0
Total System PNL	97.0		99.9	
Total System EPNL	97.2			

Table XI. Approach System Noise.

- 94.4% corrected fan speed, PCNLR
- 1.65 m^2 (2550 $in.^2$) fan exhaust nozzle area, A_{18}
- +4.3 fan blade angle, ROPDEG
- 152 m (500 ft) sideline
- 61 m (200 ft) altitude
- Fully suppressed (Reading 54)

	Maximum Noise			
	Forward Quadrant		Aft Quadrant	
	Engine	Jet/Flap	Engine	Jet/Flap
PNL	96.7	89.8	95.6	82.7
Total System PNL	97.9		96.0	
Total System EPNL	95.7			

6.0 REVERSE THRUST ACOUSTIC RESULTS

Reverse thrust testing of the fully suppressed UTW composite nacelle engine was conducted at two fan pitch blade angles. The blade angles were -95 and -100°. For these tests, the fan bypass nozzle flaps were opened to a flare position as shown in Figure 67 to provide an inlet for the reversed fan bypass flow.

6.1 FAR-FIELD DATA

Far-field PNL's are shown in Figure 68 for the peak acoustic angle of 70°. The PNL's are plotted versus reverse thrust level which is expressed as a percent of takeoff thrust. Although the reverse thrust goal of 35% was not reached due to engine temperature limitations, acoustic data were taken up to 27% of takeoff thrust. PNL's taken at -95° fan pitch blade angle are generally higher than those taken at -100°, a result that was anticipated from the model tests reported in Reference 9.

Figure 69 is a PNL directivity plot at 27% reverse thrust. The spectral distribution at 60° and 70° is shown in Figure 70. The fan BPF is evident at 800 Hz but no tones are seen at higher frequencies as confirmed by the 20 Hz narrow-band spectra presented in Figure 71.

6.2 SYSTEM NOISE LEVELS

The noise goal for the UTW engine in reverse thrust is a peak noise level of 100 PNdB or less on a 152 m (500 ft) sideline with the engine generating a reverse thrust level which is 35% of takeoff thrust. Since the UTW engine achieved a maximum of 27% reverse thrust, system noise numbers will be presented at this thrust level and not at 35%. The peak PNL occurred at 70° and was 103.3 PNdB for the single engine tested at the General Electric Peebles Test Operation. In order to convert this to a system noise level representative of a QCSEE-powered STOL aircraft, adjustments as specified in Appendix A of Reference 3 were made. They are tabulated below:

Engine size	1.1 PNdB
Number of engines	6.0 PNdB
Fuselage shielding	-3.0 PNdB
Dirt/grass ground	-1.0 PNdB
Total correction	+3.1 PNdB

With this correction, a short-haul aircraft system with four QCSEE's would achieve a maximum level of 106.4 PNdB on a 152 m (500 ft) sideline when operating at a reverse thrust which is 27% of takeoff thrust. An alternative to this would be the case where it is strictly necessary to meet the 100 PNdB goal. This stringent noise goal could be achieved at a reverse thrust level which is 18% of takeoff thrust.

ORIGINAL PAGE IS
OF POOR QUALITY

Figure 67. UTW Composite Nacelle with Fan Nozzle Flaps in the Flare Position.

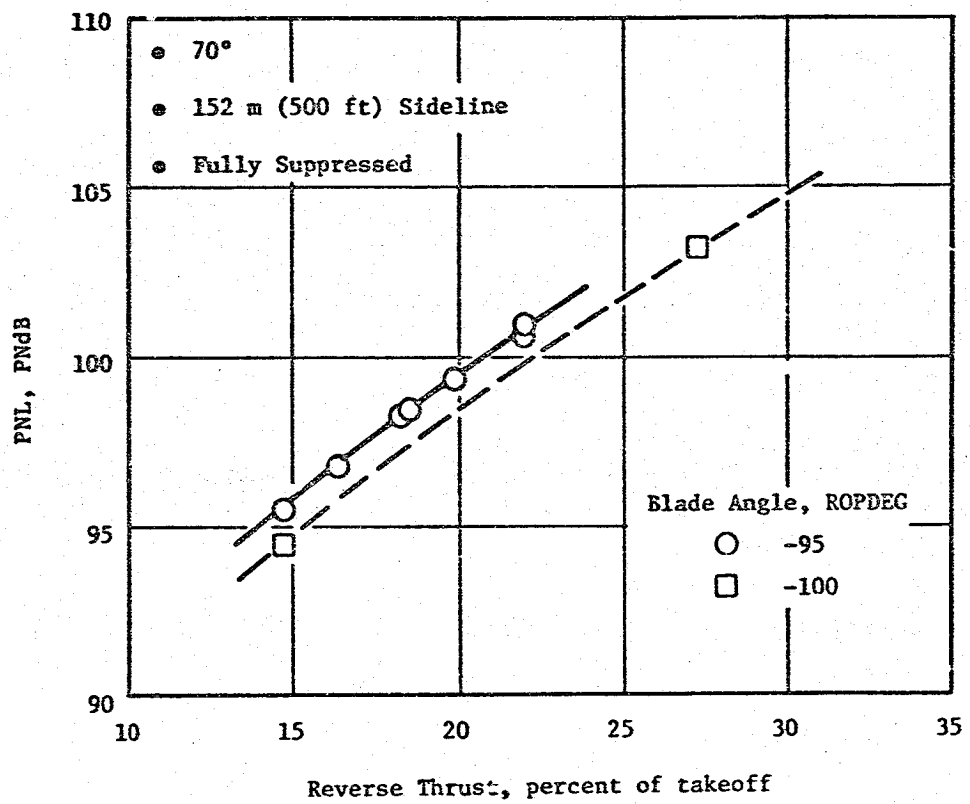

Figure 68. Peak PNL Variation with Reverse Thrust.

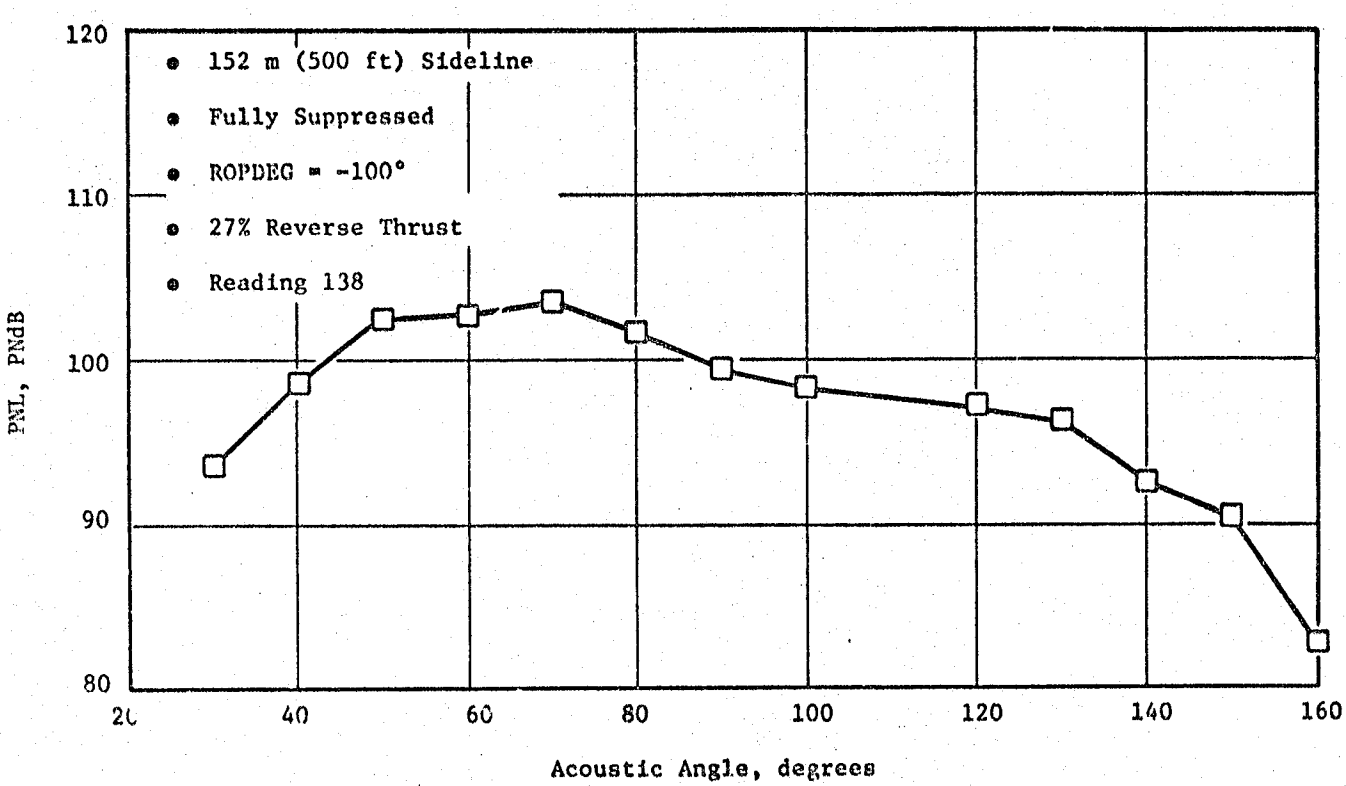

Figure 69. Reverse Thrust PNL Directivity.

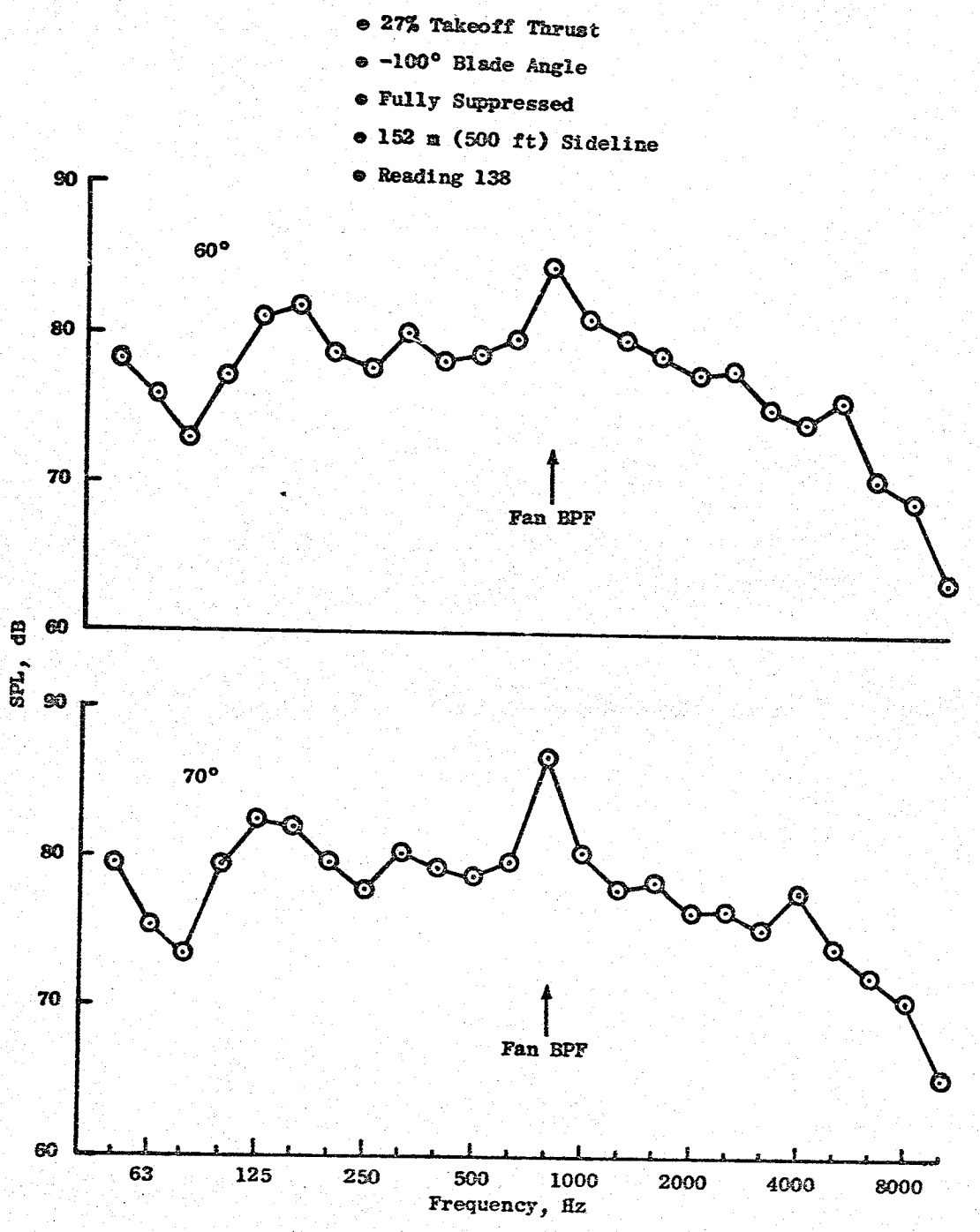

Figure 70. Reverse Thrust Spectra.

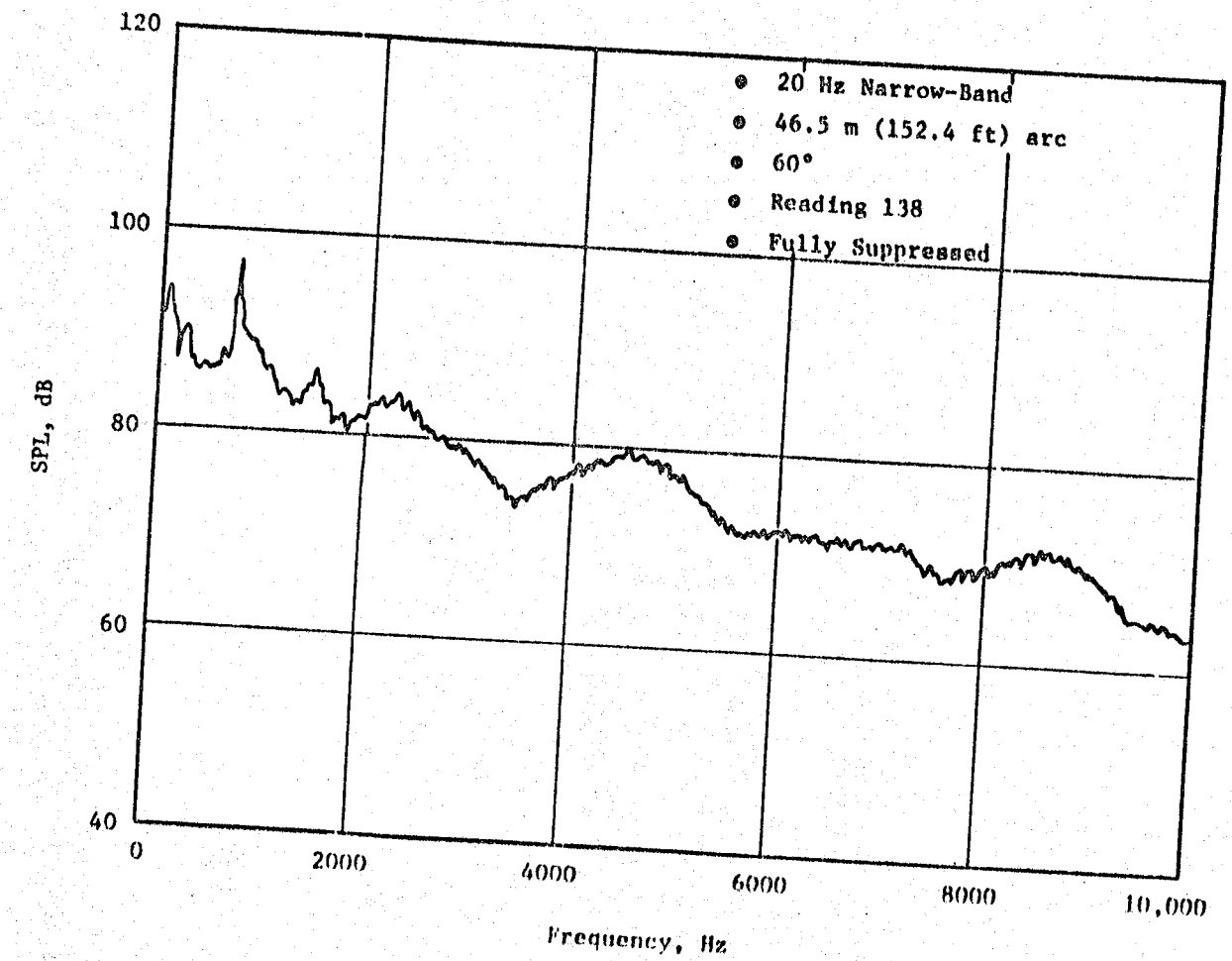

Figure 71. Reverse Thrust Narrow-Band Spectrum.

7.0 CONCLUSIONS

Because of the very challenging noise goals established for the QCSEE program, several unique noise-reduction concepts and source noise reduction features have been developed and demonstrated. The most difficult aspect of the QCSEE noise goal was to achieve simultaneous success with the prediction and suppression of several major noise components. Simultaneous success was necessary since all of these sources were contributors to the suppressed engine noise levels and, therefore, missing even one of the component levels jeopardized achievement of the noise goals.

7.1 CONCLUSIONS

- UTW takeoff system noise levels were within 2.2 EPNdB of the goal.
- UTW approach system noise levels were within 0.7 EPNdB of the goal.
- Baseline unsuppressed levels on the UTW engine were higher than anticipated but the program has provided a large data base (both aerodynamically and acoustically) for understanding and predicting variable pitch fan noise.
- The hybrid inlet achieved 14 to 15 PNdB of inlet suppression at 0.79 throat Mach number. At approach, the wall treatment provided 4 to 6 PNdB suppression.
- Aft fan suppression of up to 2 dB was demonstrated for the treated vanes. This is a significant amount of suppression for a very small amount of treatment area.
- Aft suppression for the static engine was within about 2 PNdB of predicted.
- The suppression capability of the "stacked" core suppressor was not completely evaluated due to masking by other noise sources; however, suppression at the design frequencies was demonstrated for a flight-worthy combustor noise suppressor design.
- Reverse thrust nosie levels of the variable pitch UTW fan were higher than predicted; however, the data base will provide for more accurate prediction and understanding of variable pitch fan noise in reverse thrust.

APPENDIX

FREE-FIELD CALCULATIONS

The baseline (frame treated) configuration of the QCSEE UTW composite nacelle engine was tested acoustically over two sound field surfaces - gravel and concrete. Each surface has different ground-reflection characteristics which might be considered in any correction of the data to free-field conditions. This appendix compares the free-field results from both surfaces, and documents the procedure used to correct the data over each type of surface.

Free-field corrections for the gravel sound field with 12.2 m (40 ft) microphones were established earlier on tests of the QCSEE OTW engine (Reference 10). The corrections for each 1/3-octave band are listed in Table A-1 and are added to the far field measured SPL's.

Two sets of microphones were used to acquire the data over the concrete surface. Ground microphones were 1.27 cm (0.5 in.) above the concrete and engine centerline height microphones were 4 m (13 ft) above the concrete. SPL data were corrected to free field using the following equation:

$$SPL_{FF} = A_G(SPL_G - 6.0) + A_{C/L}(SPL_{C/L} - 3.0)$$

where

A_G = weighting factor for ground microphone

$A_{C/L}$ = weighting factor for centerline microphones

$SPL_{C/L}$ = centerline microphone SPL

SPL_{FF} = free field SPL

SPL_G = ground microphone SPL

Weighting factors for each 1/3-octave band are given below:

Band	A_G	$A_{C/L}$
50 to 1000 Hz	1.00	0.00
1250	0.83	0.17
1600	0.67	0.33
2000	0.50	0.50
2500	0.33	0.67
3150	0.17	0.83
4000 to 10,000	0.00	1.00

Table A-1. Ground Reflection Corrections, 12.2 m (40 ft) High Microphone.

- Corrections are to be added to measured spectra

Frequency (Hz)	Correction (dB)
50	+3.0
63	+5.1
80	+2.3
100	-1.4
125	-3.1
160	-0.8
200	+2.7
250	-2.6
315	+1.3
400	-1.4
500	-0.9
630	-0.3
800	-0.7
1000	-0.6
1250	-0.7
1600	-0.6
2000	-0.7
2500	-0.4
3150	-0.6
4000	-0.6
5000	-0.5
6300	-0.6
8000	-0.5
10000	-0.6

The philosophy behind this composite free-field spectrum is based on the assumption that the ground microphone provides pressure doubling (6 dB) over the low frequencies while the centerline microphone provides power doubling (3 dB) in the high frequencies. For the frequencies in between, an arithmetic weighting is used to provide the free-field levels.

Free-field spectra at three angles for the gravel and concrete sound field surfaces are compared in Figures 72 and 73 at takeoff and approach, respectively. Engine operating parameters were matched as close as possible and the data separately corrected to free field using the procedures discussed above. There is excellent agreement between the two free-field spectra at each angle. On a PNL basis, the differences are less than 0.5 PNdB. There are some slight differences in the very low frequencies which are probably a result of slight shifts in the ground reflection nulls and reinforcements over the gravel. A more detailed recalculation of the ground corrections would probably collapse the low frequency data better; however, the impact on PNL would be minimal.

The comparisons in Figures 72 and 73 represent a site calibration for the QCSEE UTW engine tests and the excellent results imply that data from the two surfaces can be compared with reasonable accuracy when such comparisons are made on a free-field basis.

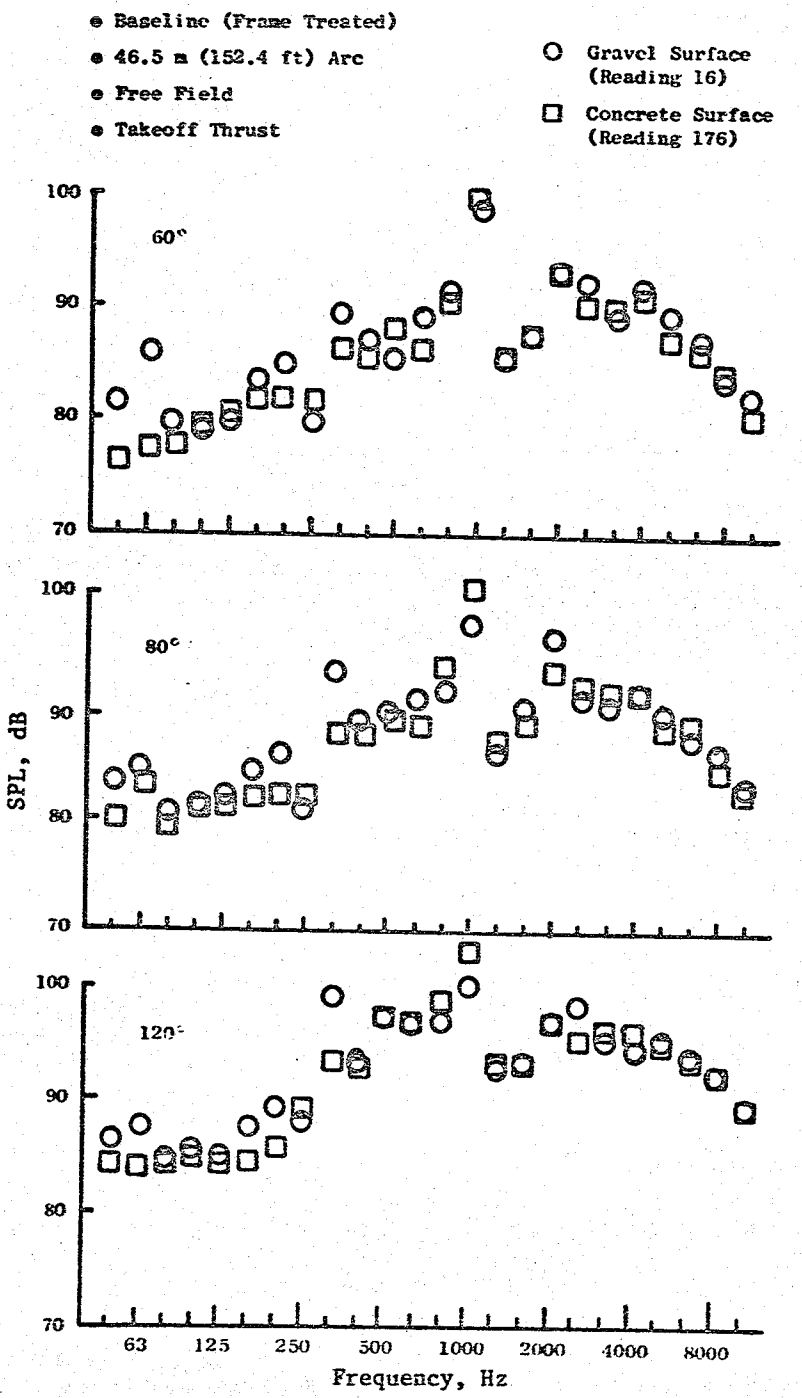

Figure 72. Comparison of Free Field Gravel and Concrete Data at Takeoff.

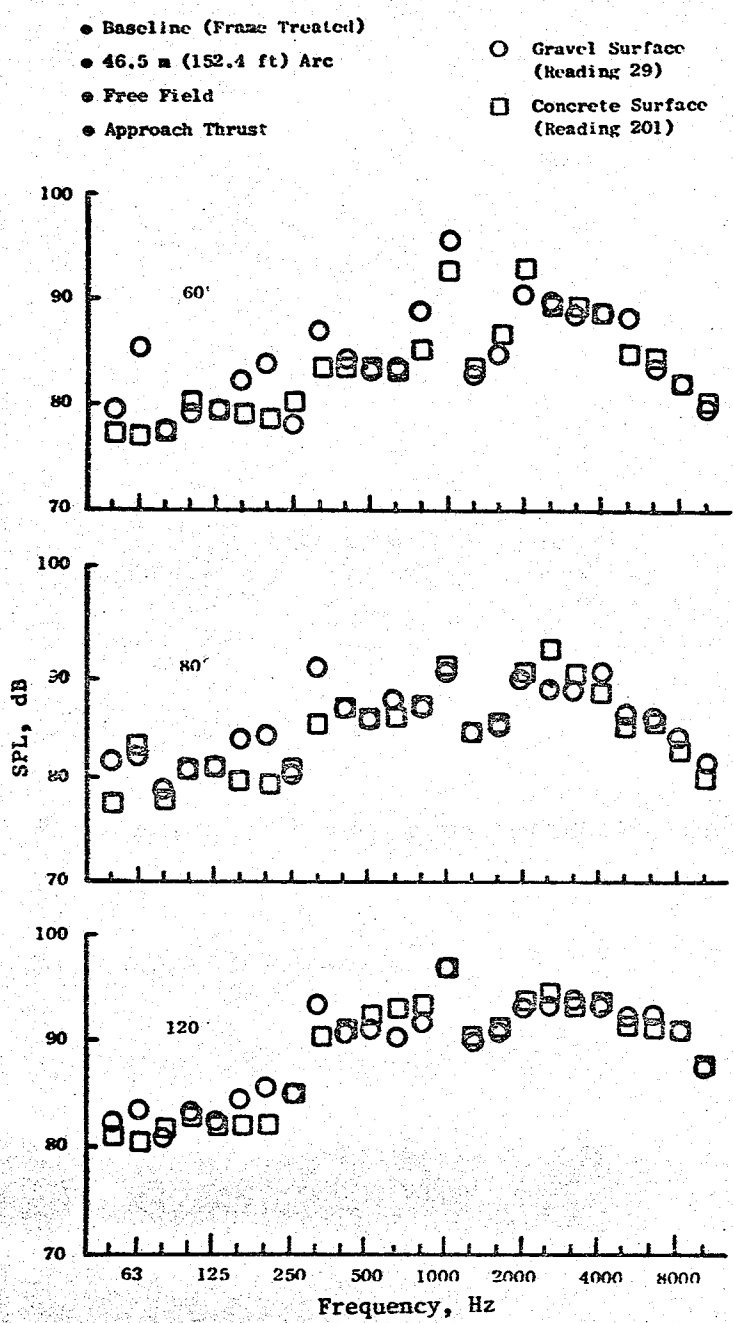

Figure 73. Comparison of Free Field Gravel and Concrete Data at Approach.

NOMENCLATURE

SYMBOL OR ABBREVIATIONS	DEFINITION	UNITS
$A_{C/L}$	Centerline microphone weighting factor	---
A_G	Ground microphone weighting factor	---
ALF	Aft looking forward	---
A18	Fan bypass nozzle area	m^2 ($in.^2$)
BPF	Blade passing frequency	Hz
D or D_F	Fan diameter	m (ft)
EPNL	Effective perceived noise level	EPNdB
FNRIN	Installed thrust	N (lb)
L	Inlet length	m (ft)
L_T	Treated length	m (ft)
OASPL	Overall sound pressure level re: 0.0002 dynes/cm^2	dB
PCNLR	Percent corrected fan speed re: 3244 rpm	---
PCRT	Percent reverse thrust re: takeoff thrust	---
PNL	Perceived noise level	PNdB
PWL	Sound power level re: 10^{-13} watts	dB
ROPDEG	Fan blade angle	degrees
SPL	Sound pressure level re: 0.0002 dynes/cm^2	dB
$SPL_{C/L}$	Centerline microphone SPL	dB
SPL_{FF}	Free-field SPL	dB
SPL_G	Ground microphone SPL	dB
UTW	Under-the-Wing engine	---
XNH	Compressor speed	rpm
XNL	Fan speed	rpm
XM11	Inlet throat Mach number	---

PRECEDING PAGE BLANK NOT FILMED

REFERENCES

1. Sowers, H.D. and Coward, W.E., "Quiet Clean Short-Haul Experimental Engine (QCSEE) Under-the-Wing (UTW) Engine Acoustic Design," NASA Contractor Report 135267, January 1978.

2. Clemons, A., "Quiet Clean Short-Haul Experimental Engine (QCSEE) Acoustic Treatment Development and Design," NASA Contractor Report 135266, January 1979.

3. Anon., "UTW/OTW Preliminary Design Report, Volumes 1 and 2," NASA Contractor Reports 134838 and 134839, October 1974.

4. Anon., "Quiet Clean Short-Haul Experimental Engine (QCSEE) Under-the-Wing (UTW) Final Design Report," NASA Contractor Report 134847, June 1977.

5. Clemons, A., Hehmann, H.W., and Radecki, K.P., "Quiet Engine Program Turbine Noise Suppression, Volume 1, General Treatment Evaluation and Measurement Techniques," NASA Contractor Report 134499, December 1973.

6. Stimpert, D.L. and Clemons, A., "Acoustic Analysis of Aft Noise Reduction Techniques Measured on a Subsonic Tip Speed 50.8 cm (20-inch) Diameter Fan," NASA Contractor Report 134891, January 1977.

7. "Standard Values of Atmospheric Absorption as a Function of Temperature and Humidity for Use in Evaluating Aircraft Flyover Noise," SAE ARP866, 1964.

8. Jutras, R.R. and Kazin, S.B., "Acoustic and Aerodynamic Testing of a Scale Model Variable Pitch Fan," NASA Contractor Report 121232, March 1974.

9. Bilwakesh, K.R., Clemons, A., and Stimpert, D.L., "Acoustic Performance of a 50.8 cm (20-inch) Diameter Variable Pitch Fan and Inlet," NASA Contractor Report 135117, April 1979.

10. Stimpert, D.L., "Quiet Clean Short-Haul Experimental Engine (QCSEE) Over-the-Wing (OTW) Propulsion Systems Test Report, Volume IV, Acoustic Performance," NASA Contractor Report 135326, February 1979.

PRECEDING PAGE BLANK NOT FILMED

End of Document